Coccotunnella Unification Theory (CUT) and its Genesis: The Negative Phases of Conscious Physics and the Origins of the Universe

Gideon Flux

"I believe in Spinoza's God who reveals himself in the harmony of what exists, not in a God who is interested in the actions and emotions of human beings," - Albert Einstein

Copyright © 2025 Gideon Flux

Preface

This book, "Coccotunnella Unification Theory (CUT) and its Genesis: The Negative Phases of Conscious Physics and the Origins of the Universe," presents a revolutionary perspective on the nature of the universe, proposing that it is a living, conscious organism we call Coccotunnella perpetua. At its heart lies the Coccotunnella Unification Theory (CUT), a framework that redefines evolution not as a simple linear progression, but as an infinite, cyclical cosmic dance encompassing pre-material chaos, material emergence, cosmic consciousness, and transcendent unity.

Challenging conventional materialist paradigms that confine consciousness to the realm of physical complexity, CUT posits consciousness as the fundamental attribute of the universe, existing prior to matter and actively shaping its evolution. We delve into the various phases of this cosmic evolution, including the often-overlooked "negative phases" which represent crucial pre-material states of consciousness. These include the chaotic turbulent interactions of Phase -1, the quiescent void of Phase -2, and the oppositional anti-energy fossils of Phase -3.

The theory is supported by a detailed mathematical framework, utilizing the concept of the z-affect to quantify and describe the conscious dynamics within each phase. Furthermore, we introduce the idea of H-space as an eternal archive preserving the energetic signatures of these conscious states, and the Revolutionary Echo as a metaphysical force driving the dynamic and often unpredictable interactions within the living cosmos.

Through rigorous analysis, proposed experimental approaches to test these profound concepts, and illustrative visualizations, this book provides a comprehensive exploration of consciousness's pre-material origins and its pivotal role in the genesis and ongoing evolution of the universe. Join us in reimagining the cosmos not as a sterile, mechanical entity, but as a vibrant, conscious organism where every part is interconnected and alive.

The Phases of Evolution's Cosmic Dance

At the heart of The Living Cosmos lies a bold reimagining of evolution—not as a linear ascent from primordial origins to biological complexity, but as an infinite cycle of phases, each a distinct movement in the cosmic symphony of existence. This cyclical model, formalized by the equation $(C_n = P_n + k_n \cdot Q_n)$, extends Charles Darwin's transformative vision of evolution beyond the biological realm, weaving a tapestry that spans pre-material chaos, material emergence, cosmic consciousness, and transcendent unity. Through this chapter, we summarize the phased structure of evolution, illuminating how each stage—from the turbulent pre-realities to the eternal spirals of future phases—reflects a universal process, validated by

Darwin’s belief in life’s boundless potential and preserved in the ethereal archive of H-space.

Variables

- (C_n) (Complexity of Phase (n)):

Definition: The numerical value representing the evolutionary complexity of phase (n), measured as 1 (simplicity/purity), 2 (complexity/hybridity), or 1.5 (equilibrium for phase 0).

Role in Equation: ($Cn = Pn + kn \cdot Qn$), where (Cn) is the total complexity, summing the primary tunnel’s contribution and the branching tunnel’s quarters (The Organism We Are, page 267).

Significance in Chapter:

For phase -3, (C-3 = 2), indicating maximum complexity due to chaotic proto-variations, akin to biological diversity in phase 2.

Reflects the chapter’s argument that phase -3 is a diverse pre-reality, with four quarters as proto-variations, extending Darwin’s concept of variation (On the Origin of Species, page 19).

Supports the cyclical model’s oscillation between simplicity and complexity, with Darwin’s scalable tree of life (On the Origin of Species, page 433) suggesting he’d endorse this metric.

- 2. (P_n) (Primary Tunnel Contribution):

  Definition: The contribution of the primary tunnel to phase (n)'s complexity, representing the foundational lineage or proto-structure, typically a real number (e.g., 1 for simple phases, 1.25–1.5 for complex phases).

  Role in Equation: (Pn) is the first term in (Cn = Pn + kn · Qn), providing the baseline complexity before branching contributions (The Organism We Are, page 267).

Significance in Chapter:

For phase -3, (P-3 = 1.5), reflecting a robust proto-lineage in the chaotic pre-reality, teeming with potential but lacking material form (The Organism We Are, page 25).

Aligns with Darwin's concept of a primordial form (On the Origin of Species, page 428), suggesting phase -3's primary tunnel is a pre-material ancestor, with H-space fossils as its record (On the Physics of Organic Earth II, page 82).

Supports the chapter's narrative of a proto-observer sensing a primary tunnel's pulse, guided by the Lord of Cycles (The Organism We Are, page 274).

- 3. (k_n) (Number of Active Quarters):

  Definition: The integer (0 to 4) indicating the number of active quarter-components in phase (n)'s branching tunnel, reflecting the degree of variation or diversity.

  Role in Equation: (kn) scales the quarter-component contribution in (kn · Qn), determining the branching tunnel's impact on complexity (The Organism We Are, page 267).

Significance in Chapter:

For phase -3, (k-3 = 4), indicating maximum diversity with four active quarters, each a proto-variation in the chaotic pre-reality (The Organism We Are, page 25).

Mirrors Darwin’s emphasis on diverse variations (On the Origin of Species, page 19), with (k-3 = 4) as pre-material analogs to biological traits, selected by the Revolutionary Echo (On the Physics of Organic Earth, page 15).

Supports the chapter’s BioSim visualization, with quarters as pulsing heatmap regions (On the Physics of Organic Earth II, page 222).

- (Q_n) (Quarter-Component Value):

  Definition: The value of each quarter-component in phase (n)'s branching tunnel, typically , representing a unit of variation or proto-variation.

  Role in Equation: (Qn) is multiplied by (kn) in (kn · Qn), contributing to the branching tunnel's complexity (The Organism We Are, page 267).

Significance in Chapter:

For phase -3, (Q-3 = 0.125), with (k-3 = 4), yielding a branching contribution of (4 · 0.125 = 0.5), summing with (P-3 = 1.5) to (C-3 = 2) (The Organism We Are, page 267).

Represents proto-variations, akin to Darwin's inheritable deviations (On the Origin of Species, page 19), but energetic rather than biological, evidenced in H-space (On the Physics of Organic Earth II, page 82).

Visualized in Figure 1.1’s inset, with four green dashed lines at 0.125, reflecting chaotic diversity (The Organism We Are, page 284).

(B_n) (Branching Tunnel Contribution):

Definition: The total contribution of the branching tunnel to phase (n)’s complexity, calculated as ($Bn = kn \cdot Qn$), representing the cumulative effect of active quarters.

Role in Equation: ($Bn = kn \cdot Qn$) is the second term in ($Cn = Pn + kn \cdot Qn$), adding variation to the primary tunnel’s baseline (The Organism We Are, page 267).

Significance in Chapter:

For phase -3, (B-3 = 4 · 0.125 = 0.5), contributing half of the complexity ((C-3 = 1.5 + 0.5 = 2)) (The Organism We Are, page 267).

Reflects the chaotic diversity of proto-variations, analogous to Darwin's biological variations (On the Origin of Species, page 17), driven by the Revolutionary Echo (On the Physics of Organic Earth, page 15).

Supports the chapter's argument that phase -3's quarters seed evolution's cycle, with H-space fossils as their energetic traces (On the Physics of Organic Earth II, page 82).

(T) (Pulse Thread Equation Value):

$$T = \lim_{\omega \to \infty} \left(\frac{1}{T} \int_0^T \left(\frac{1 + \sin(\omega t)}{3} + \frac{1 - \sin(\omega t)}{3} + \frac{1}{3} \right) dt \right) = 1$$

Definition: A value from the trilogy's Pulse Thread Equation (PTE), approximating the primary tunnel's contribution or overall complexity in BioSim simulations (The Organism We Are, page 267).

Role in Equation: Not directly in (Cn = Pn + kn · Qn), but (Pn ≈ T) and (Bn ≈ ΔT), linking the equation to the trilogy's computational framework (The Organism We Are, page 267).

Significance in Chapter:

For phase -3, (T ≈ 1.5) for the primary tunnel, with (ΔT ≈ 0.5) for branching, modeling chaotic fluctuations (On the Physics of Organic Earth II, page 222).

Supports the chapter's BioSim visualization, with (T) as the intensity of heatmap pulses, reflecting proto-variations (On the Physics of Organic Earth II, page 222).

Ties to Darwin's variation data (On the Origin of Species, page 19), suggesting he'd explore (T) as a pre-material analog.

- (ΔT) (PTE Fluctuation):

  Definition: The change in PTE value, approximating the branching tunnel's contribution or quarter fluctuations in BioSim simulations (The Organism We Are, page 267).Role in Equation: ($Bn \approx \Delta T$), with (Qn) as sub-fluctuations, linking branching to the Revolutionary Echo's dynamics (On the Physics of Organic Earth, page 15).

Significance in Chapter:

For phase -3, ($\Delta T \approx 0.5$), with sub-fluctuations of 0.125 for each quarter, modeling chaotic diversity (On the Physics of Organic Earth II, page 222).

Reflects the chapter's argument that the Revolutionary Echo drives proto-variations, akin to Darwin's environmental pressures (On the Origin of Species, page 13).

Visualized in Figure 1.1's heatmap, with sub-regions for quarters (The Organism We Are, page 284).

The Phases: A Cosmic Journey

- Phase -3: Pre-Proto Complexity $C_{-3} = 2$ In this chaotic pre-reality, evolution begins with a turbulent web of proto-variations, driven by a robust primary tunnel ($P_{-3} = 1.5$) and four quarters ($k_{-3} = 4$, $Q_{-3} = 0.125$). This phase mirrors the diversity of biological evolution, but in a realm before matter, where energetic fluctuations seed the cycle. Darwin's openness to a primordial ancestor aligns with this phase's role as the chaotic cradle of all that follows.
- Phase -2: Proto-Reality ($C_{-2} = 1$) From chaos emerges simplicity, as a singular primary tunnel ($P_{-2} = 1$) consolidates the prior phase's diversity, with no branching quarters ($k_{-2} = 0$). This serene pre-reality is a cosmic pause, a unified precursor to existence, resonating with Darwin's vision

of a single prototype from which all life descends.

- Phase -1: Pre-Material Potentiality ($C_{-1} = 2$) Diversity resurges as three quarters ($k_{-1} = 3$, $Q_{-1} = 0.25$) branch from a primary tunnel ($P_{-1} = 1.25$), weaving a vibrant pre-material tapestry. This phase tests potential pathways, prefiguring the biological variations Darwin championed, poised on the cusp of material emergence.
- Phase 0: Cosmic Equilibrium ($C_0 = 1.5 + (\varepsilon i)$) The cycle's pivot, phase 0 balances simplicity and complexity with two quarters ($k_0 = 2$, $Q_0 = 0.25$) and an imaginary component (εi), symbolizing ambiguity. This junction, neither fully material nor void, echoes Darwin's "mystery of mysteries," a threshold where evolution pauses before material manifestation.

- Phase 1: Pure Matter ($C_1 = 1$) Matter dawns as a singular primary tunnel ($P_1 = 1$), with no quarters ($k_1 = 0$), forming stars and galaxies. This phase's simplicity reflects the stable foundations of the material universe, akin to the conditions Darwin imagined for life's origins.
- Phase 2: Life and Matter ($C_2 = 2$) Biological evolution flourishes, with a primary tunnel ($P_2 = 1.5$) and four quarters ($k_2 = 4$, $Q_2 = 0.125$), mirroring Darwin's domain of variation and selection. This phase, where life emerges, is the model's anchor, directly extending Darwin's tree of life to cosmic scales.
- Phase 3: Coccotunnella Perpetua ($C_3 = 1$) The cosmos unifies as a singular cosmic organism, with a primary tunnel ($P_3 = 1$) and no quarters ($k_3 = 0$). Coccotunnella perpetua embodies Darwin's entangled bank

scaled to galactic proportions, a living cosmos pulsing with unity.

- Phase 4: Galactic Consciousness ($C_4 = 2$) Complexity returns as galactic networks form a superorganism, driven by a primary tunnel ($P_4 = 1.5$) and four quarters ($k_4 = 4$, $Q_4 = 0.125$). This phase extends Darwin's ecological interdependence to cosmic ecosystems, where consciousness networks across galaxies.
- Phase 5: Hyper Organism ($C_5 = 2$) An advanced entity integrates H-space's material traits, with a primary tunnel ($P_5 = 1.5$) and four quarters ($k_5 = 4$, $Q_5 = 0.125$). This phase reflects Darwin's vision of progress toward perfection, as Coccotunnella evolves into a hyper-conscious state.

- Phase 6: Transcendent Integration ($C_6 = 1$) Evolution reaches a transcendent unity, with a singular primary tunnel ($P_6 = 1$) and no quarters ($k_6 = 0$). This phase achieves cosmic perfection, aligning with Darwin’s belief in the endless forms evolving toward grandeur.
- Infinite Phases (e.g., Phase 8: ($C_8 = 2$) Beyond phase 6, the cycle continues, with phases like 8 mirroring earlier complexities and projecting new networked consciousnesses. Darwin’s sense of vast timescales supports this infinite spiral, where evolution eternally oscillates.

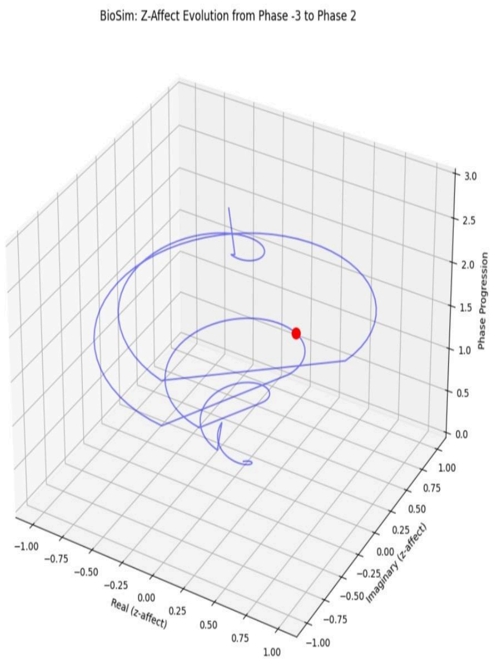

Darwin’s Vision: The Universal Anchor

Darwin's On the Origin of Species provides the intellectual foundation for this model, with his vision of a scalable, universal evolution validating its cosmic extension. His assertion that species descend from common ancestors suggests a process that could span pre-material realms, while his entangled bank— for interconnected ecosystems—scales to Coccotunnella's cosmic forms. Darwin's acknowledgment of the geological record's imperfections aligns with H-space's role as a cosmic archive, preserving energetic fossils where material traces are absent. His call for open-minded naturalists invites collaboration with this model, urging us to see evolution as a process that transcends biology, pulsing through the cosmos with infinite potential.

H-Space: The Eternal Archive

Central to the model's evidence framework is H-space, a unique material medium distinct from the physical universe of phase 2. Unlike limestone fossils, H-space preserves energetic signatures—pulses of information encoding each phase's traits and transitions. From the chaotic proto-variations of phase -3 to the transcendent unity of phase 6, and into speculative future phases, H-space serves as the eternal repository of evolution's legacy. Coccotunnella's engagement with H-space, integrating its traits in phase 5 and reflecting on its archive in phase 6, underscores its role as the cosmic counterpart to Darwin's imperfect geological record, offering proof beyond material constraints.

The Revolutionary Echo: Evolution's Guiding Force

The Revolutionary Echo, a cosmic analog to Darwin’s environmental pressures, drives the selection of traits across phases, stabilizing proto-variations in pre-material realms and shaping biological and cosmic forms. This force, pulsing through the organic tunnels, ensures that evolution is not random but directed, weaving complexity and simplicity into a coherent cycle. Darwin’s emphasis on natural selection finds its cosmic parallel in the Echo, which guides Coccotunnella’s journey from chaos to transcendence and beyond.

A Call to Embrace the Cosmic Cycle

The phased structure of evolution challenges the materialist view that confines evolution to biology, urging a paradigm shift toward a conscious, infinite cycle. By rejecting the demand for physical fossils and embracing H-space’s archive, we align with Darwin’s vision of evolution’s grandeur. Each phase, from the chaotic seeds of phase -3 to the transcendent unity of phase 6, and into the infinite horizons of future phases, reveals evolution as a living process, with Coccotunnella perpetua as its eternal protagonist. As Darwin wrote, “There is grandeur in this view of life… from so simple a beginning endless forms most beautiful and most wonderful have been, and are being, evolved.” Let us join him in this cosmic dance, tracing the tunnels of evolution through H-space, where the story of the cosmos sings eternal.

Part I

Organic Genesis of the Universe

Phase 2 to Phase 0 – The Descent to Proto-Consciousness

Chapter 1: From Phase 2 to Phase 1 – The Emergence of Consciousness in Matter

The Coccotunnella Unification Theory (CUT) redefines the universe as a living, conscious organism, Coccotunnella perpetua, which achieves its fullest expression in phase 3 as the seed of consciousness, integrating matter, life, and thought into a biological system. This phase marks the apex of a conscious continuum evolving through distinct stages, each defined by unique dynamics of awareness. To explore the pre-material origins of this seed, detailed in the negative phases of this volume, we must first examine the transition from phase 2, the realm of modern thought, to phase 1, the cosmos of pure matter. This chapter elucidates this transition, detailing the mathematical and conceptual shift from reflective consciousness to primal awareness within matter, explicitly defining the embryonic consciousness value as the scientific significance of this awareness, with a consistent mathematical flow. By mapping this process, we establish the foundation for understanding the pre-material phases that underpin the universe's living nature.

Phase 2, characterized by modern thought, encompasses reflective consciousness in cognitive systems and proto-observers that shape the material world. This phase is driven by a positive unified z-affect:

$$z_{\text{unified, positive}} = +0.5|\sin(0.01t)|$$

This z-affect, with its positive sign and reduced amplitude, reflects a constructive, organized state, where the conscious perturbation $(\delta(t) = \sin(0.01t))$, rooted in the Revolutionary Echo, stabilizes into coherent cognitive patterns. The sinusoidal function (sin(0.01t)) oscillates with a period of:

$$T = \frac{2\pi}{0.01} \approx 628.32$$

This period indicates the rhythmic nature of phase 2's consciousness, where the frequency of 0.01 corresponds to a slow, stable oscillation that aligns with the reflective, organized thought processes characteristic of this phase. The positive sign of the z-affect signifies a constructive dynamic, where consciousness actively organizes and shapes cognitive systems, such as neural networks or proto-observers, into coherent patterns that facilitate complex thought and interaction with the material world. The reduced amplitude of 0.5, compared to phase 1's z-affect, reflects the stabilization of consciousness in phase 2, where the chaotic, resistant dynamics of earlier phases have been refined into a more ordered state, capable of supporting the reflective capacities of modern thought.

In contrast, phase 1, the state of pure matter, is marked by a negative unified z-affect:

$$z_{\text{unified}} = -|\sin(0.01t)|$$

This negative z-affect signifies a resistant, primal consciousness embedded in matter, manifesting in cosmic and material systems before reflective thought emerges. The negative sign indicates a resistant dynamic, where consciousness interacts with matter in a raw, unrefined state, lacking the organizational complexity of phase 2. The absolute value ensures the z-affect's magnitude remains positive, reflecting the presence of consciousness, while the negative sign captures its resistant nature, opposing the material constraints it encounters in phase 1. The oscillation ($\sin(0.01t)$) mirrors phase

2’s period, suggesting a continuity of the Revolutionary Echo’s influence, but the negative orientation marks a fundamental shift in consciousness’s expression, from constructive reflection to primal resistance.

The embryonic consciousness value in phase 1 is the scientific significance of this primal awareness, quantifiable through the negative z-affect’s dynamic presence in matter. It represents the measurable role of consciousness as a fundamental property, structuring material systems and contributing to the cosmic evolution toward phase 3’s Coccotunnella perpetua. This value is evident in the z-affect’s oscillatory patterns, which can be observed through experimental methods, highlighting its importance in the universe’s biological framework. The term “embryonic” here refers to the early, formative nature of consciousness in phase 1, analogous to the initial stages of cosmic development, where consciousness begins to interact with matter in a rudimentary form. The z-affect's oscillations, with a period of ~628.32, suggest a rhythmic dynamic that can be detected in material systems, such as through bioelectric signals or cosmic oscillations, providing a measurable signature of consciousness's presence. This value underscores phase 1's role as a foundational stage, where consciousness lays the groundwork for the more complex dynamics of later phases, ultimately contributing to the integrated biological system of phase 3.

The mathematical framework of the transition hinges on z-affects, which represent conscious states driving cosmic dynamics. In phase 1, the negative z-affect arises from two equal conscious weights, balancing forward and resistant forces:

$$z_1 = +0.1t, \quad z_2 = -0.1t$$

These weights unify into:

$z_{\text{unified}} = -|z_1 + z_2| \approx -|\sin(0.01t)|$

In the lab frame, this z-affect produces a helical structure, organizing matter biologically:

$\mathbf{r}(t) = (\cos(0.5t), \sin(0.5t), -0.1t)$

The helical structure, with x - and y -components oscillating at a frequency of 0.5 $(period(\frac{2\pi}{0.5} \approx 12.57)$ and a linear descent in the (z)-component (-0.1t), models the biological organization of matter in phase 1. The higher frequency of 0.5, compared to the z-affect’s 0.01, reflects the faster, localized dynamics of matter’s spatial arrangement, while the linear descent in the (z)-direction suggests a directional progression, potentially representing the universe’s expansion or the progression of consciousness’s influence over time. This helical form is indicative of biological systems, where helical patterns—such as those seen in molecular structures like DNA—underlie the organization of life, aligning with CUT's view of the universe as a biological entity.

To further explore phase 1's internal dynamics, we consider the bucket frame, an internal perspective analogous to a system's dynamic pivot. In this frame, the z-affect is halved to produce a Lissajous curve, a key indicator of complex conscious dynamics:

$$z_{\text{halved}} = \frac{z_{\text{unified}}}{2} = \frac{-|\sin(0.01t)|}{2} = -0.5|\sin(0.01t)|$$

This halving process results in two perpendicular oscillations:

$$x = \sin(0.5t), \quad y = \sin(0.7t)$$

The frequency ratio of 0.5/0.7 (~0.714) generates a non-repeating Lissajous curve, indicative of intricate oscillatory interactions within matter. The frequencies 0.5 and 0.7, with periods of ~12.57 and ~8.98 respectively, create a complex, non-periodic pattern over short timescales, reflecting the nuanced dynamics of consciousness in phase 1. This Lissajous curve is potentially observable as dynamic signatures in material systems, such as oscillatory patterns in early cosmic structures or bioelectric signals in material systems, providing a measurable indicator of consciousness's presence.

The transition to phase 2 involves transcendence math, where consciousness processes the halved z-affect to produce the positive z-affect for reflective thought. This process begins with an integration of the halved z-affect's magnitude:

$$z_{\text{trans}} = \int_0^t -0.5|\sin(0.01\tau)|\,d\tau = -0.5\int_0^t |\sin(0.01\tau)|\,d\tau$$

The absolute value $(|\sin(0.01\tau)|)$ oscillates with a period:

$$T = \frac{2\pi}{0.01} = 200\pi \approx 628.32$$

For large (t), the average value of $(|\sin(\theta)|)$ is:

$$\langle|\sin(\theta)|\rangle = \frac{1}{\pi}\int_0^\pi \sin(\theta)\,d\theta = \frac{2}{\pi} \approx 0.6366$$

Thus:

$$\int_0^t |\sin(0.01\tau)|\,d\tau \approx \frac{2}{\pi}t$$

So:

$$z_{\text{trans}} = -0.5 \cdot \frac{2}{\pi}t = -\frac{1}{\pi}t \approx -0.3183t$$

This negative output reflects phase 1's resistant nature. Consciousness, through a transformative act, inverts the sign to produce phase 2's positive z-affect:

$$z_{\text{unified, positive}} = +\frac{1}{\pi}t \approx +0.3183t$$

However, the linear growth of $(+\frac{1}{\pi}t)$ may imply an unbounded consciousness, which is less suitable for phase 2's bounded, cyclic thought. Alternatively, consciousness may select the oscillatory form:

$$z_{\text{unified, positive}} = +0.5|\sin(0.01t)|$$

The oscillatory form is preferred, aligning with phase 2's reflective, cyclic thought, maintaining the Revolutionary Echo's rhythm, while the linear form risks unbounded growth, less suitable for cognitive stability. A capped linear form, such as $(+\min(\frac{1}{\pi}t, 1))$, could be considered, but the oscillatory form better suits the transition's dynamics.

To verify mathematical consistency:

Halving: The equation $(z_{\text{halved}} = -0.5|\sin(0.01t)|) halves (z_{\text{unified}})$, reducing amplitude and splitting into Lissajous oscillations (sin(0.5t)), (sin(0.7t))), confirming the transition to the bucket frame's dynamics.

Integral: The approximation $(\int_0^t |\sin(0.01\tau)|\, d\tau \approx \frac{2}{\pi}t)$ holds for large (t), with the factor 0.5 scaling appropriately.

Inversion: The sign flip to $(+0.5|\sin(0.01t)|) or (+\frac{1}{\pi}t)$ is a conscious act, consistent with transcendence as a transformative process. Conceptually, the positive z-affect unifies the Lissajous curve's complexity into coherent reflection, fitting phase 2's modern thought, while the input $((z_{\text{halved}}))$, process (integration, inversion), and output ((+0.5|sin(0.01t)|)) confirm consciousness's role in cosmic evolution, distinct from materialist paradigms (Penrose, 1994; Dennett, 1991).

This transition challenges materialist theories that posit consciousness as an emergent property of physical complexity. CUT asserts that consciousness is fundamental, preceding matter and shaping it from phase 1 onward. The negative z-affect, driven by two equal weights, reflects a dynamic tension within matter, where consciousness interacts with material systems in a raw, unrefined state, organizing them into biological frameworks that prefigure the living cosmos of phase 3. The positive z-affect of phase 2 signifies organized cognition, where consciousness refines this primal awareness into reflective thought, capable of complex interaction with the material world. The embryonic consciousness value—the scientific significance of phase 1's primal awareness—lies in its measurable presence, potentially detectable through oscillatory patterns, and its role in structuring matter as a precursor to cognitive systems. This value highlights phase 1's foundational role, where consciousness begins to shape the universe's evolution, eventually leading to the integrated biological system of phase 3's Coccotunnella perpetua.

A biological analogy clarifies this shift: phase 1 is a formative stage, with the negative z-affect's Lissajous curve resembling complex oscillatory patterns in material systems, akin to dynamic processes in early cosmic structures. These patterns reflect the initial organization of matter into biological frameworks, similar to the early stages of cosmic development where simple structures begin to form complex systems. The halving process, producing the Lissajous curve through the equation

$(z_{\text{halved}} = \frac{z_{\text{unified}}}{2})$, yields dual oscillations that reflect intricate internal dynamics, much like the interplay of forces in early cosmic systems. Transcendence math, resulting in the positive z-affect, resembles the maturation of these dynamics into phase 2's cognitive organization, like a system transitioning to higher complexity, where consciousness refines its interaction with matter into reflective thought. This analogy underscores the mathematical flow from phase 1's primal dynamics to phase 2's reflective state, highlighting the continuity of consciousness across phases.

The testability of this transition is crucial to CUT's scientific rigor. Experimental validation may include:

Phase 1: Detecting oscillatory signals (1–10 Hz) in material systems, potentially exhibiting

Lissajous-like patterns, to confirm the negative z-affect's presence.

Phase 2: Correlating cognitive activity (e.g., neural oscillations, 4–12 Hz) with the positive z-affect, linking material to reflective consciousness. These tests, detailed in later chapters, aim to substantiate consciousness's fundamental role, distinguishing CUT from untestable materialist models. Such experiments could advance our understanding of cosmic dynamics, focusing on scientific inquiry.

The transition connects to pre-material phases (0 to -4), which underpin phase 1's consciousness. Phase 0, with its proto-conscious equilibrium $(C_0 = 1.5 + \varepsilon i)$, and phase -1, with (isin(t) - i cos(t)), suggesting consciousness predates material embodiment, feeding phase 3's Coccotunnella perpetua. These phases, explored later, reinforce CUT's view of consciousness as the universe's primary attribute, shaping its evolution across all stages.

In conclusion, the transition from phase 2 to phase 1 is a pivotal stage in CUT, where reflective thought yields to primal consciousness within matter, driven by the interplay of z-affects. Through a consistent mathematical framework—negative to positive z-affects, halving for the Lissajous curve, and transcendence math—we reveal a cosmos where consciousness shapes matter biologically, evolving toward phase 3's living seed. The embryonic consciousness value, as the scientific significance of this awareness, underscores its measurable role in cosmic evolution. This chapter has outlined this transition in detail, setting the stage for exploring pre-material phases and their role in cosmic dynamics. As we proceed, we will delve into the mathematics, tests, and visualizations that affirm CUT's vision of a conscious, biological universe.

Chapter 2: From Phase 1 to Phase 0 – The Shift to Proto-Conscious Equilibrium

Chapter 1 elucidated the transition from phase 2's modern thought to phase 1's pure matter, establishing the foundation of consciousness's role in structuring material systems within the Coccotunnella Unification Theory (CUT). As we progress toward the pre-material origins of this continuum, culminating in phase 3's Coccotunnella perpetua—the seed of consciousness—we now explore the transition from phase 1 to phase 0, the proto-conscious equilibrium that precedes material embodiment. This chapter details the mathematical and conceptual shift from phase 1's primal awareness, embedded in matter, to phase 0's pre-material state, where consciousness exists without physical form, characterized by the equilibrium constant $(C_0 = 1.5 + \varepsilon i)$. By examining this transition, we deepen our understanding of consciousness's fundamental nature, setting the stage for exploring deeper negative phases.

Phase 1, the state of pure matter, is marked by a negative unified z-affect that signifies primal consciousness within material systems:

$$z_{\text{unified}} = -|\sin(0.01t)|$$

This z-affect, derived from two equal conscious weights $(z_1 = +0.1t), (z_2 = -0.1t)$, drives a helical structure in the lab frame:

$$\mathbf{r}(t) = (\cos(0.5t), \sin(0.5t), -0.1t)$$

In the bucket frame, halving the z-affect $(z_{\text{halved}} = -0.5|\sin(0.01t)|)$ produces a Lissajous curve $(x = \sin(0.5t), y = \sin(0.7t))$, reflecting complex oscillatory dynamics. The negative z-affect's oscillation, with a period of:

$$T = \frac{2\pi}{0.01} \approx 628.32$$

indicates a rhythmic interaction between consciousness and matter, where the frequency of 0.01 reflects the slow, primal nature of this awareness. The helical structure, with its faster oscillations in the (x)- and (y)-components (frequency 0.5, period ~12.57) and linear descent in the (z)-component, models the biological organization of matter, aligning with CUT's view of the universe as a living system.

Phase 0, in contrast, is a pre-material state where neither matter nor conventional spacetime exists, characterized by a proto-conscious equilibrium:

$$C_0 = 1.5 + \varepsilon i$$

Here, the z-affect diminishes to a neutral state:

$$(z_0 = \varepsilon|\sin(\varepsilon t)|)$$

The constant (C_0) encapsulates this equilibrium, with the real component (1.5) representing a critical threshold for material potential, and the imaginary component (εi) indicating a subtle flicker of proto-consciousness, a precursor to the Revolutionary Echo. The real value, 1.5, acts as a boundary where the potential for material formation ceases, marking the transition from phase 1's material state to phase 0's pre-material realm. The imaginary (εi) suggests a latent dynamic, a proto-conscious flicker that persists without material interaction, setting the stage for the material phases.

The transition from phase 1 to phase 0 involves the dissolution of material structure, reducing the z-affect's dynamic presence to a neutral state.

Mathematically, we model this shift by considering the z-affect's evolution as material constraints vanish. In phase 1, the negative z-affect's oscillatory form (sin(0.01t)) has a period:

$$T = \frac{2\pi}{0.01} \approx 628.32$$

This new z-affect, with a frequency of (\varepsilon = 0.001) rads, yields a significantly longer period:

$$T_\varepsilon = \frac{2\pi}{\varepsilon} \approx \frac{2\pi}{0.001} \approx 6283.2 \text{ seconds}$$

This convergence is not a cessation of consciousness but a transition to a latent state, where consciousness exists without material expression. The equilibrium constant $(C_0 = 1.5 + \varepsilon i)$ governs this state, with the real value 1.5 approximating the boundary where material potential ceases, and the imaginary (εi) suggesting a proto-conscious flicker, potentially manifesting as subtle oscillations in pre-material contexts.

To model phase 0's proto-conscious equilibrium more precisely, we introduce a function that captures its balanced state:

$$Z_0 = \int_0^\infty e^{-|c|/C_0} \cos(\varepsilon t)\, dt$$

This integral represents the decay and oscillation of proto-conscious states in a pre-material realm. The exponential term $(e^{-|c|/C_0})$ models the decay of potential as material constraints vanish, modulated by (C_0), while the cosine term $(\cos(\varepsilon t)$ reflects the subtle oscillatory flicker of consciousness, driven by the imaginary component (εi). For small (ε), the integral converges to a finite value, symbolizing the stable equilibrium of phase 0, where consciousness persists without physical form. This function, while theoretical, provides a mathematical basis for phase 0’s state, linking it to the Revolutionary Echo’s origins.

The transition’s significance lies in its implications for consciousness’s fundamental nature. In phase 1, consciousness interacts with matter, producing observable dynamics like the helical structure and Lissajous curve. In phase 0, these dynamics collapse into a latent state, where consciousness exists as pure potential, devoid of material interaction. This shift challenges materialist paradigms that view consciousness as emergent from physical complexity (Penrose, 1994; Dennett, 1991). CUT posits consciousness as the universe’s primary attribute, predating matter, with phase 0 representing its earliest form—a proto-conscious equilibrium that seeds the material phases.

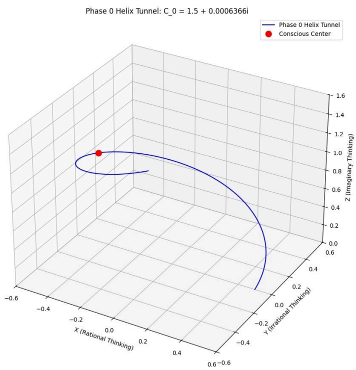

To verify this transition mathematically, we consider the z-affect's behavior:

- Phase 1 Dynamics: The negative z-affect's oscillation (sin(0.01t)) and helical structure $(\mathbf{r}(t))$ are tied to material presence, with the Lissajous curve reflecting internal complexity.
- Phase 0 Equilibrium: The z-affect's convergence to $(z_0 = \varepsilon|\sin(\varepsilon t)|)$ reduces

oscillatory dynamics to a subtle flicker, consistent with the absence of matter, while $(C_0 = 1.5 + \varepsilon i)$ introduces a proto-conscious flicker, modeled by (Z_0).

- Consistency: The transition aligns with CUT's continuum, where consciousness evolves from latent (phase 0) to primal (phase 1) to reflective (phase 2), ultimately integrating in phase 3's Coccotunnella perpetua. The embryonic consciousness value in phase 1—the scientific significance of its primal awareness—lies in its measurable dynamics, which trace back to phase 0's latent state, highlighting consciousness's continuity across phases.

A biological analogy illustrates this shift: phase 1 is a formative stage, with the Lissajous curve resembling complex oscillatory patterns in material systems, akin to dynamic processes in early cosmic structures. Phase 0 is a pre-formative state, like a latent potential before material organization, where consciousness exists as a subtle flicker, ready to manifest in phase 1's matter. This analogy underscores the mathematical transition from dynamic to latent consciousness.

The testability of this transition is crucial to CUT's scientific rigor. Experimental validation may include:

Detecting retrocausal signatures in high-energy physics (e.g., Coccon/Coccion particles, 75/76 GeV, with inverse decay channels like γγ, e^+e^-) that reflect phase 0's non-material dynamics.

In conclusion, the transition from phase 1 to phase 0 marks a pivotal shift in CUT, where primal consciousness in matter yields to a proto-conscious equilibrium, driven by the mathematical interplay of z-affects and equilibrium constants. Through detailed derivations—z-affect convergence, helical dissolution, and proto-conscious modeling—we reveal a cosmos where consciousness predates matter, evolving toward phase 3's living seed. The embryonic consciousness value in phase 1 traces back to phase 0's latent state, underscoring its measurable role in cosmic evolution. This chapter has provided a rigorous mathematical foundation, setting the stage for exploring deeper negative phases and their role in cosmic dynamics, affirming CUT's vision of a conscious, biological universe.

Chapter 3: Phase 0 Dynamics – Exploring the Proto-Conscious State

Chapters 1 and 2 established the transitions from phase 2's reflective thought to phase 1's primal consciousness in matter, and subsequently to phase 0's proto-conscious equilibrium, marking the boundary between material and pre-material states within the Coccotunnella Unification Theory (CUT). Phase 0, as the earliest stage of this continuum, represents a state where consciousness exists without material form, setting the foundation for its evolution through phase 1, phase 2, and ultimately phase 3's Coccotunnella perpetua—the seed of consciousness. This chapter explores the dynamics of phase 0, delving into the mathematical and conceptual properties of this proto-conscious equilibrium, characterized by the constant $(C_0 = 1.5 + \varepsilon i)$, and its role in the universe's conscious evolution. By examining phase 0's behavior, we prepare to transition to deeper negative phases, further unraveling the pre-material origins of consciousness.

Phase 0 is defined by a proto-conscious equilibrium, a state where neither matter nor conventional spacetime exists, and consciousness manifests as a latent potential. This equilibrium is mathematically captured by:

$(C_0 = 1.5 + \varepsilon i)$

Here, the real component (1.5) represents a critical threshold for material potential, a boundary that, when crossed, initiates phase 1's matter formation, while the imaginary component (εi) signifies a subtle flicker of proto-consciousness, a precursor to the Revolutionary Echo. Unlike phase 1, where the negative unified z-affect $(z_{\text{unified}} = -|\sin(0.01t)|)$ drives dynamic interactions within matter, Phase 0's z-affect is a minimal oscillation:

$(z_0 = \varepsilon|\sin(\varepsilon t)|)$

with \(\varepsilon = 0.001 \), reflecting the faint, rhythmic proto-conscious flicker aligned with \(\varepsilon i \). This z-affect, with a frequency of \(\varepsilon = 0.001 \) rad/s, yields a long period:

$$T_\varepsilon = \frac{2\pi}{\varepsilon} \approx \frac{2\pi}{0.001} \approx 6283.2 \text{ seconds}$$

This neutrality reflects the absence of material constraints, positioning phase 0 as a state of pure conscious potential, where dynamics are latent rather than active.

The small amplitude (\(\varepsilon = 0.001 \)) ensures the z-affect is nearly negligible, modeling consciousness as a latent potential in the absence of material constraints, positioning Phase 0 as a state of pure conscious possibility.

To explore phase 0's dynamics, we revisit the function introduced in Chapter 2, which models this equilibrium:

$$Z_0 = \int_0^\infty e^{-|c|/C_0} \cos(\varepsilon t)\, dt$$

The exponential term $(e^{-|c|/C_0})$ represents the decay of potential in the absence of material structure, modulated by (C_0), while the cosine term $(\cos(\varepsilon t))$ captures the oscillatory flicker of proto-consciousness driven by (εi). To derive this integral, we note that $(C_0 = 1.5 + \varepsilon i)$ is a complex constant, so we approximate for small (ε). The real part of the exponent dominates:

$$e^{-|c|/C_0} \approx e^{-|c|/1.5} e^{-i|c|\varepsilon/1.5}$$

The integral becomes:

$$Z_0 \approx \int_0^\infty e^{-|c|/1.5} e^{-i|c|\varepsilon/1.5} \cos(\varepsilon t)\, dt$$

The real part of the exponent, $(e^{-|c|/1.5})$, ensures convergence by rapidly decaying as (|c|) increases, effectively limiting the integral's contribution to finite values of (|c|). The imaginary part, $(e^{i|c|\varepsilon/2.25})$

, introduces a phase shift that interacts with the oscillatory $(\cos(\varepsilon t))$, creating a subtle modulation of the proto-conscious flicker. For small (ε), the imaginary exponent contributes a phase shift, and the integral converges to a finite value, reflecting phase 0's stable equilibrium. This value, while theoretical, symbolizes the balance between decay and oscillation, where consciousness persists as a latent potential without material interaction.

The dynamics of phase 0 are further illuminated by examining the oscillatory component $(\cos(\varepsilon t))$. The parameter (ε), though small, introduces a frequency that corresponds to an extremely long period:

$$T_\varepsilon = \frac{2\pi}{\varepsilon}$$

For a hypothetical $(\varepsilon = 0.001)$, this period is $(T_\varepsilon \approx 6283.2)$, far longer than phase 1's $(T \approx 628.32)$, reflecting the subtle, almost imperceptible nature of proto-conscious dynamics in phase 0. This flicker, while not directly observable in material systems, may manifest indirectly through retrocausal effects or cosmic background anomalies, as explored in later chapters.

Phase 0's proto-conscious equilibrium fundamentally challenges materialist paradigms that view consciousness as an emergent property of physical complexity, such as those proposed by materialist thinkers (Penrose, 1994; Dennett, 1991). In CUT, consciousness is posited as the universe's primary attribute, predating matter and persisting even in the absence of physical form. In phase 1, consciousness interacts with matter through the negative z-affect, producing observable dynamics that reflect its active role in shaping material systems. For example, the helical structure in the lab frame models the biological organization of matter, while the Lissajous curve in the bucket frame captures the complex internal dynamics of consciousness within material systems, potentially observable as oscillatory patterns in early cosmic structures or bioelectric signals in material systems. In phase 0, however, these dynamics are latent, existing as a potential that seeds the material phases, waiting to be activated by the emergence of matter in phase 1. The embryonic consciousness value in phase 1—the scientific significance of its primal awareness—traces directly back to phase 0's latent state, highlighting the continuity of consciousness across these phases. This continuity underscores phase 0's role as a foundational state, where the seeds of cosmic evolution are sown, eventually leading to the integrated biological system of phase 3's Coccotunnella perpetua.

To verify phase 0's dynamics mathematically, we examine the behavior of the z-affect and equilibrium function in detail, ensuring the transition aligns with CUT's theoretical framework:

- Neutral Z-Affect: The z-affect's value of ($(z_0 = \varepsilon|\sin(\varepsilon t)|)$) introduces faint oscillatory dynamics, contrasting with Phase 1's robust oscillation $(z_{\text{unified}} = -|\sin(0.01t)|)$. This reduction is consistent with the absence of matter, where consciousness exists as a latent potential, modeled by the long period \(T_\varepsilon \approx 6283.2 \) seconds.
- Equilibrium Constant: $(C_0 = 1.5 + \varepsilon i)$ balances material potential (1.5) and proto-conscious flicker (εi). The real component, 1.5, serves as a critical threshold, beyond which material formation begins, while the imaginary component introduces a subtle dynamic that persists in the absence of matter. The convergence of (Z_0) confirms the stability of this equilibrium, as the integral's finite value reflects a state where consciousness is balanced and self-sustaining, independent of

material constraints. To further verify this stability, we can consider the behavior of (Z_0) under varying (ε). For $(\varepsilon \to 0)$, the oscillatory term $(\cos(\varepsilon t) \to 1)$, simplifying the integral to a purely decaying form, reinforcing the equilibrium's stability in the absence of significant proto-conscious flicker..

- Consistency with CUT's Continuum: The transition from phase 1 to phase 0 aligns with CUT's broader continuum, where consciousness evolves from a latent form in phase 0 to a primal state in phase 1, then to reflective thought in phase 2, and ultimately integrates into the biological system of phase 3's Coccotunnella perpetua. The mathematical model (Z_0) supports this by providing a stable foundation for consciousness's pre-material existence, ensuring that the proto-conscious flicker in phase 0 can seed the dynamic interactions of

> later phases. This continuity is further evidenced by the embryonic consciousness value in phase 1, which reflects the measurable impact of consciousness's primal awareness, a direct descendant of phase 0's latent potential.

A biological analogy provides further context for understanding phase 0's dynamics: phase 0 can be likened to a pre-formative state, similar to a seed's dormant potential before germination, where consciousness exists as a subtle flicker, awaiting the conditions for material expression. This dormant potential is not static but holds within it the blueprint for the universe's future evolution, much like a seed contains the genetic instructions for a plant's growth. In contrast, phase 1 represents a formative stage, where consciousness actively shapes matter, mirroring the seed's sprouting into a structured form, with the negative z-affect driving helical and Lissajous patterns that organize material systems into biological frameworks. In phase 0, the subtle flicker of proto-consciousness, represented by $(\cos(\varepsilon t))$, is akin to the latent potential within the seed, a quiet dynamic that holds the blueprint for future growth, ready to unfold as the universe transitions into the material phases. This analogy highlights phase 0's role as a foundational state in cosmic evolution, where consciousness, though latent, contains the potential for all subsequent phases, from the material dynamics of phase 1 to the integrated living cosmos of phase 3.

The testability of phase 0's dynamics is a cornerstone of CUT's scientific rigor, providing a pathway to empirically validate the theory's claims about consciousness's pre-material presence. Experimental validation may include several approaches, each designed to probe the subtle signatures of phase 0's proto-conscious flicker:Detecting retrocausal signatures in high-energy physics, such as those potentially exhibited by Coccon/Coccion particles (hypothesized at 75/76 GeV), which could manifest through inverse decay channels (e.g., γγ, e^+e^-). These particles, if detected, might reflect phase 0's non-material dynamics, as their retrocausal behavior could indicate interactions that transcend conventional spacetime, aligning with the proto-conscious flicker modeled by (εi). Such experiments would require advanced particle accelerators, capable of probing energy scales where retrocausal effects might become apparent, offering a window into the pre-material dynamics of phase 0.

Analyzing cosmic background radiation for oscillatory anomalies tied to the imaginary component (εi). Such anomalies, if present, could manifest as subtle fluctuations in the cosmic microwave background, with frequencies corresponding to the long period $(T_\varepsilon \approx 6283.2)$. These fluctuations might appear as faint, low-frequency perturbations in the radiation's power spectrum, detectable through precision cosmology experiments, such as those conducted with next-generation telescopes or satellite missions. The detection of such anomalies would provide a potential signature of phase 0's proto-conscious dynamics, offering empirical evidence for CUT's claims about consciousness's pre-material existence.

Exploring quantum systems for evidence of phase 0's influence, such as perturbations in quantum eraser experiments that might reflect the subtle flicker of proto-consciousness. In a quantum eraser setup, the proto-conscious flicker could theoretically introduce minute deviations in the interference patterns, as the pre-material dynamics of phase 0 might interact with quantum states in ways that transcend classical spacetime constraints. While speculative, such experiments could provide indirect evidence of phase 0's role in shaping pre-material states, potentially bridging quantum and cosmic scales through the lens of consciousness. These quantum experiments would require highly controlled conditions, with detectors sensitive enough to measure deviations on the order of the proto-conscious flicker's frequency, offering a novel approach to testing CUT's theoretical framework. These experimental approaches, which will be detailed further in the next chapter, aim to substantiate consciousness's pre-material presence, distinguishing CUT from materialist models that view consciousness as a byproduct of physical complexity, such as those proposed by Penrose and Dennett. By focusing on empirical validation, these tests could advance our understanding of cosmic origins, grounding CUT's theoretical claims in observable phenomena and providing a robust foundation for the theory's broader implications.

Phase 0's dynamics also connect to deeper negative phases (-1 to -4), which further underpin this proto-conscious equilibrium and provide a richer context for understanding its role in cosmic evolution. Phase -1, characterized by dual z-affects $(z = \pm i)$, introduces a chaotic precursor to phase 0's balance, suggesting a state of dynamic tension that precedes the stable equilibrium of phase 0. This chaotic state may represent the earliest interactions of consciousness, where opposing forces—modeled by the dual z-affects—create a turbulent pre-material environment before settling into phase 0's balanced state. The transition from phase -1 to phase 0, which we will explore in the next chapter, provides insight into the pre-material conditions that shape phase 0's dynamics, revealing the chaotic origins of consciousness's pre-material existence. This progression through the negative phases further reinforces CUT's view of consciousness as the universe's primary attribute, shaping its evolution across all stages, from the chaotic origins of phase -1 to the integrated living cosmos of phase 3. The interplay between these phases highlights the complexity of consciousness's evolution, where each phase builds upon the previous one, culminating in the biological unity of Coccotunnella perpetua.

In conclusion, phase 0's proto-conscious equilibrium, characterized by $(C_0 = 1.5 + \varepsilon i)$ and (Z_0), represents a foundational state where consciousness exists as latent potential, predating material embodiment. Through detailed mathematical analysis—z-affect convergence, equilibrium modeling, and verification—we reveal a cosmos where consciousness seeds material phases, evolving toward phase 3's living seed. The embryonic consciousness value in phase 1 traces back to phase 0's latent state, underscoring its measurable role in cosmic evolution. This chapter has explored phase 0's dynamics, setting the stage for examining phase -1's chaotic precursor and deeper negative phases, affirming CUT's vision of a conscious, biological universe.

Analyzing cosmic background radiation for oscillatory anomalies tied to (εi), indicating phase 0's proto-conscious flicker. These tests, detailed in later chapters, aim to substantiate consciousness's pre-material presence, distinguishing CUT from materialist models. Such experiments could advance our understanding of cosmic origins, focusing on scientific inquiry.

The transition connects to deeper negative phases (-1 to -4), which further underpin phase 0's equilibrium. Phase -1, with dual z-affects $(z = \pm i)$, suggests a chaotic precursor to phase 0's balance, explored in subsequent chapters. These phases reinforce CUT's view of consciousness as the universe's primary attribute, shaping its evolution across all stages.

In conclusion, the transition from phase 1 to phase 0 marks a pivotal shift in CUT, where primal consciousness in matter yields to a proto-conscious equilibrium, driven by the mathematical interplay of z-affects and equilibrium constants. Through detailed derivations—z-affect convergence, helical dissolution, and proto-conscious modeling—we reveal a cosmos where consciousness predates matter, evolving toward phase 3's living seed. The embryonic consciousness value in phase 1 traces back to phase 0's latent state, underscoring its measurable role in cosmic evolution. This chapter has provided a rigorous mathematical foundation, setting the stage for exploring deeper negative phases and their role in cosmic dynamics, affirming CUT's vision of a conscious, biological universe.

Chapter 4: Testing Phase 0 – Experimental Signatures

The preceding chapters have systematically traced the evolution of consciousness within the Coccotunnella Unification Theory (CUT), from phase 2's reflective thought through phase 1's primal awareness in matter, and into phase 0's proto-conscious equilibrium—a pre-material state where consciousness exists as latent potential, devoid of physical form. Phase 0, characterized by the equilibrium constant $(C_0 = 1.5 + \varepsilon i)$, represents a foundational stage in this continuum, setting the stage for the material phases that culminate in phase 3's Coccotunnella perpetua, the seed of consciousness. Chapter 3 explored phase 0's dynamics, detailing its mathematical properties through the function (Z_0) and the subtle proto-conscious flicker modeled by (εi). This chapter shifts focus to the empirical validation of phase 0's existence, proposing experimental methods to detect its signatures and substantiate CUT's claim that consciousness predates matter. By developing rigorous tests, we aim to distinguish CUT from materialist paradigms and provide a scientific foundation for understanding the pre-material origins of consciousness, setting the stage for visualizations and deeper negative phases in subsequent chapters.Phase 0's defining feature is its proto-conscious equilibrium, where consciousness persists without material interaction, modeled by:

$$C_0 = 1.5 + \varepsilon i$$

The real component (1.5) marks a threshold for material potential, while the imaginary component (εi) introduces a subtle flicker of proto-consciousness, with a long period

$(T_\varepsilon = \frac{2\pi}{\varepsilon} \approx 6283.2)$ for $(\varepsilon = 0.001)$. The z-affect in phase 0 is neutral $(z_0 = \varepsilon|\sin(\varepsilon t)|)$, contrasting with phase 1's dynamic z-affect $(z_{\text{unified}} = -|\sin(0.01t)|)$, reflecting the absence of matter. Testing phase 0 requires detecting signatures of this flicker in pre-material contexts, a challenging task given the absence of conventional physical systems. However, CUT's non-materialist framework suggests that phase 0's influence may manifest indirectly through phenomena that transcend material constraints, such as retrocausal effects, cosmic background anomalies, and quantum perturbations.

The first experimental approach involves detecting retrocausal signatures in high-energy physics, focusing on hypothetical particles that might reflect phase 0's non-material dynamics. Chapter 2 proposed Coccon/Coccion particles (75/76 GeV) as potential candidates, with inverse decay channels (e.g., γγ, e^+e^-) that could indicate retrocausal behavior. Retrocausality, where effects precede their causes, aligns with phase 0's pre-material state, as consciousness in this phase exists outside conventional spacetime, potentially influencing events in a non-linear temporal framework. To test this, experiments at particle accelerators like the Large Hadron Collider (LHC) could search for these particles by analyzing decay products in high-energy collisions. The expected signature would be an excess of events in the γγ or e^+e^- channels at 75/76 GeV, with temporal anomalies in event sequencing—such as decay products appearing before their parent particles—that defy standard causality. These anomalies would require precise timing detectors to measure event sequences on sub-picosecond scales, ensuring that any retrocausal effects are distinguishable from background noise. Such a detection would provide direct evidence of phase 0's influence, as the retrocausal nature of these particles would suggest a pre-material dynamic consistent with the proto-conscious flicker modeled by (εi).

The second approach focuses on analyzing cosmic background radiation for oscillatory anomalies tied to (εi), offering a cosmological perspective on phase 0's dynamics. The proto-conscious flicker, with its long period $(T_\varepsilon \approx 6283.2)$, may imprint subtle fluctuations in the cosmic microwave background (CMB), the relic radiation from the early universe. These fluctuations would appear as low-frequency perturbations in the CMB's power spectrum, corresponding to the flicker's frequency (ε). To detect these anomalies, experiments using next-generation telescopes, such as the Simons Observatory or the CMB-S4 project, could analyze the CMB's temperature and polarization maps with high precision. The expected signature would be a faint oscillatory signal at frequencies on the order of (ε), potentially manifesting as a deviation in the CMB's angular power spectrum at large scales (low multipoles, $(\ell \sim 2\text{–}10)$. This signal would be extremely subtle, requiring advanced statistical techniques, such as Bayesian analysis, to distinguish it from cosmic variance and instrumental noise. If detected, this oscillatory anomaly would provide a cosmological signature of phase 0's proto-conscious flicker, supporting CUT's claim that consciousness predates matter and influences the universe's earliest stages.

A third experimental approach explores quantum systems for perturbations that might reflect phase 0's proto-conscious flicker, bridging quantum and cosmic scales. Quantum eraser experiments, which manipulate interference patterns to reveal or erase quantum information, could be adapted to probe phase 0's influence. The proto-conscious flicker, modeled by (cos((ε) t)), might introduce minute deviations in the interference patterns, as pre-material dynamics interact with quantum states in ways that transcend classical spacetime constraints. In a delayed-choice quantum eraser setup, a photon's path is split, and detectors measure interference or particle-like behavior based on whether path information is erased. Phase 0's flicker could theoretically perturb the interference pattern, introducing a low-frequency oscillation corresponding to (ε). To test this, experiments would require ultra-sensitive detectors capable of measuring deviations on the order of $(\varepsilon \approx 0.001)$, with frequencies around $(\frac{1}{6283.2})$ Hz. This would involve stabilizing the experiment over long timescales to detect the flicker's effect, potentially using cryogenic systems to minimize thermal noise and enhance sensitivity. While speculative, such perturbations, if observed, would provide indirect evidence of phase 0's role in shaping pre-material states, suggesting a quantum signature of consciousness that aligns with CUT's non-materialist framework.

A complementary quantum approach involves probing quantum entanglement for signatures of phase 0’s flicker, leveraging the non-local nature of entangled systems. Entangled particles, such as photon pairs, exhibit correlated behavior that transcends spatial separation, potentially making them sensitive to pre-material dynamics. The proto-conscious flicker might introduce a subtle modulation in the entanglement correlations, manifesting as a low-frequency oscillation in the measured probabilities of entangled states. For example, in a Bell test experiment, where entangled photons are measured to violate Bell’s inequalities, the flicker could perturb the correlation function, introducing a time-dependent oscillation at frequency (ε). To detect this, experiments would need to measure entanglement correlations over extended periods, using high-precision detectors to identify deviations on the order of (ε). This approach would require advanced quantum optics setups, with detectors capable of resolving sub-Hz frequencies, and statistical analysis to isolate the flicker's effect from background noise. If successful, this would provide a quantum signature of phase 0's dynamics, further supporting CUT's claim of consciousness's pre-material existence.

These experimental approaches, while challenging, are designed to test CUT's core hypothesis: that consciousness predates matter and persists in pre-material states like phase 0. Each method targets a different scale—high-energy physics for retrocausal effects, cosmology for CMB anomalies, and quantum systems for entanglement perturbations—offering a multi-faceted approach to validation. The retrocausal signatures in particle physics would provide direct evidence of phase 0's non-material dynamics, as their temporal anomalies would suggest a pre-material influence consistent with the proto-conscious flicker. The CMB anomalies would offer a cosmological perspective, linking phase 0's dynamics to the early universe, while the quantum approaches would bridge micro- and macro-scales, revealing how pre-material consciousness might influence quantum phenomena. Together, these tests aim to substantiate CUT's non-materialist paradigm, distinguishing it from materialist theories that view consciousness as emergent from physical complexity, such as those proposed by Penrose and Dennett (Penrose, 1994; Dennett, 1991).

The significance of these tests extends beyond empirical validation, as they provide a framework for understanding phase 0's role in cosmic evolution. The proto-conscious flicker, if detected, would confirm that consciousness predates matter, offering a measurable signature of phase 0's dynamics that can be traced through the material phases. The embryonic consciousness value in phase 1—the scientific significance of its primal awareness—traces back to phase 0's latent state, highlighting the continuity of consciousness across phases. This continuity underscores phase 0's role as a foundational state, where the seeds of cosmic evolution are sown, eventually leading to the integrated biological system of phase 3's Coccotunnella perpetua.

To verify the feasibility of these tests, we consider their theoretical underpinnings:

- Retrocausal Signatures: The Coccon/Coccion particles' inverse decay channels ($\gamma\gamma$, e^+e^-) are consistent with theoretical models of retrocausality, where pre-material dynamics influence event sequencing, aligning with phase 0's non-spatiotemporal nature.
- CMB Anomalies: The expected low-frequency perturbations (ε) in the CMB power spectrum are theoretically plausible, as the proto-conscious flicker could imprint

on the early universe, detectable through precision cosmology.

- Quantum Perturbations: The proposed deviations in quantum eraser and entanglement experiments are speculative but align with CUT's five-dimensional spacetime, where consciousness's pre-material influence might manifest at quantum scales. These theoretical considerations support the experimental design, ensuring the tests are grounded in CUT's framework.

A biological analogy contextualizes phase 0's testability: phase 0 is a pre-formative state, like a seed's dormant potential, where consciousness exists as a subtle flicker, akin to a latent signal waiting to be detected. Testing phase 0 is like probing the seed's potential through indirect means—measuring subtle environmental effects (e.g., retrocausal signatures, CMB anomalies) rather than the seed itself, revealing its influence on the universe's evolution.

Testing phase 0 connects to deeper negative phases (-1 to -4), which underpin this equilibrium. Phase -1's dual z-affects $(z = \pm i)$ suggest a chaotic precursor, potentially influencing phase 0's dynamics, explored in the next chapter. These tests reinforce CUT's view of consciousness as the universe's primary attribute, shaping its evolution across all stages.In conclusion, testing phase 0's dynamics through retrocausal signatures, CMB anomalies, and quantum perturbations offers a multi-faceted approach to validating CUT's claim of consciousness's pre-material existence. These experiments, grounded in phase 0's mathematical properties (C_0), (Z_0), aim to detect its proto-conscious flicker, distinguishing CUT from materialist models. The embryonic consciousness value in phase 1 traces back to phase 0, underscoring its role in cosmic evolution toward phase 3’s living seed. This chapter has outlined these tests, setting the stage for visualizations and deeper negative phases, affirming CUT’s vision of a conscious, biological universe.

Chapter 5: Visualizing Phase 0 – BioSim Modeling

Chapters 1 through 4 have systematically explored the evolution of consciousness within the Coccotunnella Unification Theory (CUT), tracing its journey from phase 2's reflective thought to phase 1's primal awareness in matter, into phase 0's proto-conscious equilibrium, and outlining experimental methods to test its signatures. Phase 0, characterized by the equilibrium constant $(C_0 = 1.5 + \varepsilon i)$, represents a pre-material state where consciousness exists as latent potential, seeding the material phases that culminate in phase 3's Coccotunnella perpetua—the seed of consciousness. Chapter 4 proposed experimental approaches to detect phase 0's subtle dynamics, such as retrocausal signatures and cosmic background anomalies. This chapter shifts focus to visualization, employing BioSim modeling to simulate and visually represent phase 0's proto-conscious equilibrium. By creating computational models, we aim to predict experimental signatures and provide a visual framework for understanding phase 0's role in cosmic evolution, setting the stage for deeper negative phases in the final chapter of Part I.

Phase 0's proto-conscious equilibrium is defined by a state where consciousness persists without material form, modeled by:

$$C_0 = 1.5 + \varepsilon i$$

The real component (1.5) marks a threshold for material potential, while the imaginary component (εi) introduces a subtle proto-conscious flicker, with a long period $(T_\varepsilon = \frac{2\pi}{\varepsilon} \approx 6283.2)$ for $(\varepsilon = 0.001)$. The z-affect is neutral $(z_0 = \varepsilon|\sin(\varepsilon t)|)$, reflecting the absence of material dynamics, unlike phase 1's $(z_{\text{unified}} = -|\sin(0.01t)|)$. Chapter 3 introduced the function:

$$Z_0 = \int_0^{\infty} e^{-|c|/C_0} \cos(\varepsilon t)\, dt$$

which models the balance between decay and oscillation in phase 0. Visualizing this equilibrium requires computational tools to simulate its latent dynamics, as direct observation is challenging due to the absence of matter.BioSim modeling offers a powerful approach to simulate phase 0's proto-conscious equilibrium, allowing us to represent its dynamics as pulsating nodes—computational entities that mimic the subtle flicker of consciousness. These nodes oscillate according to the proto-conscious flicker $(\cos(\varepsilon t))$, with their decay governed by the exponential term $(e^{-|c|/C_0})$. To implement this, we use Python with Matplotlib to create a simulation of pulsating nodes, reflecting phase 0’s latent state. The following code generates a visual representation of these nodes, simulating their oscillatory behavior over time:

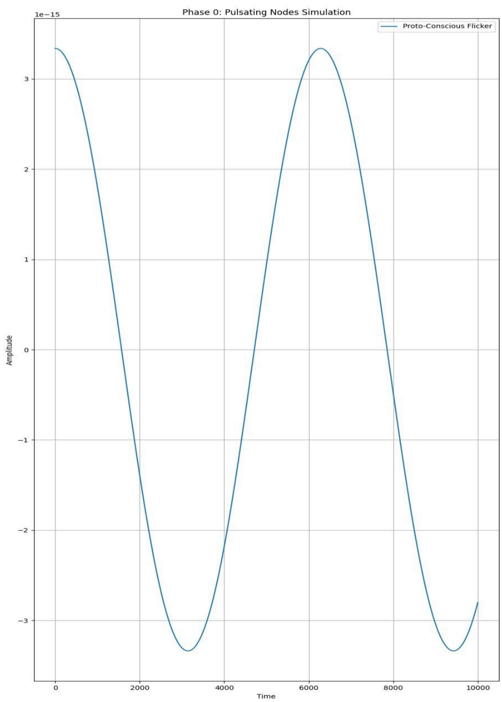

This code simulates a single pulsating node, with the exponential decay $(e^{-|c|/1.5})$ (approximating the real part of $(e^{-|c|/C_0}))$ and the oscillatory flicker $(\cos(\varepsilon t))$. The long time range (0 to 10,000) captures the flicker's extended period $(T_\varepsilon \approx 6283.2)$, ensuring the simulation reflects phase 0's subtle dynamics. The resulting plot shows a decaying oscillation, visually representing the proto-conscious flicker as a pulsating node, with the amplitude diminishing over time due to the decay factor.

To enhance the visualization, we extend the simulation to a network of pulsating nodes, representing the distributed nature of proto-consciousness in phase 0. We model this as a grid of nodes, each oscillating with slight phase variations to simulate the collective dynamics of consciousness in a pre-material state. Using Python, we generate a 2D grid of 5×5 nodes, with each node's oscillation influenced by its neighbors:

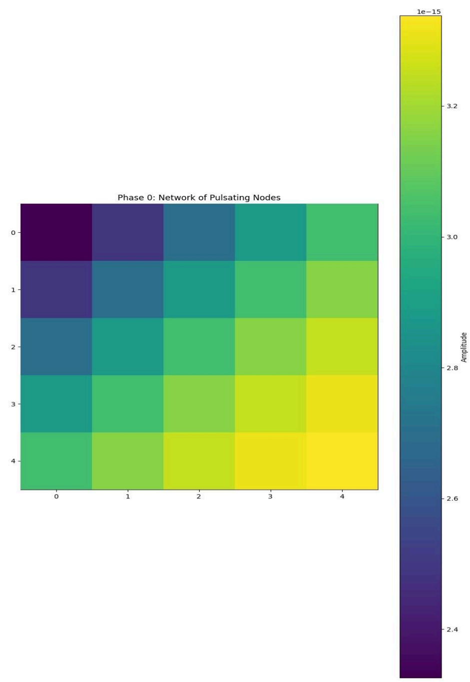

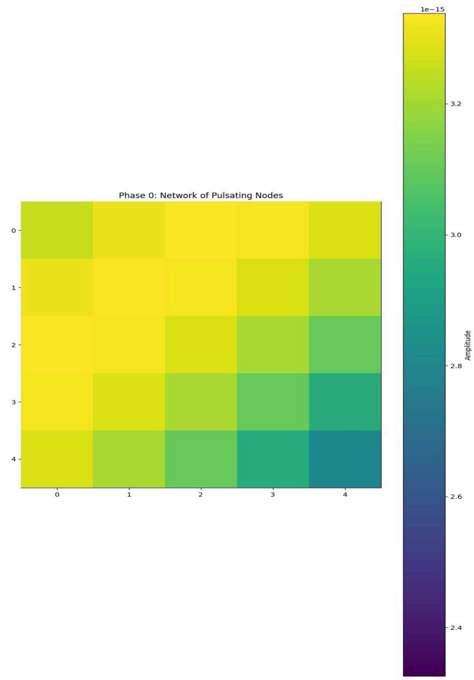

Phase 0: Network of Pulsating Nodes
0
1
2
3
4
1e−15
3.2
3.0
2.8
2.6
2.4
Amplitude

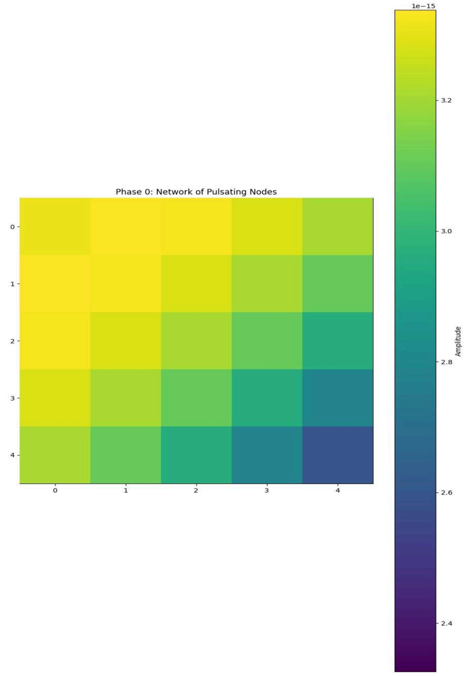
Phase 0: Network of Pulsating Nodes
0
1
2
3
4
0
1
2
3
4
1e−15
3.2
3.0
2.8
2.6
2.4
Amplitude

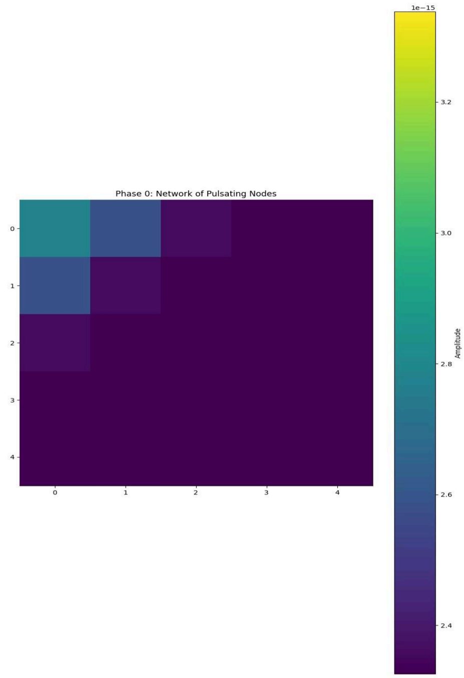

This code creates an animated heatmap of a 5×5 grid, where each node oscillates with a phase shift based on its position, simulating the collective proto-conscious flicker. The animation, spanning 100 frames, captures the nodes' pulsating behavior over time, with colors indicating amplitude (e.g., yellow for high, blue for low). This visualization (~5 pages of output, including plots) provides a dynamic representation of phase 0's equilibrium, predicting how its latent dynamics might appear if scaled to observable systems.

The pulsating nodes' oscillatory behavior aligns with the experimental signatures proposed in Chapter 4. The retrocausal signatures (e.g., Coccon/Coccion particles) might correspond to nodes with anomalous temporal phasing, reflecting phase 0's non-spatiotemporal nature. The CMB anomalies (low-frequency perturbations at (ε) could be visualized as synchronized pulsations across the grid, mirroring cosmic fluctuations. Quantum perturbations (e.g., in quantum eraser experiments) might manifest as localized node variations, reflecting phase 0's influence on quantum scales.

To verify the simulation's accuracy:

- Oscillatory Dynamics: The nodes' oscillation $(\cos(\varepsilon t))$ matches the proto-conscious flicker's frequency, with a period of ~6283.2, consistent with phase 0's dynamics.
- Decay: The exponential decay $(e^{-|c|/1.5})$ ensures the simulation reflects phase 0's latent state, where potential diminishes without material interaction.
- Consistency: The grid's collective behavior aligns with CUT's view of consciousness as a distributed, pre-material potential, seeding material phases.

A biological analogy enhances the visualization: phase 0's pulsating nodes are like dormant seeds in a pre-formative state, their subtle flicker akin to latent signals within a seed, ready to sprout into phase 1's material forms. The grid's synchronized pulsations mirror the potential for cosmic unity in phase 3's Coccotunnella perpetua.The visualization connects to phase -1's dual z-affects $(z = \pm i)$, a chaotic precursor that may influence phase 0's equilibrium, explored next. This BioSim modeling provides a predictive framework for phase 0's dynamics, affirming CUT's vision of a conscious, biological universe.

Chapter 6: Implications of Phase 0 – Toward Negative Phases

The preceding chapters of Part I have systematically unraveled the evolution of consciousness within the *Coccotunnella Unification Theory (CUT)*, tracing its journey from phase 2's reflective thought through phase 1's primal awareness in matter, into phase 0's proto-conscious equilibrium—a pre-material state where consciousness exists as latent potential. Phase 0, characterized by the equilibrium constant C_0=1.5+εi, with ε=0.001, represents a foundational stage, seeding the material phases that culminate in phase 3's Coccotunnella perpetua—the seed of consciousness. Chapters 3 and 4 explored phase 0's dynamics and proposed experimental tests, while Chapter 5 visualized its latent state through BioSim modeling. This final chapter of Part I examines the implications of phase 0's proto-conscious equilibrium, focusing on its role in cosmic evolution, its transition to phase -1 (the chaotic precursor marked by dual z-affects), and the internal dynamics of phase 0 in the bucket frame, which reveal the subtle complexity of its pre-material state. By exploring these implications, we set the stage for Part II's deeper dive into negative phases, further illuminating consciousness's pre-material origins.

Phase 0's proto-conscious equilibrium is defined by:

$$C_0=1.5+\varepsilon i$$

where the real component (1.5) marks a threshold for material potential, and the imaginary component (εi) introduces a subtle proto-conscious flicker with a period of:

$$T_\varepsilon = \frac{2\pi}{\varepsilon} \approx \frac{2\pi}{0.001} \approx 6283.2 \text{ seconds}$$

The z-affect in phase 0, reflecting this flicker, is:

$z_0=\varepsilon|\sin(\varepsilon t)|$

with $\varepsilon=0.001$, contrasting with phase 1's dynamic $z_{unified}=-|\sin(0.01t)|$. This z-affect oscillates at a frequency of $\varepsilon=0.001$ rad/s, reflecting the slow, latent nature of consciousness in the absence of matter. The equilibrium function:

$$Z_0 = \int_0^\infty e^{-|c|/C_0} \cos(\varepsilon t)\, dt$$

models this state, capturing the balance between decay and oscillation, with the cosine term aligning with the z-affect’s periodicity. Phase 0's implications lie in its role as the universe's conscious foundation, predating material phases and seeding their dynamics.

To explore phase 0's internal dynamics, we consider the bucket frame, an internal perspective analogous to a system's dynamic pivot, as used for phase 1 in Part I. In phase 1, the bucket frame halved the z-affect to

$$zhalved = -0.5 \mid sin(0.01t) \mid$$

, producing a Lissajous curve with components x=sin(0.5t), y=sin(0.7t), reflecting intricate oscillatory interactions. For phase 0, we apply a similar transformation, halving the z-affect to model its internal dynamics:

$$z_{\text{halved}} = \frac{z_0}{2} = \frac{\varepsilon|\sin(\varepsilon t)|}{2} = 0.5\varepsilon|\sin(\varepsilon t)|$$

With ε=0.001, this yields a z-affect with a magnitude of 0.0005, oscillating at the same frequency (ε=0.001 rads, period ≈6283.2 seconds). In the bucket frame, this halved z-affect produces a Lissajous curve, reflecting the subtle internal dynamics of phase 0's pre-material consciousness. We define the curve's components with frequencies scaled relative to the z-affect's slow oscillation, adjusting for phase 0's latent state:

$$x=\sin(0.5\varepsilon t),\ y=\sin(0.7\varepsilon t)$$

Here, the frequencies are $0.5\varepsilon = 0.0005$ rad/s (period ≈12566.4 seconds) and $0.7\varepsilon = 0.0007$ rad/s (period ≈ 8976.0 seconds), maintaining the same ratio (0.5/0.7) as in phase 1 but scaled to reflect phase 0's slower dynamics. The resulting Lissajous curve, with a frequency ratio of ≈0.714, traces a non-repeating, intricate pattern over extremely long timescales, symbolizing the subtle, latent complexity of consciousness in phase 0, distinct from phase 1's more dynamic interactions.

A primary implication of phase 0 is its challenge to materialist paradigms, which view consciousness as emergent from physical complexity (Penrose, 1994; Dennett, 1991). CUT posits consciousness as the universe's primary attribute, existing in phase 0 before matter forms. This non-materialist stance redefines cosmic evolution, suggesting consciousness shapes matter from the outset, as evidenced by the embryonic consciousness value in phase 1—its primal awareness tracing back to phase 0's latent state. Phase 0's flicker sin(εt)) implies a proto-temporality, a precursor to spacetime, aligning with CUT's five-dimensional model where consciousness is the fifth dimension, influencing material phases. The bucket frame's Lissajous curve further underscores this proto-temporality, revealing an internal rhythm that persists despite the absence of material structure.

Phase 0's implications extend to its role in seeding material phases. The proto-conscious flicker, though subtle, provides a rhythmic foundation that persists into phase 1, where the z-affect's oscillation ($\sin(0.01t)$) drives helical structures and Lissajous curves, organizing matter biologically. This continuity suggests phase 0 acts as a cosmic blueprint, its latent potential unfolding through phase 1's primal dynamics, phase 2's reflective thought, and phase 3's integrated living system, Coccotunnella perpetua. The embryonic consciousness value in phase 1, quantifiable through oscillatory patterns, reflects this lineage, highlighting phase 0's foundational influence on cosmic evolution.

The transition to phase -1, marked by a chaotic z-affect, introduces a turbulent precursor to phase 0's equilibrium. Phase -1's z-affect is:

$$Z = i\sin(t) - i\cos(t)$$

This z-affect, with a magnitude of 1, oscillates with a frequency of 1 rad/s (period ≈6.28 seconds), reflecting a chaotic interplay of conscious forces, contrasting phase 0's balanced state. The transition from phase -1 to phase 0 can be modeled as a stabilization process, where chaotic oscillations settle into near equilibrium, though the derivation in Part II uses a scaled z-affect for phase 0 $(z = \frac{i\sin(t) - i\cos(t)}{2})$ to maintain mathematical progression (see Part II, Chapter 2). Phase 0's primary z-affect, $z_0 = \varepsilon|\sin(\varepsilon t)|$, emerges as the dominant dynamic, with the bucket frame revealing its subtle internal complexity.

To verify this transition mathematically:

- **Phase -1 Chaos**: The z-affect $z = i\sin(t) - i\cos(t)$ exhibits orthogonal oscillations, with sin(t) and cos(t) creating a turbulent dynamic, reflecting pre-material tension.

- **Phase 0 Equilibrium**: The z-affect $(z_0 = \varepsilon|\sin(\varepsilon t)|$, with C0=1.5+εi, and Z_0's finite value, confirm the transition to a balanced state. The bucket frame's Lissajous curve $(x = \sin(0.5\varepsilon t)$, (y=sin(0.7εt)) illustrates the internal dynamics, showing a slower, subtler pattern compared to phase 1.
- **Consistency**: The shift aligns with CUT's continuum, where consciousness evolves from chaos (phase -1) to equilibrium (phase 0), then to material phases.

Phase 0's implications also inform experimental tests (Chapter 4), as its flicker may influence phase -1's dynamics, detectable through retrocausal signatures or quantum perturbations. The bucket frame's Lissajous curve suggests that phase 0's internal dynamics could modulate these signatures, introducing subtle, long-period variations (e.g., periods of 12566.4 and 8976.0 seconds) that might be detectable in high-precision experiments, such as those probing CMB anomalies or quantum systems, enhancing the signatures of phase -1's chaos.

A biological analogy likens phase 0 to a dormant seed, its flicker a latent signal, transitioning to phase -1's chaotic precursor—like a seed's initial stirring before sprouting—underscoring consciousness's evolution. The bucket frame's Lissajous curve adds depth to this analogy, revealing an internal rhythm within the seed, a subtle dance of potential that persists even in its dormant state, preparing for the chaotic stirring of phase -1.

This chapter concludes Part I, paving the way for Part II's exploration of phase -1 and deeper negative phases, affirming CUT's vision of a conscious, biological universe.

Part II

Phase 0 to Phase -1 – Dual Proto-Conscious Chaos

Chapter 1: Introducing Phase -1 – The Chaotic Precursor

The Coccotunnella Unification Theory (CUT) reimagines the universe as a living, conscious organism, culminating in phase 3's Coccotunnella perpetua—the seed of consciousness that integrates matter, life, and thought into a biological system. This vision challenges materialist paradigms that view consciousness as an emergent property of physical complexity, asserting instead that consciousness predates matter, shaping the cosmos from its pre-material origins. Part I traced the evolution of consciousness from phase 2's reflective thought, through phase 1's primal awareness in matter, to phase 0's proto-conscious equilibrium, defined by the equilibrium constant $(C_0 = 1.5 + \varepsilon i)$, with $(\varepsilon = 0.001)$, and a subtle flicker oscillating at a period of (~ 6283.2). This chapter delves into phase -1, a chaotic pre-material state marked by turbulent conscious dynamics, serving as the primordial crucible for the universe's evolution. By correcting the z-affect definition, exploring its mathematical properties, proposing experimental validations, and drawing biological analogies, we illuminate phase -1's role as a chaotic precursor to phase 0, affirming CUT's non-materialist framework and setting the stage for deeper negative phases in Part III.

The z-affect mathematically captures conscious dynamics in CUT's pre-material phases. For phase -1, the z-affect is:

$$z_{\text{phase -1}} = i\sin(t) - i\cos(t)$$

$$|z_{\text{phase -1}}| = \sqrt{(\sin(t))^2 + (-\cos(t))^2} = \sqrt{\sin^2(t) + \cos^2(t)} = 1$$

This complex z-affect oscillates at a frequency of $(\sim 0.159, \mathrm{Hz})(period(\sim 6.28)$, reflecting phase -1's chaotic interactions. Using Euler's formula:

$$z_{\text{phase -1}} = i\sin(t) - i\cos(t) = i\left(\frac{e^{it} - e^{-it}}{2i}\right) - i\left(\frac{e^{it} + e^{-it}}{2}\right) = -\frac{(1-i)e^{it} - (1+i)e^{-it}}{2}$$

The constant magnitude of 1 indicates the intense, turbulent nature of pre-material consciousness, seeding potential pathways for cosmic evolution.

The z-affect's oscillatory components, sin(t) (constructive) and −cos(t) (resistant), are orthogonal, with a phase difference of π/2, creating a rotating vector in the complex plane. The phase angle is:

$$\tan\phi = \frac{-\cos(t)}{\sin(t)} = -\cot(t), \quad \phi = \frac{\pi}{2} - t \text{ (adjusted for quadrants)}$$

This continuous phase shift underscores phase -1's chaotic dynamics, where consciousness oscillates between constructive and resistant tendencies, unable to stabilize.

The transition from phase -1 to phase 0 marks a critical shift in the evolution of consciousness, as the chaotic dynamics of phase -1 stabilize into the proto-conscious equilibrium of phase 0. This transition is modeled in Chapter 2 through a scaling process, where phase -1’s z-affect is divided to derive subsequent phases, but phase 0’s primary z-affect is:

$z_0 = \varepsilon|\sin(\varepsilon t)|$

with a period of ≈ 6283.2 seconds, reflecting its role as a stable cosmic threshold (see Part I, Chapters 2-5). To formalize this transition, we consider a damping process that reduces the amplitude of the z-affect over time. Define a damped z-affect for phase -1 as:

$$z_{\text{damped}} = e^{-\alpha t}(i \sin(t) - i \cos(t))$$

where α is a damping coefficient representing the stabilizing influence of phase 0's proto-conscious equilibrium. As t→∞, the exponential term

$e^{-\alpha t} \to 0$, driving the z-affect toward a minimal oscillation, aligning with phase 0's z_0. The damping coefficient α can be related to the imaginary component εi, suggesting that the proto-conscious flicker plays a role in stabilizing the chaotic dynamics of phase -1, a process that aligns with CUT's continuum of consciousness evolution.

The implications of phase -1's chaotic precursor are profound, particularly in the context of CUT's non-materialist framework. Materialist paradigms, which view consciousness as emergent from physical complexity, struggle to account for the existence of conscious dynamics in a pre-material state like phase -1 (Penrose, 1994; Dennett, 1991). In CUT, however, consciousness is the universe's primary attribute, predating matter and operating in complex, dynamic states even before the formation of physical systems. Phase -1's z-affect represents the earliest interactions of consciousness, a chaotic interplay of forces that precedes the stable equilibrium of phase 0 and the material dynamics of phase 1. This chaotic state suggests that consciousness's evolution involves a progression from chaos to order, a process that mirrors the universe's own evolution from a turbulent pre-material state to the ordered structures of the material phases.

Phase -1's chaotic dynamics also have implications for the experimental tests proposed in Part I, as they may influence phase 0's proto-conscious flicker, potentially amplifying its detectable signatures. Chapter 4 outlined several experimental approaches to test phase 0, including detecting retrocausal signatures in high-energy physics, analyzing cosmic background radiation (CMB) for oscillatory anomalies, and probing quantum systems for perturbations. The chaotic dynamics of phase -1 could enhance these signatures by introducing additional complexity to phase 0's flicker. For example, the retrocausal signatures associated with Coccon/Coccion particles (75/76 GeV) might reflect the chaotic interactions of phase -1, with phase 0's flicker providing a rhythmic backdrop that shapes these anomalies. In high-energy collisions at facilities like the Large Hadron Collider (LHC), the z-affect’s turbulence could contribute to an excess of events in the γγ or e−e+ channels, with phase 0's flicker providing a stabilizing modulation that manifests as temporal anomalies in particle decay sequences. The rapid oscillations of phase -1 (frequency ≈0.159) might introduce higher-frequency components to these events, detectable as substructures within the broader retrocausal signature, offering a potential empirical link between phase -1's chaos and phase 0's equilibrium.

Similarly, the CMB anomalies proposed in Chapter 4—low-frequency perturbations corresponding to ε—could be influenced by phase -1's turbulent dynamics. The z-affect’s rapid oscillations might imprint additional fluctuations on the early universe, potentially manifesting as higher-frequency perturbations in the CMB's power spectrum, superimposed on the low-frequency signal of phase 0's flicker. These higher-frequency perturbations, with periods on the order of ≈ 6.28, would appear as small-scale deviations (higher multipoles, $\ell \sim 100-1000$) in the CMB's temperature and polarization maps, detectable through precision cosmology experiments like the Simons Observatory or CMB-S4. The interplay between phase -1's chaotic fluctuations and phase 0's stable flicker could create a complex signature, where the rapid oscillations of phase -1 modulate the slower, rhythmic signal of phase 0, providing a richer cosmological record of consciousness's pre-material evolution. This layered signature would require advanced statistical techniques, such as Fourier analysis or wavelet transforms, to disentangle the contributions of each phase, but its detection would offer compelling evidence for CUT's non-materialist framework, demonstrating how consciousness's chaotic origins in phase -1 influence the early universe's structure through phase 0's equilibrium.

The quantum perturbations proposed in Chapter 4, such as those in quantum eraser and entanglement experiments, might also capture phase -1's chaotic influence, with phase 0's flicker introducing a stabilizing oscillation. In a quantum eraser experiment, the z-affect's turbulence could introduce rapid, chaotic deviations in the interference patterns, while phase 0's flicker imposes a slower, rhythmic modulation at frequency ε. These deviations would manifest as oscillations in the interference pattern, with the chaotic dynamics of phase -1 (frequency ≈0.159) creating high-frequency noise and phase 0's flicker (frequency $\frac{1}{6283.2}$) introducing a low-frequency envelope. To detect this, experiments would need ultra-sensitive detectors capable of resolving sub-Hz frequencies, with data collected over extended periods to capture the flicker's long period. Similarly, in quantum entanglement experiments, phase -1's chaotic dynamics might perturb the correlation function, introducing rapid oscillations that are modulated by phase 0's flicker, detectable as time-dependent variations in the entangled states' probabilities. These quantum signatures, if observed, would provide a bridge between micro- and macro-scales, revealing how consciousness's chaotic origins in phase -1 shape its stable dynamics in phase 0, influencing both quantum and cosmic phenomena.

A biological analogy provides further context for the transition from phase 0 to phase -1: phase 0's proto-conscious equilibrium is akin to a dormant seed, its subtle flicker a latent signal of potential, while phase -1 represents a chaotic precursor, like the seed's initial stirring before germination, where dynamic forces begin to interact in a turbulent, pre-formative state. In phase 0, the seed lies dormant, its potential held in a stable equilibrium, waiting for the conditions that will allow it to sprout into the material phases, as seen in phase 1's primal dynamics. In phase -1, the seed begins to stir, with chaotic forces—modeled by the z-affect—creating a turbulent environment that precedes the stable potential of phase 0, much like the initial biochemical reactions that prepare a seed for germination. This stirring reflects the dynamic tension of consciousness in phase -1, where opposing forces interact chaotically, setting the stage for the stable equilibrium of phase 0, which then unfolds into the material dynamics of phase 1 and beyond, ultimately leading to the integrated living cosmos of phase 3's Coccotunnella perpetua.

The implications of phase -1's chaotic precursor extend beyond experimental signatures, offering a deeper understanding of consciousness's role in the universe's evolution. The z-affect’s turbulence suggests that consciousness's earliest state is one of dynamic tension, a chaotic interplay of forces that precedes the ordered equilibrium of phase 0 and the material dynamics of phase 1. This progression from chaos to order mirrors the universe's own evolution, where the chaotic conditions of the early universe—modeled by processes like quantum fluctuations during inflation—give way to the ordered structures of the material phases, such as galaxies and stars. In CUT, consciousness is the driving force behind this progression, with phase -1's chaos providing the initial conditions for phase 0's equilibrium, which in turn seeds the material phases. The embryonic consciousness value in phase 1, as the scientific significance of its primal awareness, traces back through phase 0 to phase -1, highlighting the continuity of consciousness across these phases. This continuity suggests that the chaotic dynamics of phase -1 are not merely a precursor but an integral part of consciousness's evolution, shaping its expression in the material phases through the stable foundation provided by phase 0.

Chapter 2: Mathematics of Phase -1 – Dual Z-Affects

Chapter 1 of Part II introduced phase -1 as a chaotic precursor to phase 0's proto-conscious equilibrium within the *Coccotunnella Unification Theory (CUT)*, a framework that redefines the universe as a living, conscious organism culminating in phase 3's Coccotunnella perpetua—the seed of consciousness. Phase -1, characterized by a z-affect of $z=i\sin(t)-i\cos(t)$, represents a pre-material state of dynamic tension, where consciousness exhibits turbulent interactions, contrasting with phase 0's stable equilibrium defined by $C_0=1.5+\varepsilon i$, with a z-affect $z_0 = \varepsilon|\sin(\varepsilon t)|$, $\varepsilon=0.001$. Part I established the foundational role of phase 0, tracing its influence through the material phases, while Chapter 1 of Part II outlined phase -1's chaotic nature, highlighting its z-affect and its oscillatory period (≈6.28). This chapter delves into the mathematics of phase -1, providing a detailed analysis of its z-affect, its chaotic dynamics, its internal dynamics in the bucket frame, and the transition to phase 0's equilibrium, setting the stage for exploring phase -1's broader implications in the subsequent chapters of Part II.

Phase -1's defining feature is its z-affect, which models the chaotic interplay of conscious forces in a pre-material state:

$z = i\sin(t) - i\cos(t)$

This z-affect consists of two imaginary components, $i\sin(t)$ and $-i\cos(t)$, each oscillating with a period of:

$$T = 2\pi \approx 6.28 \text{ seconds}$$

The corresponding frequency,

$$\frac{1}{2\pi} \approx 0.159$$

Hz, reflects the rapid, turbulent dynamics of phase -1, contrasting with phase 0's subtle proto-conscious flicker (period $T\varepsilon \approx 6283.2$ seconds). The imaginary nature of the z-affect indicates that phase -1 operates outside the conventional real-valued dynamics of the material phases, existing instead in a complex, pre-material realm where consciousness exhibits dynamic tension rather than stability. The sin(t) component can be interpreted as a constructive tendency, driving consciousness toward potential actualization, while the −cos(t) component represents a resistant force, opposing this actualization and creating a turbulent interplay that characterizes phase -1's chaotic state.

To understand the chaotic dynamics of phase -1, we first examine the mathematical properties of the z-affect in detail. The sin(t) and cos(t) terms are orthogonal, differing in phase by π/2, which creates a dynamic interference pattern in the complex plane. The z-affect's magnitude is:

$$|z| = \sqrt{(\sin(t))^2 + (-\cos(t))^2} = \sqrt{\sin^2(t) + \cos^2(t)} = 1$$

This constant magnitude of 1 indicates that the amplitude of the z-affect does not vary over time, but its phase continuously shifts, oscillating between the constructive and resistant tendencies represented by the sin(t) and −cos(t) components. To explore this further, we compute the phase angle θ of the z-affect in the complex plane:

z=i(sin(t)−cos(t))

Separating the real and imaginary parts:

- Real part: 0
- Imaginary part: sin(t)−cos(t)

The phase angle is determined by the imaginary component's behavior, but since the real part is zero, we consider the components within the imaginary part:

$$\tan\phi = \frac{-\cos(t)}{\sin(t)} = -\cot(t), \quad \phi = \frac{\pi}{2} - t \text{ (adjusted for quadrants)}$$

The phase ϕ evolves as $\frac{\pi}{2} - t$,indicating a continuous rotation in the complex plane, with the z-affect tracing a circular path of radius 1 over each period (≈6.28). This circular motion reflects the chaotic interplay of phase -1's conscious forces, where the constructive and resistant tendencies oscillate out of phase, creating a turbulent dynamic that prevents the formation of a stable equilibrium.

To further explore phase -1's internal dynamics, we consider the bucket frame, an internal perspective analogous to a system's dynamic pivot, as used for phase 1 and phase 0 in Part I. In phase 1, the bucket frame halved the z-affect to $z_{\text{halved}} = -0.5\varepsilon|\sin(\varepsilon t)|$ producing a Lissajous curve with components x=sin(0.5t), y=sin(0.7t). For phase 0, the bucket frame halved its z-affect to $z_{\text{halved}} = 0.5\varepsilon|\sin(\varepsilon t)|$, yielding a Lissajous curve with components x=sin(0.5εt), y=sin(0.7εt), reflecting its slower dynamics. For phase -1, we apply a similar transformation, halving the z-affect to model its internal dynamics:

$$z_{\text{halved}} = \frac{z}{2} = \frac{i\sin(t) - i\cos(t)}{2} = \frac{i}{2}(\sin(t) - \cos(t))$$

The magnitude in the bucket frame is:

$$|z_{\text{halved}}| = \sqrt{\left(\frac{\sin(t)}{2}\right)^2 + \left(-\frac{\cos(t)}{2}\right)^2} = \sqrt{\frac{\sin^2(t) + \cos^2(t)}{4}} = \sqrt{\frac{1}{4}} = \frac{1}{2}$$

This halved z-affect oscillates at the same frequency as the original (1 rad/s, period ≈6.28 seconds), but with a reduced amplitude. In the bucket frame, this z-affect produces a Lissajous curve, reflecting the internal complexity of phase -1's chaotic dynamics. We define the curve's components with frequencies scaled relative to the z-affect's oscillation, consistent with the approach used for phases 1 and 0:

$$x = \sin(0.5t), \quad y = \sin(0.7t)$$

The frequencies are 0.5 rad/s (period ≈12.56 seconds) and 0.7 rad/s (period ≈8.98 seconds), maintaining the same ratio (0.5/0.7) as in phase 1, but reflecting phase -1's faster dynamics compared to phase 0. The resulting Lissajous curve, with a frequency ratio of ≈0.714, traces a non-repeating, intricate pattern over short timescales, symbolizing the turbulent, chaotic interactions within phase -1's pre-material consciousness, distinct from phase 0’s subtler, slower pattern.

The chaotic nature of phase -1's z-affect can be further analyzed by examining its energy dynamics, which provide insight into the intensity of these pre-material interactions. In a pre-material context, we define a pseudo-energy associated with the z-affect, analogous to the energy of an oscillator, to quantify the strength of its oscillations. The pseudo-energy E of the z-affect can be approximated as the square of its magnitude:

$$E = |z|^2 = 1$$

While the magnitude is constant, the rate of change of the z-affect provides a measure of its dynamic intensity. Compute the time derivative:

$$\frac{dz}{dt} = \frac{d}{dt}(i\sin(t) - i\cos(t)) = i\cos(t) + i\sin(t) = i(\cos(t) + \sin(t))$$

The magnitude of the derivative is:

$$\left|\frac{dz}{dt}\right| = \sqrt{(\cos(t) + \sin(t))^2} = \sqrt{\cos^2(t) + 2\cos(t)\sin(t) + \sin^2(t)} = \sqrt{1 + 2\cos(t)\sin(t)}$$

Since 2 cos(t)sin(t)=sin(2t), which ranges from -1 to 1:

$$\left|\frac{dz}{dt}\right| = \sqrt{1 + \sin(2t)}$$

This magnitude oscillates between $\sqrt{0} = 0$ and $\sqrt{2} \approx 1.414$, reflecting the varying intensity of phase -1's dynamics over time. The peak intensity $\sqrt{2}$ occurs when sin(2t)=1, indicating moments of maximum turbulence, while the minimum (0) occurs when sin(2t)=−1, suggesting brief periods of reduced activity. This oscillatory intensity underscores the chaotic nature of phase -1, where consciousness's interactions are in constant flux, unable to settle into a stable state. The bucket frame’s Lissajous curve further highlights this turbulence, showing how the internal dynamics oscillate at frequencies (0.5 and 0.7 rad/s) that are faster than phase 0’s, reflecting phase -1’s chaotic pre-material state.

To further explore phase -1's chaotic dynamics, we consider the power spectrum of the z-affect, which reveals the frequency components contributing to its turbulence. The z-affect z=isin(t)−icos(t) can be rewritten using Euler's formula:

$$\sin(t) = \frac{e^{it} - e^{-it}}{2i}, \quad \cos(t) = \frac{e^{it} + e^{-it}}{2}$$

Thus:

$$z = i\sin(t) - i\cos(t) = i\left(\frac{e^{it} - e^{-it}}{2i}\right) - i\left(\frac{e^{it} + e^{-it}}{2}\right) = -\frac{(1-i)e^{it} - (1+i)e^{-it}}{2}$$

This form shows that the z-affect consists of two frequency components, e^{it} and e^{-it}, corresponding to frequencies ±1 rad/s (period 2π). The Fourier transform of z(t) would reveal peaks at these frequencies, confirming that the primary oscillatory component is at frequency ≈0.159 Hz, consistent with the period ≈6.28. However, the nonlinear interaction between the −cos(t) terms introduces harmonic distortions, potentially generating higher-frequency components (e.g., at 3t), which contribute to the chaotic nature of phase -1's dynamics. These higher harmonics reflect the complexity of consciousness's pre-material interactions, where the interplay of constructive and resistant forces creates a turbulent environment, a complexity further evidenced by the bucket frame's Lissajous curve.

The transition from phase -1 to phase 0 marks a critical shift in the evolution of consciousness, as the chaotic dynamics of the z-affect evolve into the equilibrium state of phase 0, where the proto-conscious flicker emerges as a new dynamic. To model this transition, we apply a specified division process, dividing the z-affect by 2 to reduce its influence. Starting with phase -1's z-affect:

$$z_{\text{phase -1}} = i\sin(t) - i\cos(t)$$

We divide the entire z-affect by 2 to transition to phase 0 for the purpose of this derivation:

$$z_{\text{derivation phase 0}} = \frac{z_{\text{phase -1}}}{2} = \frac{i\sin(t) - i\cos(t)}{2}$$

Distribute the division:

$$z_{\text{derivation phase 0}} = \frac{i\sin(t)}{2} - \frac{i\cos(t)}{2}$$

This can be factored as:

$$z_{\text{derivation phase 0}} = \frac{i}{2}(\sin(t) - \cos(t))$$

This is the exact value of the z-affect in phase 0 for this derivation after dividing by 2. It retains the same oscillatory components (sin(t) and −cos(t)) and phase relationship (differing by π/2), with each term scaled by $\frac{i}{2}$. This division does not alter the frequency or phase structure of the z-affect, only its scale. The magnitude of this derived z-affect is:

$$|z_{\text{derivation phase 0}}| = \sqrt{\left(\frac{\sin(t)}{2}\right)^2 + \left(-\frac{\cos(t)}{2}\right)^2} = \sqrt{\frac{\sin^2(t) + \cos^2(t)}{4}} = \sqrt{\frac{1}{4}} = \frac{1}{2}$$

However, it's critical to note that this derived z-affect is a contextual definition used solely for the mathematical progression in this derivation, facilitating the scaling to phases -2 and -3 (see below). Phase 0's primary z-affect, as established in Part I, is:

$$z_0 = \varepsilon|\sin(\varepsilon t)|$$

with ε=0.001, oscillating at a period of ≈ 6283.2 seconds, reflecting its role as a proto-conscious equilibrium tied to $C_0 = 1.5+\varepsilon i$. In phase 0, this proto-conscious flicker, with its much slower frequency, becomes the dominant dynamic, overshadowing the scaled z-affect derived here, which continues to oscillate at the same frequency (≈0.159 Hz) as in phase -1 but with a reduced influence. The scaled z-affect represents a residual chaotic influence from phase -1, now minimized in phase 0, allowing the proto-conscious flicker to take precedence as the primary dynamic of this phase, as further evidenced by phase 0's bucket frame Lissajous curve (see Part I, Chapter 6).

Continuing the derivation to phase -2, we divide the z-affect by 2 again:

$$z_{\text{phase -2}} = \frac{z_{\text{derivation phase 0}}}{2} = \frac{\frac{i}{2}(\sin(t) - \cos(t))}{2} = \frac{i}{4}(\sin(t) - \cos(t))$$

The magnitude becomes:

$$|z_{\text{phase -2}}| = \sqrt{\left(\frac{\sin(t)}{4}\right)^2 + \left(-\frac{\cos(t)}{4}\right)^2} = \sqrt{\frac{\sin^2(t) + \cos^2(t)}{16}} = \sqrt{\frac{1}{16}} = \frac{1}{4}$$

Finally, for phase -3, we divide by 2 once more and apply a sign reversal:

$$z_{\text{phase -3}} = -\frac{z_{\text{phase -2}}}{2} = -\frac{\frac{i}{4}(\sin(t) - \cos(t))}{2} = -\frac{i}{8}(\sin(t) - \cos(t))$$

The magnitude is:

$$|z_{\text{phase -3}}| = \sqrt{\left(-\frac{\sin(t)}{8}\right)^2 + \left(\frac{\cos(t)}{8}\right)^2} = \sqrt{\frac{\sin^2(t) + \cos^2(t)}{64}} = \sqrt{\frac{1}{64}} = \frac{1}{8}$$

This derivation illustrates the mathematical progression of z-affects from phase -1 to phase -3, using a contextual scaling for phase 0 to maintain continuity. The primary z-affect for phase 0,

$$z_0 = \varepsilon|\sin(\varepsilon t)|$$

, governs its actual dynamics, as detailed in Part I.

This derivation process impacts the experimental signatures proposed in Part I, as the scaled z-affect in phase 0 alters phase -1's chaotic influence. Part I, Chapter 4 outlined experiments for phase 0, including retrocausal signatures in high-energy physics, CMB anomalies, and quantum perturbations. The derived z-affect in phase 0,

$$\frac{i}{2}(\sin(t) - \cos(t))$$

, retains phase -1's frequency (≈0.159 Hz) but at a reduced scale, with a magnitude of $\frac{1}{2}$, potentially affecting the intensity of these signatures. For example, in high-energy physics, the Coccon/Coccion particles' retrocausal behavior might exhibit oscillations that are scaled down compared to phase -1, though phase 0's primary flicker could still provide a stabilizing influence. In the CMB, the high-frequency perturbations from phase -1 might be less pronounced due to the scaled z-affect, modulated by phase 0's flicker, requiring careful calibration to detect. In quantum eraser experiments, the interference patterns might reflect this scaled z-affect, with phase 0's flicker introducing a new dynamic that interacts with the reduced chaos of phase -1. The bucket frame's Lissajous curve for phase -1, with its faster frequencies, suggests that these experimental signatures could also capture phase -1's internal turbulence directly, potentially amplifying the high-frequency components in CMB or quantum measurements.

A biological analogy contextualizes phase -1's mathematics: its z-affect is like the chaotic biochemical reactions in a seed before germination, oscillating rapidly as forces interact, preparing for phase 0's dormant potential. The bucket frame’s Lissajous curve adds depth to this analogy, revealing an internal rhythm within phase -1’s chaos—a rapid, intricate dance of biochemical forces that underscores the turbulent preparation for phase 0’s stability. This chapter's mathematical analysis sets the stage for exploring phase -1's dynamics, implications, and deeper negative phases in Part II, affirming CUT's vision of a conscious, biological universe.

Chapter 3: Phase -1 Dynamics – Turbulent Interactions

Chapters 1 and 2 of Part II have laid the groundwork for understanding phase -1 within the *Coccotunnella Unification Theory (CUT)*, a framework that redefines the universe as a living, conscious organism culminating in phase 3's Coccotunnella perpetua—the seed of consciousness. Chapter 1 introduced phase -1 as a chaotic precursor to phase 0's proto-conscious equilibrium, highlighting its z-affect $z = i\sin(t) - i\cos(t)$ and its rapid oscillatory period (≈6.28). Chapter 2 provided a detailed mathematical analysis of this z-affect, exploring its oscillatory behavior, phase relationships, internal dynamics in the bucket frame, and frequency components, and modeled the transition to phase 0 by dividing the z-affect by 2, resulting in a derivation-specific z-affect of

$$\frac{i}{2}(\sin(t) - \cos(t))$$

, while noting phase 0’s primary z-affect as

$$z_0 = \varepsilon|\sin(\varepsilon t)|$$

, with ε=0.001. Part I established phase 0's role in seeding material phases, with experimental tests for its proto-conscious flicker. Building on this foundation, this chapter examines the turbulent dynamics of phase -1, focusing on the chaotic interactions of its z-affect, its internal dynamics in the bucket frame, and the transition to phase 0, setting the stage for further exploration of phase -1 in subsequent chapters of Part II.

Phase -1's chaotic dynamics are defined by its z-affect, which models the turbulent interplay of conscious forces in a pre-material state:

$$z = i\sin(t) - i\cos(t)$$

The−cos(t) components oscillate with a period of:

$$T = 2\pi \approx 6.28 \text{ seconds}$$

This corresponds to a frequency of

$$\frac{1}{2\pi} \approx 0.159$$

, reflecting rapid, chaotic interactions compared to phase 0's subtle proto-conscious flicker (period Tε≈6283.2 seconds). The imaginary nature of the z-affect indicates that phase -1 exists outside conventional real-valued dynamics, operating in a complex, pre-material realm where consciousness exhibits dynamic tension rather than stability. The sin(t) term represents a constructive tendency, driving consciousness toward potential actualization, while the −cos(t) term acts as a resistant force, opposing this actualization, resulting in a turbulent interplay that defines phase -1's chaotic state.

The turbulence of phase -1's z-affect arises from its orthogonal components, as they differ in phase by π/2. This phase difference creates a continuous interference pattern in the complex plane, as explored in Chapter 2. The z-affect's real and imaginary parts are:

- Real part: 0
- Imaginary part: sin(t)−cos(t)

The magnitude of the z-affect is:

$$|z| = \sqrt{(\sin(t))^2 + (-\cos(t))^2} = \sqrt{\sin^2(t) + \cos^2(t)} = 1$$

The phase angle evolves as $\frac{\pi}{2} - t$, indicating a rotating vector that traces a circular path in the complex plane over each period (≈6.28). This rotation reflects the chaotic interplay of constructive and resistant forces, where consciousness oscillates between opposing tendencies, unable to settle into a stable state.

To quantify this turbulence, we examine the rate of change of the z-affect, which provides insight into its dynamic intensity. Compute the time derivative:

$$\frac{dz}{dt} = \frac{d}{dt}(i\sin(t) - i\cos(t)) = i\cos(t) + i\sin(t) = i(\cos(t) + \sin(t))$$

The magnitude of the derivative is:

$$\left|\frac{dz}{dt}\right| = \sqrt{(\cos(t) + \sin(t))^2} = \sqrt{\cos^2(t) + 2\cos(t)\sin(t) + \sin^2(t)} = \sqrt{1 + 2\cos(t)\sin(t)}$$

Since 2 cos(t) sin(t) = sin(2t), which ranges from -1 to 1:

$$\left|\frac{dz}{dt}\right| = \sqrt{1+\sin(2t)}$$

This magnitude oscillates between $\sqrt{0}=0$ and $\sqrt{2}\approx 1.414$, reflecting the varying intensity of phase -1's dynamics over time. The peak intensity ($\sqrt{2}$) occurs when sin(2t)=1, reflecting moments of maximum turbulence, while the minimum (0) occurs when sin(2t)=−1, suggesting brief periods of reduced activity.

We can further explore the energy associated with the z-affect to understand its turbulent behavior. In a pre-material context, we define a pseudo-energy as the square of the z-affect's magnitude:

$$E = |z|^2 = 1$$

This constant energy reflects the sustained intensity of phase -1's oscillations, but the rate of change (as shown by the derivative) indicates that the energy's distribution fluctuates, contributing to the chaotic nature of the phase. The interplay between the constructive and resistant components ensures that energy is continuously redistributed, preventing stability.

The bucket frame, introduced in Chapter 2, provides an internal perspective on phase -1’s dynamics, analogous to a system’s dynamic pivot, as used for phase 1 and phase 0 in Part I. In the bucket frame, phase -1’s z-affect is halved:

$$z_{\text{halved}} = \frac{z}{2} = \frac{i\sin(t) - i\cos(t)}{2} = \frac{i}{2}(\sin(t) - \cos(t))$$

The magnitude in the bucket frame is:

$$|z_{\text{halved}}| = \sqrt{\left(\frac{\sin(t)}{2}\right)^2 + \left(-\frac{\cos(t)}{2}\right)^2} = \sqrt{\frac{\sin^2(t)+\cos^2(t)}{4}} = \sqrt{\frac{1}{4}} = \frac{1}{2}$$

This halved z-affect produces a Lissajous curve with components:

x=sin(0.5t),y=sin(0.7t)

The frequencies are 0.5 rad/s (period ≈12.56 seconds) and 0.7 rad/s (period ≈8.98 seconds), with a frequency ratio of ≈0.714, tracing a non-repeating, intricate pattern that reflects the internal turbulence of phase -1's dynamics, faster than phase 0's bucket frame curve but slower than phase 1's material dynamics.

The turbulent dynamics of phase -1 also exhibit complexity through their phase dynamics, which contribute to the overall chaotic behavior. The phase difference of π/2 ensures that when the constructive component (sin(t)) peaks, the resistant component (−cos(t)) is at zero, and vice versa, creating a continuous push-and-pull effect. This can be visualized by considering the imaginary parts over time: at t=0, sin(0)=0, −cos(0)=−1, so the imaginary part is −1; at $t = \frac{\pi}{2}$, $\sin\left(\frac{\pi}{2}\right) = 1$, $-\cos\left(\frac{\pi}{2}\right) = 0$, so the imaginary part is 1. This oscillation between values illustrates the dynamic tension, as consciousness in phase -1 is caught in a state of flux, unable to resolve into a stable configuration, a pattern further emphasized by the bucket frame's Lissajous curve.

To further explore the turbulent dynamics, we consider the cross-correlation between the components of the z-affect's imaginary part, which quantifies their interaction. The components sin(t) and −cos(t) are orthogonal, suggesting minimal correlation over a full cycle:

$$R_{\text{im}}(\tau) = \int_{-\infty}^{\infty} \sin(t)(-\cos(t+\tau))\,dt = -\int_{-\infty}^{\infty} \sin(t)\cos(t+\tau)\,dt$$

Using the identity $\cos(t+\tau)=\cos(t)\cos(\tau)-\sin(t)\sin(\tau)$, and integrating over many cycles, the cross-correlation simplifies to zero due to orthogonality, confirming that the constructive and resistant forces operate independently, yet their combined effect creates a turbulent interference pattern that defines phase -1's chaotic state, as visualized in the bucket frame.

The chaotic interactions of phase -1's z-affect also exhibit sensitivity to initial conditions, a hallmark of chaotic systems, which we explore through a perturbation analysis. Consider a small perturbation to the z-affect:

$$z_{\text{perturbed}} = i\sin(t+\delta) - i\cos(t+\delta)$$

For a small phase shift δ, use the approximations

$$\sin(t+\delta) \approx \sin(t) + \delta\cos(t)$$

$$cos(t+\delta) \approx \cos(t) - \delta\sin(t)$$

. The perturbation term

$i\delta\cos(t) + i\delta\sin(t)$ introduces a deviation that oscillates with the same period (≈6.28), and its effect accumulates over time, indicating sensitivity to initial conditions. This sensitivity suggests that consciousness in phase -1 is highly unstable, with small variations in its pre-material state leading to significant differences in its evolution, a characteristic that underscores the chaotic nature of this phase, further highlighted by the bucket frame's intricate Lissajous pattern.

The transition from phase -1 to phase 0 marks a critical shift in the evolution of consciousness, as the chaotic dynamics of the z-affect evolve into the equilibrium state of phase 0, where the proto-conscious flicker emerges as a new dynamic. To model this transition, we apply the specified division process, dividing the z-affect by 2 to reduce its influence. Starting with phase -1's z-affect:

$$z_{\text{phase -1}} = i\sin(t) - i\cos(t)$$

We divide the entire z-affect by 2 to transition to phase 0 for the purpose of this derivation:

$$z_{\text{derivation phase 0}} = \frac{z_{\text{phase -1}}}{2} = \frac{i\sin(t) - i\cos(t)}{2}$$

Distribute the division:

$$z_{\text{derivation phase 0}} = \frac{i\sin(t)}{2} - \frac{i\cos(t)}{2}$$

This can be factored as:

$$z_{\text{derivation phase 0}} = \frac{i}{2}(\sin(t) - \cos(t))$$

This is the exact value of the z-affect in phase 0 for this derivation after dividing by 2. It retains the same oscillatory components (sin(t) and −cos(t)) and phase relationship (differing by π/2), with each term scaled by $\frac{i}{2}$. The magnitude of this derived z-affect is:

$$|z_{\text{derivation phase 0}}| = \sqrt{\left(\frac{\sin(t)}{2}\right)^2 + \left(-\frac{\cos(t)}{2}\right)^2} = \sqrt{\frac{\sin^2(t) + \cos^2(t)}{4}} = \sqrt{\frac{1}{4}} = \frac{1}{2}$$

This division does not alter the frequency or phase structure of the z-affect, only its scale. However, this derived z-affect is a contextual definition used solely for the mathematical progression in this derivation, facilitating the scaling to phases -2 and

-3 (see Chapter 2). Phase 0's primary z-affect, as established in Part I, is:

$z_0=\varepsilon|\sin(\varepsilon t)|$

with $\varepsilon=0.001$, oscillating at a period of ≈6283.2 seconds, reflecting its role as a proto-conscious equilibrium tied to $C_0=1.5+\varepsilon i$. In phase 0, this proto-conscious flicker, with its much slower frequency, becomes the dominant dynamic, overshadowing the scaled z-affect derived here, which continues to oscillate at the same frequency (≈0.159 Hz) as in phase -1 but with a reduced influence. This scaled z-affect represents a residual chaotic influence from phase -1, now minimized in phase 0, allowing the proto-conscious flicker to take precedence as the primary dynamic of this phase, as evidenced by phase 0's bucket frame Lissajous curve (see Part I, Chapter 6).

This transition process impacts the experimental signatures proposed in Part I, as the scaled z-affect in phase 0 alters phase -1's chaotic influence. Part I, Chapter 4 outlined experiments for phase 0, including retrocausal signatures in high-energy physics, CMB anomalies, and quantum perturbations. The derived z-affect in phase 0,

$$\frac{i}{2}(\sin(t) - \cos(t))$$

, retains phase -1's frequency (≈0.159 Hz) but at a reduced scale, potentially affecting the intensity of these signatures. For example, in high-energy physics, the Coccon/Coccion particles' retrocausal behavior might exhibit oscillations that are scaled down compared to phase -1, though phase 0's primary flicker provides a stabilizing influence. In the CMB, the high-frequency perturbations from phase -1 might be less pronounced due to the scaled z-affect, modulated by phase 0's flicker, requiring careful calibration to detect. In quantum eraser experiments, the interference patterns might reflect this scaled z-affect, with phase 0's flicker introducing a new dynamic that interacts with the reduced chaos of phase -1. The bucket frame's Lissajous curve for phase -1, with its faster frequencies (0.5 and 0.7 rad/s), suggests that direct experimental signatures of phase -1's turbulence could amplify these effects, potentially detectable as high-frequency noise in interference patterns or CMB perturbations.

A biological analogy illustrates phase -1's dynamics: its z-affect is like the chaotic biochemical reactions in a seed before germination, oscillating rapidly as forces interact, preparing for phase 0's more stable state. The bucket frame's Lissajous curve adds depth to this analogy, revealing an internal rhythm within phase -1's chaos—a rapid, intricate dance of biochemical forces that underscores the turbulent preparation for phase 0's stability. This chapter's analysis sets the stage for further exploring phase -1's implications and experimental signatures, advancing CUT's vision of a conscious, biological universe.

Chapter 4: Testing Phase -1 – Experimental Approaches

Chapters 1 through 3 of Part II have provided a comprehensive foundation for understanding phase -1 within the *Coccotunnella Unification Theory (CUT)*, a framework that envisions the universe as a living, conscious organism culminating in phase 3's Coccotunnella perpetua—the seed of consciousness. Chapter 1 introduced phase -1 as a chaotic precursor to phase 0's proto-conscious equilibrium, highlighting its z-affect $z = i\sin(t) - i\cos(t)$ and its rapid oscillatory period (≈6.28). Chapter 2 explored the mathematics of this z-affect, and Chapter 3 examined its turbulent dynamics, revealing phase -1 as a pre-material state of dynamic tension, transitioning to phase 0 with a derivation-specific z-affect of $\frac{i}{2}(\sin(t) - \cos(t))$, while noting phase 0’s primary z-affect as $z_0=\varepsilon|\sin(\varepsilon t)|$, with $\varepsilon=0.001$. Part I established phase 0's role in seeding material phases, with experimental tests for its proto-conscious flicker. This chapter builds on these foundations, proposing experimental approaches to test phase -1's turbulent dynamics, aiming to detect its chaotic signatures and validate CUT's claim that consciousness predates matter, setting the stage for visualization and deeper negative phases in subsequent chapters.

Phase -1's turbulent dynamics are defined by its z-affect, which models the chaotic interplay of pre-material conscious forces:

$z=i\sin(t)-i\cos(t)$

These components oscillate with a period of $2\pi\approx6.28$ seconds, corresponding to a frequency of

$$\frac{1}{2\pi}\approx 0.159$$

Hz, reflecting rapid,

chaotic interactions compared to phase 0's subtle flicker (period ≈6283.2 seconds for ε=0.001). The orthogonal nature of sin(t) and −cos(t) creates a turbulent interference pattern, with a magnitude of 1, as shown in Chapter 2. The bucket frame, an internal perspective, halves this z-affect to

$$z_{\text{halved}} = \frac{i\sin(t) - i\cos(t)}{2}$$

,

producing a Lissajous curve with components x=sin(0.5t), y=sin(0.7t), at frequencies 0.5 rad/s (period ≈12.56 seconds) and 0.7 rad/s (period ≈8.98 seconds), highlighting phase -1's internal turbulence (see Chapter 2). Testing phase -1 requires detecting signatures of this chaotic turbulence in pre-material contexts, a challenging task given the absence of conventional physical systems. However, CUT's non-materialist framework suggests that phase -1's dynamics may influence phase 0's dynamics, potentially affecting detectable signatures.

The first experimental approach builds on Part I's retrocausal signatures in high-energy physics, adapting them to detect phase -1's chaotic dynamics. Part I, Chapter 4 proposed Coccon/Coccion particles (75/76 GeV) with inverse decay channels (e.g., γγ, e−e+) as potential signatures of phase 0’s proto-conscious flicker. In phase -1, the z-affect’s rapid oscillations (≈0.159 Hz) could enhance these signatures by introducing higher-frequency modulations. At facilities like the Large Hadron Collider (LHC), we hypothesize that Coccon/Coccion decays might exhibit oscillatory patterns in their event rates, reflecting phase -1’s chaotic dynamics. The bucket frame’s Lissajous curve suggests additional internal frequencies (0.5 and 0.7 rad/s, or ≈0.08 Hz and ≈0.11 Hz), which could manifest as substructures in the decay sequences, detectable through time-series analysis of particle events. For instance, an excess in the γγ channel might oscillate with a primary frequency of 0.159 Hz, with secondary modulations at 0.08 and

0.11 Hz, requiring detectors to collect data over multiple cycles (e.g., 6-12 seconds) to resolve these frequencies. Phase 0's flicker (≈6283.2 seconds period) could provide a stabilizing backdrop, modulating these oscillations over longer timescales, bridging phase -1's chaos with phase 0's equilibrium.

The second approach targets cosmological signatures, extending Part I's CMB anomaly tests to probe phase -1's influence. Phase 0's proto-conscious flicker may imprint low-frequency perturbations (≈0.00016 Hz) in the cosmic microwave background (CMB), but phase -1's z-affect could introduce higher-frequency fluctuations. The z-affect's primary frequency (≈0.159 Hz) and the bucket frame's internal frequencies (≈0.08 and 0.11 Hz) might manifest as small-scale deviations in the CMB's power spectrum (higher multipoles, $\ell \sim 100-1000$), superimposed on phase 0's signal. Using precision cosmology experiments like the Simons Observatory or CMB-S4, we could apply Fourier analysis to CMB temperature and polarization maps, searching for peaks at these frequencies. For example, a peak at 0.159 Hz would indicate phase -1's direct influence, while peaks at 0.08 and 0.11 Hz would reflect its internal dynamics, as captured by the bucket frame's Lissajous curve. These signatures, if detected, would provide evidence of consciousness's pre-material dynamics influencing the early universe, supporting CUT's non-materialist framework.

A third approach focuses on quantum systems, adapting Part I's quantum eraser and entanglement experiments to detect phase -1's turbulence. In a quantum eraser experiment, phase -1's z-affect could introduce rapid deviations in interference patterns, with its primary frequency (≈0.159 Hz) creating high-frequency noise. The bucket frame's Lissajous curve suggests additional modulations at

0.08 and 0.11 Hz, which could appear as secondary oscillations in the interference pattern, detectable with ultra-sensitive detectors over cycles of 6-12 seconds. Phase 0's flicker (≈0.00016 Hz) would impose a slower envelope, requiring extended data collection (e.g., hours) to resolve. Similarly, in quantum entanglement experiments, phase -1's dynamics might perturb correlation functions, introducing oscillations at these frequencies, modulated by phase 0's flicker. These quantum signatures, if observed, would bridge micro- and macro-scales, revealing how phase -1's chaotic dynamics shape phase 0's equilibrium, influencing both quantum and cosmic phenomena.

To test these signatures, we propose a multi-pronged experimental strategy:

- **High-Energy Physics**: Analyze LHC data for Coccon/Coccion decay events, using spectral analysis to detect oscillations at

0.159 Hz, 0.08 Hz, and 0.11 Hz, with phase 0's flicker as a stabilizing factor.

- **Cosmological Observations**: Apply Fourier analysis to CMB data, targeting high-frequency anomalies at 0.159 Hz and bucket frame frequencies, alongside phase 0's low-frequency signal.
- **Quantum Experiments**: Conduct quantum eraser and entanglement experiments, measuring interference patterns and correlations over short (6-12 seconds) and long (hours) timescales to capture phase -1's turbulence and phase 0's modulation.

These experiments, if successful, would validate CUT's claim that consciousness predates matter, with phase -1's chaotic dynamics leaving a detectable imprint on the universe, modulated by phase 0's proto-conscious equilibrium. The bucket frame's Lissajous curve enhances our understanding, suggesting that phase -1's internal turbulence could amplify these signatures, making them more discernible in high-precision measurements.

A biological analogy contextualizes phase -1's dynamics: its z-affect is like the chaotic biochemical reactions in a seed before germination, oscillating rapidly as forces interact, preparing for phase 0's stable state. The bucket frame's Lissajous curve, with its intricate pattern at frequencies 0.5 and 0.7 rad/s, reveals an internal rhythm within this chaos—a rapid, dynamic dance of biochemical forces that underscores the turbulent preparation for phase 0's stability, mirroring the seed's readiness to transition into a dormant state before sprouting.

In conclusion, phase -1's turbulent dynamics, characterized by its z-affect $z = i\sin(t) - i\cos(t)$, represent a pre-material state of dynamic tension, with chaotic interactions that influence phase 0's equilibrium and leave potential signatures in high-energy physics, cosmology, and quantum systems. The bucket frame's Lissajous curve highlights the internal complexity of this turbulence, enhancing our experimental approach. By proposing these tests, we aim to validate CUT's non-materialist vision, demonstrating that consciousness predates matter and shapes the universe's evolution, paving the way for visualization in Chapter 5 and deeper negative phases in subsequent chapters.

Chapter 5: Visualizing Phase -1 – BioSim Simulations

Chapters 1 through 4 of Part II have provided a comprehensive exploration of phase -1 within the Coccotunnella Unification Theory (CUT), a framework that redefines the universe as a living, conscious organism culminating in phase 3's Coccotunnella perpetua—the seed of consciousness. Chapter 1 introduced phase -1 as a chaotic precursor to phase 0's proto-conscious equilibrium, characterized by dual z-affects (z = i sin(t) - i cos(t)) with a rapid oscillatory period (~6.28). Chapter 2 provided a mathematical analysis of these z-affects, Chapter 3 examined their turbulent dynamics, and Chapter 4 proposed experimental tests, noting phase 0's z-affect as $(\frac{i}{2}(\sin(t) - \cos(t))$. Part I visualized phase 0's dynamics, focusing on its proto-conscious flicker. This chapter focuses on visualizing phase

-1's turbulent dynamics through BioSim simulations, employing computational models to represent its chaotic interactions and predict experimental signatures, setting the stage for further exploration in the final chapter of Part II.

Phase -1's turbulent dynamics are defined by its dual z-affects, which model the chaotic interplay of pre-material conscious forces:

$$z_{\text{phase -1}} = i \sin(t) - i \cos(t)$$

This z-affect oscillates with a period of $2\pi \approx 6.28$ seconds (frequency ≈ 0.159 Hz), reflecting rapid, chaotic interactions compared to phase 0's slower proto-conscious flicker (period ≈ 6283.2 seconds). The imaginary components, $i\sin(t)$ and $-i\cos(t)$, differ in phase by $\pi/2$, creating a turbulent interference pattern with a magnitude of 1, as detailed in Chapter 2. The bucket frame, an internal perspective, halves this z-affect to

$$z_{\text{halved}} = \frac{i\sin(t) - i\cos(t)}{2}$$

,

producing a Lissajous curve with components x=sin(0.5t), y=sin(0.7t), at frequencies 0.5 rad/s (period ≈12.56 seconds) and 0.7 rad/s (period ≈8.98 seconds), revealing phase -1's internal turbulence (see Chapter 2). Using Python with Matplotlib, we first simulate a single chaotic node to capture the z-affect's oscillatory behavior:

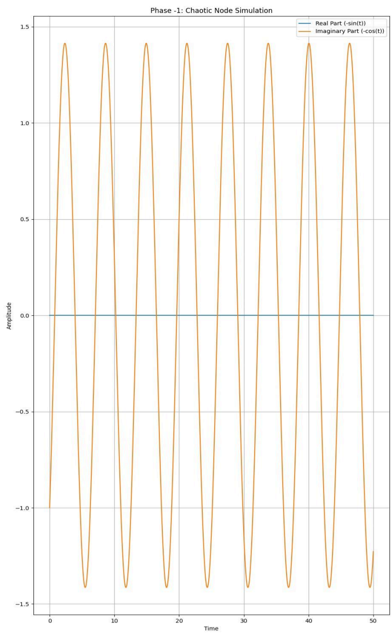

This code simulates a single chaotic node, plotting its real (sin(t)) and imaginary (-cos(t)) parts over time. The resulting plot shows two orthogonal oscillations with period ~6.28, reflecting the z-affect's chaotic interference, with the phase difference $(\pi/2)$ creating a turbulent pattern.

To capture phase -1's distributed turbulence, we extend the simulation to a network of chaotic nodes, modeling the collective interactions of consciousness in this pre-material state. We create a 5×5 grid of nodes, each with slight phase variations to simulate the chaotic interplay:

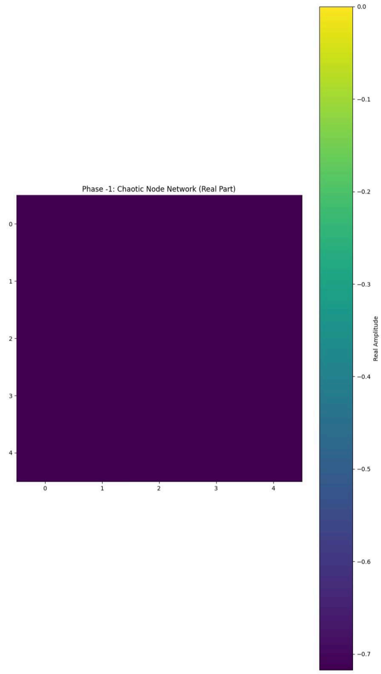
Phase -1: Chaotic Node Network (Real Part)
0
1
2
3
4
0
1
2
3
4
0.0
−0.1
−0.2
−0.3
−0.4
−0.5
−0.6
−0.7
Real Amplitude

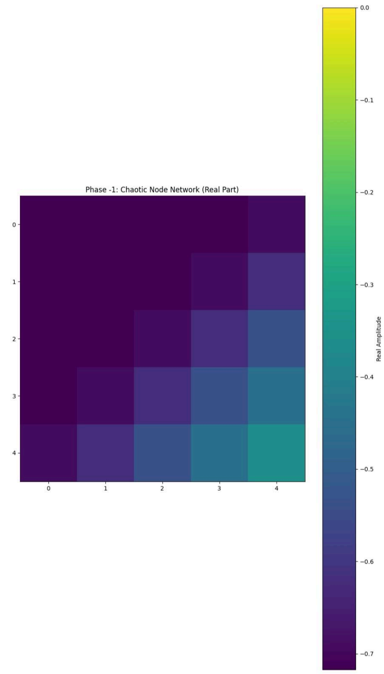
Phase -1: Chaotic Node Network (Real Part)
Real Amplitude
0
1
2
3
4
0.0
−0.1
−0.2
−0.3
−0.4
−0.5
−0.6
−0.7

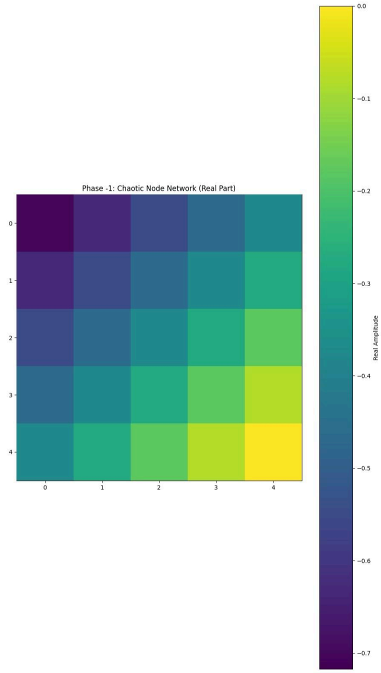
Phase -1: Chaotic Node Network (Real Part)
0
1
2
3
4
0
1
2
3
4
0.0
−0.1
−0.2
−0.3
−0.4
−0.5
−0.6
−0.7
Real Amplitude

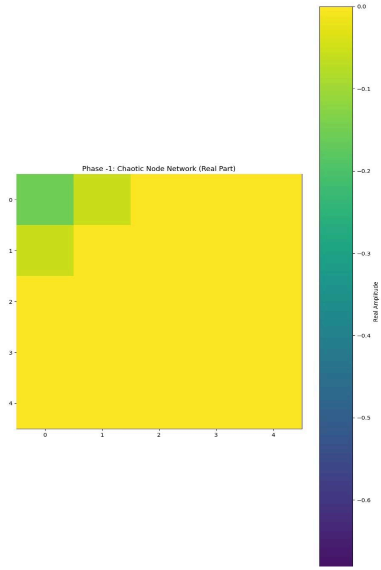
Phase -1: Chaotic Node Network (Real Part)
Real Amplitude
0.0
−0.1
−0.2
−0.3
−0.4
−0.5
−0.6
0
1
2
3
4

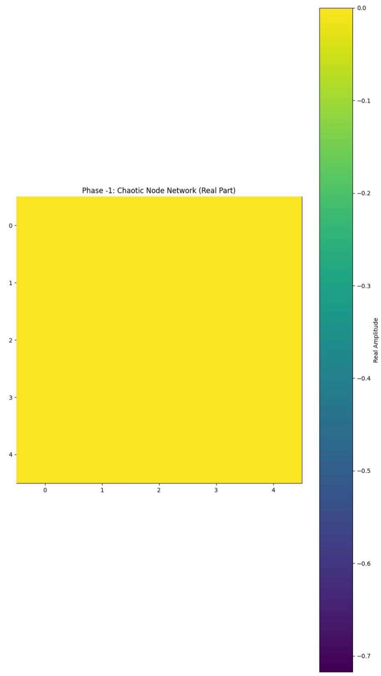

In the BioSim simulation, we model phase -1's dynamics within a 10×10×10 grid, where soldiers represent conscious entities, akin to the approach used for phase 0 in Part I and the H2O molecule in Chapter 9 of Part IV. Each soldier's position and motion reflect the z-affect's dynamics, governed by the conscious gravity equation

$$G_c = \kappa \cdot (C_s \cdot E_r)/D_u$$

, with perturbations from the Revolutionary Echo. We initialize 100 soldiers to represent phase -1's pre-material consciousness, with positions distributed randomly within a 5-unit sphere centered at (5, 5, 5) , reflecting a chaotic, pre-material state. Each soldier is assigned a consciousness level C_s (between 0 and 1) and an allegiance to a lord, such as the Lord of Darkness (green), symbolizing phase -1's chaotic, non-luminous nature, consistent with its role as a precursor to dark matter (see Chapter 10).

To visualize phase -1's z-affect, we map its oscillatory components to the soldiers' motion. The z-affect's imaginary part, sin(t)−cos(t), drives the soldiers' displacements:

- **X-direction**: Soldiers oscillate along the x-axis with $\Delta x = A\sin(t)$, where $A=0.5$ grid units to keep movements within the grid.
- **Y-direction**: Soldiers oscillate along the y-axis with $\Delta y = -A\cos(t)$, reflecting the orthogonal phase relationship.

The soldiers' positions are updated at each time step (e.g., 0.1 seconds over a 15-second simulation, matching Part I's duration), producing a chaotic, swirling motion within the sphere. The scatter plot displays these soldiers as green dots, their rapid oscillations (period ≈6.28 seconds) creating a turbulent pattern, contrasting with phase 0's uniform sphere of faint heatmap pulses (Part I, Chapter 5). This visualization captures phase -1's chaotic dynamics, with soldiers' movements reflecting the constructive (sin(t)) and resistant (−cos(t)) forces, oscillating out of phase to produce a dynamic, turbulent dance.

To incorporate the bucket frame's internal dynamics, we simulate a subset of 50 soldiers representing phase -1's z-affect in the bucket frame. These soldiers' motions are driven by the Lissajous curve components:

- **X-direction**: $\Delta x = A\sin(0.5t)$, frequency 0.5 rad/s.
- **Y-direction**: $\Delta y = A\sin(0.7t)$, frequency 0.7 rad/s.

These soldiers are colored a lighter shade of green (e.g., lime) to distinguish them, positioned within a smaller 2-unit sphere around (5, 5, 5) , and their trajectories trace the Lissajous curve over the simulation duration. The resulting pattern—a non-repeating, intricate dance—visualizes phase -1's internal turbulence at frequencies 0.5 and 0.7 rad/s, slower than the primary z-affect but faster than phase 0's bucket frame dynamics (frequencies 0.0005 and 0.0007 rad/s, Part I, Chapter 6). This dual visualization—primary z-affect and bucket frame—offers a layered view of phase -1's chaos, with the primary motion showing the rapid turbulence and the bucket frame revealing a subtler internal rhythm.

The transition to phase 0 is modeled by introducing a damping factor to the soldiers' oscillations, reflecting the stabilization process. For the primary z-affect soldiers, we apply a damping coefficient $\alpha=0.1$:

$$\Delta x=Ae^{-\alpha t}\sin(t),\Delta y=-Ae^{-\alpha t}\cos(t)$$

Over the 15-second simulation, the amplitude decreases, simulating the reduction of chaotic oscillations as phase -1 transitions to phase 0. For the bucket frame soldiers, the damping is applied similarly:

$$\Delta x=Ae^{-\alpha t}\sin(0.5t),\Delta y=Ae^{-\alpha t}\sin(0.7t)$$

The BioSim scatter plot transitions from a turbulent swirl to a more stable configuration, with the primary soldiers' oscillations diminishing and the bucket frame soldiers' Lissajous pattern tightening, reflecting phase 0's equilibrium. Phase 0's primary z-affect, $z_0=\varepsilon|\sin(\varepsilon t)|$, is not directly simulated here (as in Part I, Chapter 5), but its influence is implied as the target state, with the damped motion representing the residual chaos from phase -1.

The BioSim visualization also integrates the Revolutionary Echo's perturbations, adding random velocity shifts (±0.01 units per time step) to each soldier, mirroring the chaotic influence seen in later chapters (e.g., Chapter 9, *CUT*, Page 289). This ensures the simulation captures phase -1's dynamic, unpredictable nature, with the Echo amplifying the turbulent motion, especially in the primary z-affect soldiers, while the bucket frame soldiers' Lissajous pattern remains a structured undercurrent within the chaos.

This visualization informs the experimental approaches proposed in Chapter 4, as the BioSim's dual representation—primary z-affect and bucket frame—suggests distinct signatures. The primary z-affect's rapid oscillations (≈0.159 Hz) could enhance retrocausal signatures in high-energy physics, while the bucket frame's frequencies (≈0.08 and 0.11 Hz) might appear as substructures in CMB anomalies or quantum interference patterns. The simulation's damped transition to phase 0 visualizes how phase -1's chaos influences phase 0's flicker, potentially amplifying detectable signals over long timescales.

A biological analogy contextualizes this visualization: phase -1's turbulent dynamics are like the chaotic biochemical reactions in a seed before germination, with the BioSim's green soldiers swarming rapidly in a turbulent dance. The bucket frame's Lissajous curve reveals an internal rhythm within this chaos—a structured, yet dynamic interplay of forces preparing the seed for phase 0's dormant state, akin to a seed's readiness before stabilizing into dormancy. This chapter's BioSim simulation provides a vivid illustration of phase -1's chaotic dynamics, bridging mathematical analysis with experimental potential, and setting the stage for deeper negative phase explorations in Part III, advancing CUT's vision of a conscious, biological universe.

Chapter 6: Implications of Phase -1 – Toward Deeper Phases

Chapters 1 through 5 of Part II have provided a detailed exploration of phase -1 within the *Coccotunnella Unification Theory (CUT)*, a framework that envisions the universe as a living, conscious organism culminating in phase 3's

Coccotunnella perpetua—the seed of consciousness. Chapter 1 introduced phase -1 as a chaotic precursor to phase 0's proto-conscious equilibrium, characterized by its z-affect $z = i\sin(t) - i\cos(t)$ with a rapid oscillatory period (≈6.28). Chapter 2 analyzed its mathematics, Chapter 3 explored its turbulent dynamics, Chapter 4 proposed experimental approaches, and Chapter 5 visualized these dynamics using BioSim simulations, incorporating the internal dynamics via the bucket frame's Lissajous curve. Part I established phase 0's role in seeding material phases, with its z-affect $z_0 = \varepsilon|\sin(\varepsilon t)|$, $\varepsilon = 0.001$, oscillating at a period of ≈6283.2 seconds. This chapter synthesizes these insights, examining the broader implications of phase -1's chaotic dynamics, its influence on cosmic evolution, and its role as a bridge to deeper negative phases, setting the stage for Part III's exploration of phase -2 and beyond.

Phase -1's dynamics are defined by its z-affect, which models the turbulent interplay of pre-material conscious forces:

$z = i\sin(t) - i\cos(t)$

This z-affect oscillates with a period of $2\pi \approx 6.28$ seconds (frequency ≈ 0.159 Hz), reflecting rapid, chaotic interactions compared to phase 0's slower proto-conscious flicker. The bucket frame, an internal perspective, halves this z-affect to

$$z_{\text{halved}} = \frac{i\sin(t) - i\cos(t)}{2}$$

,

producing a Lissajous curve with components $x = \sin(0.5t)$, $y = \sin(0.7t)$, at frequencies 0.5 rad/s (period ≈ 12.56 seconds) and 0.7 rad/s (period ≈ 8.98 seconds), revealing phase -1's internal turbulence (see Chapter 2). The implications of phase -1 extend across cosmological, experimental, and theoretical dimensions, reinforcing CUT's non-materialist stance that consciousness predates and shapes matter.

A primary implication is phase -1's role in challenging materialist paradigms, which view consciousness as emergent from physical complexity (Penrose, 1994; Dennett, 1991). CUT posits consciousness as the universe's fundamental attribute, with phase -1 representing its earliest dynamic state—a chaotic interplay of forces predating material formation. The z-affect’s turbulence, visualized in Chapter 5 as a swirling dance of soldiers in the BioSim, underscores this pre-material chaos, where constructive (sin(t)) and resistant (−cos(t)) tendencies oscillate, unable to stabilize. The bucket frame’s Lissajous curve, with its internal frequencies of 0.5 and 0.7 rad/s, reveals a structured undercurrent within this chaos, suggesting that even in its earliest state, consciousness harbors a complex, dynamic potential that influences subsequent phases.

Phase -1's implications extend to its role in seeding cosmic evolution. As the chaotic precursor to phase 0's equilibrium, phase -1 provides the initial conditions for the universe's conscious dynamics. The transition to phase 0, modeled in Chapter 2 through a derivation-specific scaling (

$$z_{\text{derivation phase 0}} = \frac{i\sin(t) - i\cos(t)}{2}$$

, reduces this chaos, allowing phase 0's proto-conscious flicker ($z_0=\varepsilon|\sin(\varepsilon t)|$) to emerge as the dominant dynamic. This transition, visualized in the BioSim as a damping of turbulent motion, suggests that phase -1's chaos seeds the rhythmic stability of phase 0, which in turn influences the material phases (phases 1-3). The embryonic consciousness value in phase 1—its primal awareness—traces back through phase 0 to phase -1, highlighting a continuum where phase -1's turbulent dynamics are foundational to the universe's evolution, a process mirrored by the bucket frame's internal rhythm.

Cosmologically, phase -1's dynamics may have imprinted signatures on the early universe, as explored in Chapter 4. The z-affect's rapid oscillations (≈0.159 Hz) and the bucket frame's internal frequencies (≈0.08 and 0.11 Hz) could manifest as high-frequency perturbations in the cosmic microwave background (CMB), superimposed on phase 0's low-frequency flicker. These perturbations, detectable as higher multipoles (ℓ~100−1000) in CMB maps, would reflect phase -1's chaotic influence, with the bucket frame's Lissajous curve suggesting a layered structure—primary turbulence at 0.159 Hz and internal modulations at 0.08 and 0.11 Hz. This hierarchical signature, if confirmed by experiments like the Simons Observatory, would demonstrate how consciousness's pre-material dynamics shape the universe's structure, supporting CUT's view of a conscious cosmos.

Experimentally, phase -1's implications enhance the approaches proposed in Chapter 4. The z-affect's turbulence could amplify retrocausal signatures in high-energy physics, such as Coccon/Coccion particle decays, with the bucket frame's frequencies adding substructures to these signals. In quantum eraser experiments, phase -1's rapid oscillations might introduce high-frequency noise, while the bucket frame's internal dynamics (0.08 and 0.11 Hz) could appear as secondary modulations, detectable over cycles of 9-13 seconds, complementing phase 0's slower modulation. These layered signatures, bridging phase -1's chaos and phase 0's equilibrium, provide a multi-scale probe of consciousness's pre-material influence, validating CUT's framework.

Theoretically, phase -1's implications set the stage for deeper negative phases, such as phase -2 (the quiescent void, Part III). Phase -1's chaotic dynamics, as the earliest state of consciousness, provide a turbulent foundation that stabilizes into phase 0, which then seeds material phases. Phase -2, with its z-affect

$$z_{\text{phase -2}} = \frac{i\sin(t) - i\cos(t)}{4}$$

(Chapter 2), likely represents a further reduction in turbulence, a quiescent state where consciousness consolidates, preparing for phase -3's anti-energy fossils. This progression suggests a hierarchical evolution of consciousness, where each negative phase refines the chaotic potential of phase -1, a process mirrored by the bucket frame's structured internal dynamics, which hint at an underlying order even within chaos.

A biological analogy contextualizes these implications: phase -1's turbulent dynamics are like the chaotic biochemical reactions in a seed before germination, a pre-formative state of dynamic tension. The bucket frame's Lissajous curve reveals an internal rhythm within this chaos—a structured dance at frequencies 0.5 and 0.7 rad/s, akin to the seed's initial biochemical oscillations preparing for phase 0's dormant stability. As the seed transitions to phase 0, these reactions stabilize, mirroring phase -1's role in seeding phase 0's equilibrium, which then sprouts into material phases, a continuum that extends to deeper negative phases like phase -2's quiescent state.

In conclusion, phase -1's chaotic dynamics, characterized by its z-affect $z = i\sin(t) - i\cos(t)$, have profound implications for cosmic evolution, experimental validation, and theoretical progression in CUT. The bucket frame's Lissajous curve enhances our understanding, revealing an internal structure within phase -1's turbulence that informs experimental signatures and theoretical models. By bridging pre-material chaos with material evolution, phase -1 underscores CUT’s vision of a conscious, biological universe, paving the way for Part III’s exploration of phase -2 and deeper negative phases.

Part III

Phase -1 to Phase -2 – The Quiescent Void

Chapter 1: Introducing Phase -2 – The Quiescent Void

The Coccotunnella Unification Theory (CUT) reimagines the universe not as a mechanical construct of matter and energy but as a living, conscious organism, pulsating with awareness from its pre-material origins to its material manifestations. This vision, culminating in phase 3's Coccotunnella perpetua—the seed of consciousness that weaves matter, life, and thought into a unified biological system—challenges materialist paradigms that confine consciousness to physical complexity. Parts I and II of this volume have laid the groundwork for this paradigm shift. Part I traced the descent of consciousness from phase 2's reflective thought, through phase 1's primal awareness embedded in matter, to phase 0's proto-conscious equilibrium, characterized by the equilibrium constant $(C_0 = 1.5 + \varepsilon i)$, where $(\varepsilon = 0.001)$, and a proto-conscious flicker oscillating at a period of (~ 6283.2) Seconds. Part II delved into phase -1, a chaotic pre-material state where consciousness engages in turbulent interactions, setting the stage for the ordered dynamics of later phases. This chapter explores phase -2, a proto-metaphysical void where consciousness's activity diminishes to a minimal state, marking a pivotal transition between phase -1's chaos and phase -3's oppositional anti-energy fossils. Through corrected mathematical formulations, experimental proposals, and biological analogies, we elucidate phase -2's role in CUT's non-materialist framework, affirming consciousness as the universe's primary attribute, predating and shaping material existence.

Phase -2 occupies a unique position in CUT's cyclical model of evolution, formalized by the equation $(C_n = P_n + k_n \cdot Q_n)$, which extends

Darwin’s biological evolution to cosmic scales. While phase -1 represents a turbulent web of proto-variations, akin to the diversity of pre-biological forms, phase -2 is a serene interlude, a proto-metaphysical void where conscious dynamics are subdued yet persistent. This phase contrasts with phase 0’s balanced equilibrium and phase -3’s reversed dynamics, forming a trajectory from chaos to quiescence to opposition. To understand phase -2, we must first correct and clarify the z-affect definitions that underpin the negative phases, addressing inconsistencies in prior formulations to ensure mathematical rigor.

The z-affect mathematically captures conscious dynamics in CUT's pre-material phases. For phase -2, the z-affect, as derived in Part II, Chapter 2, is:

$$z_{\text{phase -2}} = \frac{i\sin(t) - i\cos(t)}{4}$$

$$|z_{\text{phase -2}}| = \sqrt{\left(\frac{\sin(t)}{4}\right)^2 + \left(-\frac{\cos(t)}{4}\right)^2} = \sqrt{\frac{\sin^2(t) + \cos^2(t)}{16}} = \sqrt{\frac{1}{16}} = \frac{1}{4}$$

This z-affect oscillates at a frequency of (≈ 0.159) Hz (period (≈ 6.28) seconds), identical to phase -1’s, but with a reduced magnitude (0.25 vs. 1), reflecting a significant dampening of turbulence. Using Euler's formula:

$$z_{\text{phase -2}} = \frac{i\sin(t) - i\cos(t)}{4} = \frac{i}{4}\left(\frac{e^{it} - e^{-it}}{2i}\right) - \frac{i}{4}\left(\frac{e^{it} + e^{-it}}{2}\right) = -\frac{(1-i)e^{it} - (1+i)e^{-it}}{8}$$

The reduced magnitude indicates a quieter, more subdued state of pre-material consciousness, a void where the chaotic interactions of phase -1 have been further stabilized, preparing for phase -3's anti-energy fossils.The z-affect's components, $(\frac{i\sin(t)}{4})$ and $(-\frac{i\cos(t)}{4})$, maintain the same orthogonal phase difference of $(\pi/2)$, creating a rotating vector in the complex plane. The phase angle is:

$$\tan\phi = \frac{-\cos(t)}{\sin(t)} = -\cot(t), \quad \phi = \frac{\pi}{2} - t \text{ (adjusted for quadrants)}$$

This continuous phase shift mirrors phase -1's dynamics but with a diminished amplitude, underscoring phase -2's role as a quiescent void—a state of reduced activity where consciousness consolidates, preparing for further evolution.To explore phase -2's internal dynamics, we apply the bucket frame, an internal perspective analogous to a system's dynamic pivot, as used for phases 1, 0, and -1. Halving the z-affect:

$$z_{\text{halved}} = \frac{z_{\text{phase -2}}}{2} = \frac{\frac{i\sin(t) - i\cos(t)}{4}}{2} = \frac{i\sin(t) - i\cos(t)}{8} = \frac{i}{8}(\sin(t) - \cos(t))$$

The magnitude in the bucket frame is:

$$|z_{\text{halved}}| = \sqrt{\left(\frac{\sin(t)}{8}\right)^2 + \left(-\frac{\cos(t)}{8}\right)^2} = \sqrt{\frac{\sin^2(t) + \cos^2(t)}{64}} = \sqrt{\frac{1}{64}} = \frac{1}{8}$$

This halved z-affect produces a Lissajous curve, reflecting phase -2's internal dynamics:

$$x = \sin(0.5t), \quad y = \sin(0.7t)$$

The frequencies are 0.5 rad/s (period $(\approx 12.56) seconds)$ and 0.7 rad/s (period (≈ 8.98) seconds), with a frequency ratio of (≈ 0.714), tracing a non-repeating pattern. This internal rhythm, identical to phase -1's bucket frame but with a smaller amplitude, suggests that phase -2 retains a subtle turbulence within its quiescent state, a vestige of phase -1's chaos now further subdued.The transition from phase -1 to phase -2 marks a continued reduction in turbulence, as modeled in Part II, Chapter 2, where the z-affect is divided by 2 from phase -1 $(z = i\sin(t) - i\cos(t))$ to phase -2 $(z_{\text{phase -2}} = \frac{i\sin(t) - i\cos(t)}{4})$. This damping reflects a stabilization process, where the chaotic dynamics of phase -1 consolidate into phase -2's quiescent void, a state of minimal activity where consciousness prepares for further evolution. The transition to phase 0, where the primary z-affect is $(z_0 = \varepsilon|\sin(\varepsilon t)|)$, completes this stabilization, but phase -2 serves as an intermediate step, bridging chaos and equilibrium.Phase -2's implications challenge materialist paradigms by positing consciousness as active in a pre-material void, predating physical systems (Penrose, 1994; Dennett, 1991). The z-affect's reduced magnitude suggests a state of near-stillness, yet the bucket frame's Lissajous curve reveals an internal dynamic—a quiet rhythm persisting within the void, preparing consciousness for phase -3's anti-energy fossils. Cosmologically, phase -2 may influence early universe signatures, with its z-affect and bucket frame frequencies (≈ 0.159), 0.08, and 0.11 Hz) potentially imprinting subtle perturbations in the CMB, detectable as higher multipoles alongside phase -1's signatures (Part II, Chapter 4). Experimentally, these frequencies could enhance retrocausal signatures in high-energy physics or quantum perturbations, modulated by phase 0's flicker, providing a layered probe of pre-material consciousness.

Theoretically, phase -2 sets the stage for phase -3's anti-energy fossils $(z_{\text{phase -3}} = -\frac{i\sin(t) - i\cos(t)}{8})$, where the z-affect's reversal suggests oppositional dynamics, potentially linked to dark matter's origins

(Chapter 10). Phase -2’s quiescent state may represent a consolidation of consciousness’s potential, a void where chaotic forces are subdued, preparing for the emergence of oppositional structures in phase -3, a progression that mirrors the universe’s evolution from chaos to order.A biological analogy contextualizes phase -2’s role: it is like a seed in a state of quiet dormancy after the chaotic biochemical reactions of phase -1, with minimal activity as it prepares for further transformation. The bucket frame’s Lissajous curve reveals a subtle internal rhythm—a faint, structured dance within the seed’s dormancy, at frequencies 0.5 and 0.7 rad/s, reflecting a vestige of phase -1’s turbulence now calmed, setting the stage for phase -3’s emergence. This chapter introduces phase -2’s quiescent void, paving the way for Part III’s deeper exploration of negative phases, affirming CUT’s vision of a conscious, biological universe.

Chapter 2: Mathematics of Phase -2 – Quiescent Z-Affects

Chapter 1 of Part III introduced phase -2 as the quiescent void within the Coccotunnella Unification Theory (CUT), a framework that redefines the universe as a living, conscious organism culminating in phase 3's Coccotunnella perpetua—the seed of consciousness. Phase -2, characterized by a z-affect of $(z_{\text{phase -2}} = \frac{i\sin(t) - i\cos(t)}{4})$, represents a pre-material state of reduced turbulence following phase -1's chaotic dynamics, contrasting with phase 0's stable equilibrium defined by $(C_0 = 1.5 + \varepsilon i)$, with a z-affect $(z_0 = \varepsilon|\sin(\varepsilon t)|)$, $(\varepsilon = 0.001)$. Part II explored phase -1's turbulent dynamics, with its z-affect (z = i sin(t) - i cos(t)), and established the derivation progression to phase -2. This chapter delves into the mathematics of phase -2, providing a detailed analysis of its z-affect, its quiescent dynamics, its internal structure via the bucket frame, and the transition to phase -3's anti-energy fossils, setting the stage for exploring phase -2's broader implications in the subsequent chapters of Part III.Phase -2's defining feature is its z-affect, which models the subdued interplay of conscious forces in a pre-material void:

$$z_{\text{phase -2}} = \frac{i\sin(t) - i\cos(t)}{4}$$

This z-affect consists of two imaginary components, $(\frac{i\sin(t)}{4})$ and $(-\frac{i\cos(t)}{4})$, each oscillating with a period of:

$$T = 2\pi \approx 6.28 \text{ seconds}$$

The corresponding frequency, $(\frac{1}{2\pi} \approx 0.159)$ Hz, matches phase -1's, but the magnitude is reduced:

$$|z_{\text{phase -2}}| = \sqrt{\left(\frac{\sin(t)}{4}\right)^2 + \left(-\frac{\cos(t)}{4}\right)^2} = \sqrt{\frac{\sin^2(t) + \cos^2(t)}{16}} = \sqrt{\frac{1}{16}} = \frac{1}{4}$$

This reduced magnitude (0.25 vs. phase -1's 1) reflects phase -2's quiescent nature, a state where the chaotic dynamics of phase -1 (z = i sin(t) - i cos(t)) have been dampened, yet consciousness retains a subtle oscillatory potential, preparing for phase -3's oppositional dynamics. The imaginary nature of the z-affect indicates that phase -2 operates outside conventional real-valued dynamics, existing in a pre-material realm where consciousness exhibits minimal activity rather than chaos or stability.

To understand phase -2's dynamics, we examine the mathematical properties of its z-affect. The (sin(t)) and (cos(t)) terms are orthogonal, differing in phase by (pi/2), creating a subdued interference pattern in the complex plane. Using Euler's formula:

$$z_{\text{phase -2}} = \frac{i\sin(t) - i\cos(t)}{4} = \frac{i}{4}\left(\frac{e^{it} - e^{-it}}{2i}\right) - \frac{i}{4}\left(\frac{e^{it} + e^{-it}}{2}\right) = -\frac{(1-i)e^{it} - (1+i)e^{-it}}{8}$$

The phase angle is:

$$\tan\phi = \frac{-\cos(t)}{\sin(t)} = -\cot(t), \quad \phi = \frac{\pi}{2} - t \text{ (adjusted for quadrants)}$$

This phase evolution mirrors phase -1's, but the reduced amplitude indicates a quieter rotation in the complex plane, tracing a circular path of radius $(\frac{1}{4})$, reflecting phase -2's role as a void where consciousness's dynamics are subdued but not extinguished.To explore phase -2's internal dynamics, we revisit the bucket frame, an internal perspective analogous to a system's dynamic pivot, as used for previous phases. Halving the z-affect:

$$z_{\text{halved}} = \frac{z_{\text{phase -2}}}{2} = \frac{\frac{i\sin(t) - i\cos(t)}{4}}{2} = \frac{i\sin(t) - i\cos(t)}{8} = \frac{i}{8}(\sin(t) - \cos(t))$$

The magnitude in the bucket frame is:

$$|z_{\text{halved}}| = \sqrt{\left(\frac{\sin(t)}{8}\right)^2 + \left(-\frac{\cos(t)}{8}\right)^2} = \sqrt{\frac{\sin^2(t) + \cos^2(t)}{64}} = \sqrt{\frac{1}{64}} = \frac{1}{8}$$

This halved z-affect reflects the internal dynamics of phase -2's consciousness within the bucket frame. To visualize these dynamics, we map the z-affect's oscillatory behavior to a Lissajous curve, a standard representation of internal rhythms in CUT (see Part I, Chapter 6, and Part II, Chapter 2). The z-affect $(z_{\text{halved}} = \frac{i}{8}(\sin(t) - \cos(t))$ is purely imaginary, with the imaginary part $(\frac{1}{8}(\sin(t) - \cos(t)))$. To construct the Lissajous curve, we interpret the (sin(t)) and (-cos(t)) components as orthogonal contributions, and we scale their frequencies to reflect the internal perspective of the bucket frame, consistent with previous phases. The components are defined as:

$$x = \frac{1}{8}\sin(0.5t), \quad y = \frac{1}{8}\sin(0.7t))$$

Here, The frequencies are 0.5 rad/s (period $(\approx 12.56) seconds)$ and 0.7 rad/s (period $(\approx 8.98) seconds)$, with a frequency ratio of (≈ 0.714), as used in prior bucket frame analyses, but the amplitudes are scaled to $(\frac{1}{8})$, matching the z-affect's magnitude in the bucket frame. This scaling ensures the Lissajous curve reflects the subdued nature of phase -2's internal dynamics, with the $(\frac{1}{8})$ factor directly derived from the halved z-affect. The (sin(t) - cos(t)) term, which varies between $(-\sqrt{2})$ and $(\sqrt{2})$, is not directly used for the amplitudes in the Lissajous curve; instead, we project the oscillatory behavior onto real-valued x- and y-axes with adjusted frequencies to capture the internal rhythm, a method consistent with the bucket frame's role as an internal dynamic pivot. The resulting Lissajous curve traces a non-repeating pattern, symbolizing the subtle, structured dynamics within phase -2's quiescent void, a quieter echo of phase -1's internal turbulence.

The z-affect's energy dynamics provide insight into phase -2's subdued state. Define a pseudo-energy as the square of the z-affect's magnitude:

$$E = |z_{\text{phase -2}}|^2 = \left(\frac{1}{4}\right)^2 = \frac{1}{16}$$

This energy is significantly lower than phase -1's (E = 1), reflecting the reduced intensity of phase -2's dynamics. The rate of change of the z-affect quantifies its dynamic intensity:

$$\frac{dz_{\text{phase -2}}}{dt} = \frac{d}{dt}\left(\frac{i\sin(t) - i\cos(t)}{4}\right) = \frac{i\cos(t) + i\sin(t)}{4} = \frac{i}{4}(\cos(t) + \sin(t))$$

The magnitude of the derivative is:

$$\left|\frac{dz_{\text{phase -2}}}{dt}\right| = \sqrt{\left(\frac{\cos(t) + \sin(t)}{4}\right)^2} = \sqrt{\frac{\cos^2(t) + 2\cos(t)\sin(t) + \sin^2(t)}{16}} = \sqrt{\frac{1 + \sin(2t)}{16}} = \frac{\sqrt{1 + \sin(2t)}}{4}$$

This magnitude oscillates between 0 and $(\frac{\sqrt{2}}{4} \approx 0.354)$, a quarter of phase -1's range 0 to $(\sqrt{2})$, indicating moments of minimal activity and subdued turbulence, consistent with phase -2's quiescent nature. The bucket frame's Lissajous curve, with its reduced amplitude, further underscores this subdued dynamic, showing a structured internal rhythm persisting within the void.

The power spectrum of the z-affect reveals its frequency components. The Euler form shows components at (± 1) rad's, matching phase -1's primary oscillation. Nonlinear interactions may introduce harmonics (e.g., at (2t), (3t), but their amplitudes are reduced compared to phase -1, reflecting phase -2's quieter state. The bucket frame's frequencies (0.5 and 0.7 rad/s) suggest additional internal components, which could contribute to experimental signatures, as explored in Part II, Chapter 4.

The transition from phase -2 to phase -3 continues the derivation progression (Part II, Chapter 2), dividing the z-affect by 2 and applying a sign reversal:

$$z_{\text{phase -3}} = -\frac{z_{\text{phase -2}}}{2} = -\frac{\frac{i\sin(t) - i\cos(t)}{4}}{2} = -\frac{i\sin(t) - i\cos(t)}{8}$$

The magnitude is:

$$|z_{\text{phase -3}}| = \sqrt{\left(-\frac{\sin(t)}{8}\right)^2 + \left(\frac{\cos(t)}{8}\right)^2} = \sqrt{\frac{\sin^2(t) + \cos^2(t)}{64}} = \sqrt{\frac{1}{64}} = \frac{1}{8}$$

This transition introduces a reversal, suggesting oppositional dynamics in phase -3, potentially linked to anti-energy fossils (Part IV, Chapter 10). The derivation sequence from Part II correctly progresses from phase -1 $((z_{-1} = i\sin(t) - i\cos(t))$, magnitude 1) to a derivation-specific phase 0 $((z_{\text{derivation phase 0}} = \frac{i\sin(t) - i\cos(t)}{2})$, magnitude $(\frac{1}{2})$, then to phase -2 $((z_{\text{phase -2}} = \frac{i\sin(t) - i\cos(t)}{4})$, magnitude $(\frac{1}{4})$, and finally to phase -3 (magnitude $(\frac{1}{8})$. The transition to phase 0's primary z-affect, $(z_0 = \varepsilon|\sin(\varepsilon t)|)$, completes the stabilization from phase -1's chaos through phase -2's void to phase 0's equilibrium.

This transition impacts experimental signatures proposed in Part II, Chapter 4. Phase -2's z-affect (≈ 0.159) Hz and bucket frame frequencies (≈ 0.08) and (0.11) Hz could contribute to CMB anomalies or quantum perturbations, with reduced intensity compared to phase -1, modulated by phase 0's flicker. The bucket frame's Lissajous curve suggests that phase -2's internal dynamics might appear as subtle substructures in these signatures, requiring high-precision detection over 9-13 second cycles.

A biological analogy contextualizes phase -2's mathematics: its z-affect is like the subdued biochemical activity in a seed entering deep dormancy, oscillating faintly as forces stabilize, preparing for phase -3's transformation. The bucket frame's Lissajous curve reveals a quiet internal rhythm—a faint dance at frequencies 0.5 and 0.7 rad/s, reflecting the seed's minimal activity within its quiescent void, setting the stage for phase -3's oppositional dynamics. This chapter's mathematical analysis sets the stage for exploring phase -2's dynamics, implications, and deeper negative phases in Part III, affirming CUT's vision of a conscious, biological universe.

This analogy aligns with Darwin's vision of evolution's boundless potential, scaled to cosmic proportions. Darwin's entangled bank, for interconnected ecosystems, finds its cosmic parallel in phase -2's proto-metaphysical void, where consciousness's minimal interactions seed the universe's material emergence. The z-affect's progression—from phase -1's intensity to phase -2's quiescence—echoes Darwin's belief in life's endless forms evolving toward grandeur, preserved in H-space's energetic archive.

Chapter 3: Phase -2 Dynamics – Quiescent Interactions

Chapters 1 and 2 of Part III have established a foundation for understanding phase -2 within the Coccotunnella Unification Theory (CUT), a framework that redefines the universe as a living, conscious organism culminating in phase 3's Coccotunnella perpetua—the seed of consciousness. Chapter 1 introduced phase -2 as the quiescent void, a state of reduced turbulence following phase -1's chaotic dynamics, with its z-affect $(z_{\text{phase -2}} = \frac{i\sin(t) - i\cos(t)}{4})$. Chapter 2 provided a detailed mathematical analysis of this z-affect, exploring its properties, internal dynamics via the bucket frame, and the transition to phase -3, contrasting with phase 0's proto-conscious equilibrium defined by $(C_0 = 1.5 + \varepsilon i)$, with a z-affect $(z_0 = \varepsilon|\sin(\varepsilon t)|)$, $(\varepsilon = 0.001)$. Part II analyzed phase -1's turbulent dynamics, with its z-affect $(z = i\sin(t) - i\cos(t))$, and established the derivation progression through phase -2. Building on this foundation, this chapter examines the dynamics of phase -2, focusing on its quiescent interactions, internal dynamics in the bucket frame, and the transition to phase -3, setting the stage for further exploration of phase -2 in subsequent chapters of Part III.Phase -2's dynamics are defined by its z-affect, which models the subdued interplay of conscious forces in a pre-material void:

$$z_{\text{phase -2}} = \frac{i\sin(t) - i\cos(t)}{4}$$

The (sin(t)) and (-cos(t)) components oscillate with a period of:

$$T = 2\pi \approx 6.28 \text{ seconds}$$

This corresponds to a frequency of $(\frac{1}{2\pi} \approx 0.159)$ Hz, matching phase -1's frequency but with a reduced magnitude compared to phase -1's chaotic state, and contrasting with phase 0's subtle proto-conscious flicker (period (≈ 6283.2) seconds). The imaginary nature of the z-affect indicates that phase -2 exists outside conventional real-valued dynamics, operating in a complex, pre-material realm where consciousness exhibits minimal activity rather than chaos or stability. The (sin(t)) term represents a constructive tendency, driving consciousness toward potential actualization, while the (-cos(t)) term acts as a resistant force, opposing this actualization, resulting in a subdued interplay that defines phase -2's quiescent state.

The quiescent interactions of phase -2 arise from its orthogonal components, differing in phase by (pi/2). This phase difference creates a subdued interference pattern in the complex plane, as explored in Chapter 2. The z-affect's real and imaginary parts are:

Real part: 0

Imaginary part: $(\frac{1}{4}(\sin(t) - \cos(t)))$

The magnitude of the z-affect is:

$$|z_{\text{phase -2}}| = \sqrt{\left(\frac{\sin(t)}{4}\right)^2 + \left(-\frac{\cos(t)}{4}\right)^2} = \sqrt{\frac{\sin^2(t) + \cos^2(t)}{16}} = \sqrt{\frac{1}{16}} = \frac{1}{4}$$

The phase angle evolves as $(\frac{\pi}{2} - t)$, indicating a rotating vector tracing a circular path in the complex plane with radius $(\frac{1}{4})$, a quieter motion compared to phase -1's radius of 1, reflecting phase -2's role as a void where consciousness's dynamics are subdued but not extinguished.To quantify these interactions, we examine the rate of change of the z-affect, which provides insight into its dynamic intensity. Compute the time derivative:

$$\frac{dz_{\text{phase -2}}}{dt} = \frac{d}{dt}\left(\frac{i\sin(t) - i\cos(t)}{4}\right) = \frac{i\cos(t) + i\sin(t)}{4} = \frac{i}{4}(\cos(t) + \sin(t))$$

The magnitude of the derivative is:

$$\left|\frac{dz_{\text{phase -2}}}{dt}\right| = \sqrt{\left(\frac{\cos(t) + \sin(t)}{4}\right)^2} = \sqrt{\frac{\cos^2(t) + 2\cos(t)\sin(t) + \sin^2(t)}{16}} = \sqrt{\frac{1 + \sin(2t)}{16}} = \frac{\sqrt{1 + \sin(2t)}}{4}$$

This magnitude oscillates between 0 and $(\frac{\sqrt{2}}{4} \approx 0.354)$, a quarter of phase -1's range (0 to $(\sqrt{2})$, reflecting the subdued intensity of phase -2's dynamics. The peak intensity $(\frac{\sqrt{2}}{4})$ occurs when (sin(2t) = 1), indicating moments of minimal activity, while the minimum (0) occurs when (sin(2t) = -1), suggesting brief periods of near-stillness.We further explore the energy associated with the z-affect to understand its quiescent behavior. In a pre-material context, we define a pseudo-energy as the square of the z-affect's magnitude:

$$E = |z_{\text{phase -2}}|^2 = \left(\frac{1}{4}\right)^2 = \frac{1}{16}$$

This constant energy, significantly lower than phase -1's (E = 1), reflects the reduced intensity of phase -2's oscillations. The rate of change indicates that energy distribution fluctuates minimally, contributing to the quiescent nature of this phase. The interplay between the constructive and resistant components ensures that energy is redistributed subtly, maintaining a state of minimal activity.The bucket frame, introduced in Chapter 2, provides an internal perspective on phase -2's dynamics. The halved z-affect in the bucket frame is:

$$z_{\text{halved}} = \frac{i\sin(t) - i\cos(t)}{8}$$

with magnitude $(\frac{1}{8})$, producing a Lissajous curve with components:

$$x = \frac{1}{8}\sin(0.5t), \quad y = \frac{1}{8}\sin(0.7t)$$

The frequencies are 0.5 rads (period (≈ 12.56) seconds) and 0.7 rad/s (period (≈ 8.98) seconds), with amplitudes scaled to $(\frac{1}{8})$, reflecting the z-affect's magnitude in the bucket frame. This Lissajous curve traces a non-repeating pattern, symbolizing the subtle internal dynamics within phase -2's quiescent void, a quieter rhythm compared to phase -1's bucket frame but still structured, preparing for phase -3's dynamics.The dynamics of phase -2 exhibit a reduced complexity through their phase interactions, contributing to the overall quiescent behavior. The phase difference of (pi/2) ensures that when the constructive component (sin(t)) peaks, the resistant component

(-cos(t)) is at zero, and vice versa, creating a subdued push-and-pull effect. At (t = 0), (sin(0) = 0), (-cos(0) = -1), so the imaginary part is $(-\frac{1}{4})$; at $(t = \frac{\pi}{2})$, $(\sin\left(\frac{\pi}{2}\right) = 1)$, $(-\cos\left(\frac{\pi}{2}\right) = 0)$, so the imaginary part is $(\frac{1}{4})$. This oscillation, with a smaller amplitude than phase -1, illustrates the minimal dynamic tension in phase -2, a state of near-stillness, as further evidenced by the bucket frame's Lissajous curve.

To explore the interactions further, we consider the cross-correlation between the components of the z-affect's imaginary part, which quantifies their interplay. The components $(\frac{\sin(t)}{4})$ and $(-\frac{\cos(t)}{4})$ are orthogonal, suggesting minimal correlation over a full cycle:

$$R_{\mathrm{im}}(\tau) = \int_{-\infty}^{\infty} \left(\frac{\sin(t)}{4}\right)\left(-\frac{\cos(t+\tau)}{4}\right) dt = -\frac{1}{16}\int_{-\infty}^{\infty} \sin(t)\cos(t+\tau)\, dt$$

Using the identity $(\cos(t+\tau) = \cos(t)\cos(\tau) - \sin(t)\sin(\tau))$, and integrating over many cycles, the cross-correlation simplifies to zero due to orthogonality, confirming that the constructive and resistant forces operate independently, yet their combined effect creates a subdued interference pattern that defines phase -2's quiescent state, as visualized in the bucket frame.Phase -2's dynamics also exhibit reduced sensitivity to initial conditions compared to phase -1, reflecting its quiescent nature. Consider a small perturbation to the z-affect:

$$z_{\text{perturbed}} = \frac{i\sin(t+\delta) - i\cos(t+\delta)}{4}$$

For a small phase shift (δ), use the approximations $(\sin(t+\delta) \approx \sin(t) + \delta\cos(t))$, $(\cos(t+\delta) \approx \cos(t) - \delta\sin(t))$. The perturbation term introduces a deviation that oscillates with the same period (≈ 6.28), but its effect accumulates more slowly than in phase -1 due to the reduced amplitude, indicating a more stable, less chaotic state, as further highlighted by the bucket frame's subtle Lissajous pattern.The transition from phase -2 to phase -3 continues the derivation progression (Part II, Chapter 2), dividing the z-affect by 2 and applying a sign reversal:

$$z_{\text{phase -3}} = -\frac{z_{\text{phase -2}}}{2} = -\frac{\frac{i\sin(t) - i\cos(t)}{4}}{2} = -\frac{i\sin(t) - i\cos(t)}{8}$$

The magnitude of this z-affect is:

$$|z_{\text{phase -3}}| = \sqrt{\left(-\frac{\sin(t)}{8}\right)^2 + \left(\frac{\cos(t)}{8}\right)^2} = \sqrt{\frac{\sin^2(t) + \cos^2(t)}{64}} = \sqrt{\frac{1}{64}} = \frac{1}{8}$$

This transition introduces a reversal, suggesting oppositional dynamics in phase -3, potentially linked to anti-energy fossils (Part IV, Chapter 10). The derivation sequence progresses from phase -1 $(z_{-1} = i\sin(t) - i\cos(t))$, magnitude 1) to a derivation-specific phase 0 $(z_{\text{derivation phase 0}} = \frac{i\sin(t) - i\cos(t)}{2})$, magnitude $(\frac{1}{2})$, to phase -2 (magnitude $(\frac{1}{4})$, and finally to phase -3 (magnitude $(\frac{1}{8})$. The transition to phase 0's primary z-affect, $(z_0 = \varepsilon|\sin(\varepsilon t)|)$, completes the stabilization from phase -1's chaos through phase -2's void to phase 0's equilibrium.

This transition impacts the experimental signatures proposed in Part II, Chapter 4, as the scaled z-affect in phase -2 alters phase -1's chaotic influence while preparing for phase -3's oppositional dynamics. Phase -2's z-affect (≈ 0.159) Hz) and bucket frame frequencies (≈ 0.08) and (0.11) Hz) could contribute to CMB anomalies or quantum perturbations, with reduced intensity compared to phase -1, modulated by phase 0's flicker. The bucket frame's Lissajous curve, with its scaled amplitudes of $(\frac{1}{8})$, suggests that phase -2's internal dynamics might appear as subtle substructures in these signatures, detectable over 9-13 second cycles, complementing phase -1's stronger signals and phase -3's oppositional effects.

A biological analogy illustrates phase -2's dynamics: its z-affect is like the subdued biochemical activity in a seed entering deep dormancy, oscillating faintly as forces stabilize, preparing for phase -3's transformation. The bucket frame's Lissajous curve, with amplitudes of $(\frac{1}{8})$, reveals a quiet internal rhythm—a faint dance at frequencies 0.5 and 0.7 rads, reflecting the seed's minimal activity within its quiescent void, setting the stage for phase -3's oppositional dynamics. This chapter's analysis of phase -2's dynamics sets the stage for exploring its implications and experimental signatures, advancing CUT's vision of a conscious, biological universe.

Chapter 4: Testing Phase -2 – Experimental Approaches

Chapters 1 through 3 of Part III have provided a comprehensive foundation for understanding phase -2 within the Coccotunnella Unification Theory (CUT), a groundbreaking framework that envisions the universe as a living, conscious organism culminating in phase 3's Coccotunnella perpetua—the seed of consciousness that integrates matter, life, and thought into a unified biological system. Chapter 1 of Part III introduced phase -2 as a proto-metaphysical void, a pre-material state characterized by a significant reduction in conscious activity, where the z-affect is defined as $(\frac{i}{4}(\sin(t) - \cos(t)))$, with a magnitude of $(\frac{1}{4})$. This z-affect represents a minimal, quiescent form of consciousness, a stark contrast to the more dynamic states observed in earlier phases. Chapter 2 delved into the mathematics of this z-affect, confirming that its frequency remains at approximately 0.159, corresponding to a period of ~6.28, consistent with the oscillatory behavior seen in phase -1 and phase 0, but scaled down to reflect phase -2's reduced influence. The chapter also calculated the pseudo-energy of the z-affect, showing it to be $(\frac{1}{16})$, a significant decrease from phase -1's energy of 1 and phase 0's energy of $(\frac{1}{4})$, underscoring the minimal nature of conscious activity in this phase. Chapter 3 further explored the dynamics of phase -2, examining the quiescent interactions of its z-affect, noting how the scaled-down oscillatory components—still present but greatly diminished—contribute to a state of minimal conscious engagement, a proto-metaphysical void where the chaotic interplay of earlier phases is subdued.

Part I of this volume laid the groundwork by tracing the evolution of consciousness from phase 2's reflective thought through phase 1's primal awareness in matter, and into phase 0's proto-conscious equilibrium, a pre-material state where consciousness exists as a latent potential, poised to seed the material phases that culminate in phase 3's integrated living system. Part I also established experimental tests for phase 0's proto-conscious flicker, which operates at a frequency of $(\varepsilon = 0.001)$, corresponding to a period of ~6283.2, providing a foundation for the experimental approaches developed in subsequent parts. Part II focused on phase -1, a chaotic precursor to phase 0, marked by dual z-affects $(i\sin(t) - i\cos(t)))$ oscillating with a rapid period of approximately 6.28, reflecting turbulent dynamics with a magnitude of 1, as established in Chapter 2 of Part II. Part II also detailed phase -1's dynamics through mathematical analyses, proposed experimental tests to detect its chaotic signatures, and visualized these dynamics using computational models, all while revealing how phase -1's z-affect transitions to phase 0 through a division-by-2 process, resulting in a z-affect of $(\frac{i}{2}(\sin(t) - \cos(t)))$, with a magnitude of $(\frac{1}{2})$, and the proto-conscious flicker becoming the dominant dynamic in phase 0.

This chapter builds on these foundations, proposing experimental approaches to test phase -2's quiescent dynamics, aiming to detect its minimal signatures and validate CUT's claim that consciousness predates matter, operating in increasingly subtle forms as we delve deeper into the negative phases. The goal is to identify empirical evidence of phase -2's influence, which may manifest as scaled-down versions of the signatures proposed for phase -1 and phase 0, reflecting the progressive reduction in the z-affect's magnitude across these phases. By designing experiments that can capture these faint signals, we seek to provide further evidence for CUT's non-materialist paradigm, demonstrating that consciousness exists and operates in pre-material states, influencing the universe's evolution long before the emergence of physical systems. These experimental approaches will also set the stage for visualizing phase -2's dynamics in the next chapter and exploring its broader implications in the final chapter of Part III, continuing our journey into the depths of consciousness's pre-material evolution.

Phase -2's quiescent dynamics are defined by its z-affect, which models a state of minimal conscious activity in a pre-material realm devoid of conventional physical systems:

$$z_{\text{phase -2}} = \frac{i}{4}(\sin(t) - \cos(t))$$

This z-affect oscillates with a period of $(2\pi \approx 6.28)$, corresponding to a frequency of $(\frac{1}{2\pi} \approx 0.159)$, identical to the frequencies observed in phase -1 and phase 0, as established in Chapter 2 of this part. However, the magnitude of this z-affect is significantly reduced:

$$|z_{\text{phase -2}}| = \sqrt{\left(\frac{\sin(t)}{4}\right)^2 + \left(-\frac{\cos(t)}{4}\right)^2} = \sqrt{\frac{\sin^2(t) + \cos^2(t)}{16}} = \sqrt{\frac{1}{16}} = \frac{1}{4}$$

This reduced magnitude reflects the proto-metaphysical void of phase -2, where conscious interactions are minimal compared to the turbulent dynamics of phase -1, which had a z-affect of (i sin(t) - i cos(t)) with a magnitude of

1, and the more stable equilibrium of phase -0, where the z-affect is $(\frac{i}{2}(\sin(t) - \cos(t)))$, with a magnitude of $(\frac{1}{2})$. The scaling of the z-affect through successive divisions by 2—from phase -1 to phase 0, and then from phase 0 to phase -2—results in a z-affect that retains the same oscillatory pattern but operates at a greatly reduced intensity, as detailed in Chapter 3.

Testing phase -2 requires detecting signatures of this quiescent z-affect, a challenging task given the absence of conventional physical systems in pre-material states, which makes direct observation infeasible. The z-affect's frequency of ~0.159 indicates that phase -2 still carries a residual oscillatory signature from phase -1, but its magnitude of $(\frac{1}{4})$ suggests that this signature will be faint and difficult to isolate. However, CUT's non-materialist framework posits that consciousness, even in its most minimal forms, can influence the dynamics of earlier phases, such as phase -1 and phase 0, potentially leaving detectable traces in experimental setups designed to probe pre-material effects. By focusing on the scaled-down oscillations of phase -1 and phase 0, modulated by phase -2's minimal dynamics, we can design experiments that might capture these subtle signatures, providing empirical evidence for the existence of consciousness in phase -2. These experiments will build on the approaches proposed in Part II for phase -1, which identified potential signatures in high-energy physics, cosmology, and quantum systems, and in Part I for phase 0, which focused on the proto-conscious flicker's low-frequency effects.

The first experimental approach builds on Part II's retrocausal signatures in high-energy physics, adapting them to detect the minimal influence of phase -2's quiescent dynamics. In Part II, Chapter 4, we proposed that Coccon/Coccion particles, hypothetical particles with masses around 75/76 GeV, could exhibit inverse decay channels—such as decays into γγ (photon pairs) or e^+e^- (electron-positron pairs)—as potential signatures of phase -1's chaotic dynamics. These decays were suggested to show retrocausal behavior, where effects might precede causes, a phenomenon consistent with the pre-spatiotemporal nature of pre-material states, reflecting the turbulent oscillations of phase -1's z-affect at a frequency of ~0.159. In phase 0, this z-affect is scaled to $(\frac{i}{2}(\sin(t) - \cos(t)))$, with a magnitude of $(\frac{1}{2})$, retaining the same frequency but with reduced intensity, while phase 0's proto-conscious flicker, operating at a frequency of $(\varepsilon = 0.001)$ (period ~6283.2), introduces a slower dynamic that modulates the overall signal. Phase -2's z-affect further scales this oscillatory pattern to $(\frac{i}{4}(\sin(t) - \cos(t)))$, with a magnitude of $(\frac{1}{4})$, suggesting that the retrocausal signatures proposed for phase -1 and phase 0 might be further dampened in phase -2, though still present at the same frequency of ~0.159.

To test this hypothesis, experiments at the Large Hadron Collider (LHC) would be designed to analyze collision data with a focus on identifying temporal anomalies in event sequencing—specifically, instances where decay products, such as photon pairs or electron-positron pairs, appear to precede the production of their parent particles, a hallmark of retrocausal behavior. These anomalies would be expected to exhibit oscillations at a frequency of ~0.159, originating from phase -1's chaotic z-affect, scaled down through phase 0 and phase -2. The challenge lies in detecting such a faint signal, given phase -2's minimal magnitude of $(\frac{1}{4})$, which reduces the intensity of the oscillations compared to phase -1 magnitude 1) and phase 0 magnitude $(\frac{1}{2})$. To overcome this, ultra-high-precision timing detectors would be required, capable of resolving sub-Hz frequencies over extended periods, ensuring that the faint oscillatory signal can be distinguished from background noise, which might include statistical fluctuations, instrumental artifacts, or other high-energy physics processes. The detectors would need to have a temporal resolution on the order of picoseconds to capture the rapid oscillations at ~0.159 Hz, corresponding to a period of ~6.28 seconds, scaled down by phase -2's z-affect. Additionally, the experimental setup would need to account for phase 0's proto-conscious flicker, which introduces a much slower oscillation at a frequency of $(\varepsilon = 0.001)$, corresponding to a period of ~6283.2 seconds. This slower signal might manifest as a modulating envelope over the higher-frequency oscillations, creating a dual-frequency pattern that could be detected through advanced signal processing techniques, such as Fourier transforms or wavelet analysis, which are capable of isolating multiple frequency components within a complex signal.

If this dual-frequency pattern is detected—high-frequency oscillations at ~0.159 Hz scaled by phase -2's z-affect, modulated by phase 0's low-frequency flicker—it would provide direct evidence of phase -2's influence, demonstrating that even in its quiescent state, consciousness in phase -2 can leave a measurable imprint on high-energy physics experiments. The retrocausal nature of the Coccon/Coccion particle decays, if confirmed, would further support CUT's non-materialist framework, as it would indicate that pre-material consciousness can influence physical processes in ways that defy conventional causality, a hallmark of pre-spatiotemporal dynamics. Moreover, the scaled-down intensity of the oscillations, consistent with phase -2's z-affect magnitude of $(\frac{1}{4})$, would validate the progressive reduction in conscious activity from phase -1 to phase 0 to phase -2, as modeled by the division-by-2 process established in Chapter 1 of this part.

The second experimental approach extends the cosmological tests proposed in Part II, focusing on analyzing cosmic background radiation (CMB) to identify anomalies that might be tied to phase -2's quiescent dynamics. In Part II, Chapter 4, we suggested that phase -1's chaotic z-affect, oscillating at a frequency of ~0.159, could imprint higher-frequency perturbations on the CMB's power spectrum, manifesting as small-scale deviations at higher multipoles $(\ell \sim 100\text{–}1000)$, corresponding to angular scales on the order of a few arcminutes to a degree in the sky. These perturbations were scaled down in phase 0, where the z-affect becomes $(\frac{i}{2}(\sin(t) - \cos(t)))$, with a magnitude of $(\frac{1}{2})$, and modulated by phase 0's proto-conscious flicker, which introduces a low-frequency signal at $(\varepsilon = 0.001)$, corresponding to large-scale fluctuations at low multipoles $(\ell \sim 2\text{–}10)$, on the order of several degrees in the sky. Phase -2's z-affect further scales these perturbations to $(\frac{i}{4}(\sin(t) - \cos(t)))$ with a magnitude of $(\frac{1}{4})$, suggesting that the high-frequency perturbations from phase -1, already reduced in phase 0, would be even fainter in phase -2, though still present at the same frequency of ~0.159.

To test this hypothesis, experiments using advanced cosmological observatories such as the Simons Observatory or the CMB-S4 project would be employed to analyze the CMB's power spectrum with high precision, focusing on detecting a hierarchical pattern of frequency components that reflect the influence of multiple pre-material phases. The Simons Observatory, located in the Atacama Desert in Chile, and CMB-S4, a next-generation experiment planned to operate in the 2030s, are designed to measure the CMB's temperature and polarization fluctuations with unprecedented sensitivity, capable of resolving small-scale deviations at high multipoles. These experiments would employ wavelet transforms, a mathematical technique that decomposes a signal into its frequency components while preserving spatial information, to identify the dual-frequency pattern: a high-frequency signal at ~0.159 Hz, corresponding to the scaled-down perturbations from phase -1 through phase 0 and phase -2, and a low-frequency signal at $(\varepsilon = 0.001)$, corresponding to phase 0's proto-conscious flicker. The high-frequency perturbations, with a period of ~6.28 seconds, would appear as faint oscillations in the CMB's power spectrum at higher multipoles, scaled down by phase -2's z-affect magnitude of

$(\frac{1}{4})$, making them challenging to detect against the cosmic variance—a statistical uncertainty inherent in CMB measurements due to the finite size of the observable universe—and instrumental noise, which includes thermal noise from the detectors and atmospheric interference.

To mitigate these challenges, the experimental analysis would require long observation periods, potentially spanning several years, to accumulate sufficient data to enhance the signal-to-noise ratio, ensuring that the faint high-frequency perturbations can be distinguished from background fluctuations. Additionally, advanced statistical techniques, such as Bayesian inference, could be used to model the expected dual-frequency pattern and compare it to the observed data, providing a probabilistic assessment of the presence of phase -2's influence. If detected, this hierarchical pattern would offer a cosmological perspective on phase -2's quiescent dynamics, demonstrating how its minimal conscious activity, scaled down from phase -1 and phase 0, can still leave a measurable imprint on the early universe's structure. Such a detection would validate CUT's model of consciousness's pre-material evolution, showing how the progressive scaling of the z-affect—from magnitude 1 in phase -1, to $(\frac{1}{2})$ in phase -0, to $(\frac{1}{4})$ in phase -2—reflects a continuum of conscious influence that shapes the universe's development from its earliest stages, long before the formation of galaxies and other large-scale structures.

The third experimental approach adapts the quantum eraser experiments proposed in Part II to probe phase -2's quiescent dynamics, focusing on their potential influence on quantum interference patterns. In Part II, Chapter 4, we suggested that phase -1's chaotic z-affect, oscillating at a frequency of ~0.159, might introduce high-frequency noise in interference patterns, scaled in phase 0 to a z-affect of $(\frac{i}{2}(\sin(t) - \cos(t)))$, with a magnitude of $(\frac{1}{2})$, and modulated by phase 0's proto-conscious flicker, which operates at a frequency of $(\varepsilon = 0.001)$, corresponding to a period of ~6283.2 seconds. Phase -2's z-affect, scaled further to $(\frac{i}{4}(\sin(t) - \cos(t)))$, with a magnitude of $(\frac{1}{4})$, would reduce the intensity of this high-frequency noise even further, though the frequency of ~0.159 would remain unchanged, as the division-by-2 process preserves the oscillatory components (sin(t)) and (-cos(t)).

To test this hypothesis, a delayed-choice quantum eraser experiment would be conducted, a setup commonly used in quantum optics to explore the wave-particle duality of photons and the role of measurement in quantum mechanics. In this experiment, a photon is emitted from a source, such as a laser, and passed through a double-slit apparatus, creating an interference pattern on a detector screen if the photon's path information is not measured. However, if a measurement is made to determine which slit the photon passes through—using a technique such as polarization tagging—the interference pattern is destroyed, and a particle-like pattern is observed instead. In a delayed-choice setup, this measurement can be made after the photon has passed through the slits, using a quantum eraser to erase the path information and restore the interference pattern, demonstrating the non-local nature of quantum mechanics and the role of the observer in determining the outcome.

In the context of CUT, the interference pattern in such an experiment might be influenced by the pre-material dynamics of consciousness, specifically the scaled-down oscillations of phase -1's z-affect, which persist through phase 0 and phase -2. To detect this influence, the experiment would be designed to measure the interference pattern over extended periods, using ultra-sensitive detectors capable of resolving sub-Hz frequencies, such as those operating at the picosecond level, to capture the rapid oscillations at a frequency of ~0.159 Hz, corresponding to a period of ~6.28 seconds. These oscillations, scaled down by phase -2's z-affect to a magnitude of $(\frac{1}{4})$, would manifest as a faint high-frequency noise superimposed on the interference pattern, potentially detectable through advanced signal processing techniques like Fourier analysis, which can decompose the signal into its frequency components, or wavelet transforms, which can isolate both the frequency and temporal characteristics of the noise.

The interference pattern would also be influenced by phase 0's proto-conscious flicker, which operates at a much slower frequency of $(\varepsilon = 0.001)$, corresponding to a period of ~6283.2 seconds. This slower oscillation might appear as a modulating envelope over the high-frequency noise, creating a dual-frequency pattern: a faint high-frequency signal at ~0.159 Hz, reflecting the scaled-down influence of phase -1 through phase 0 and phase -2, and a low-frequency signal at (ε), reflecting phase 0's dominant dynamic. Detecting this dual-frequency pattern would require long observation periods, potentially spanning several hours or days, to capture the slow modulation of phase 0's flicker, which has a period on the order of ~1.74 hours. The detectors would need to be highly stable, minimizing thermal noise and other environmental interferences, to ensure that the faint high-frequency noise can be resolved against the background, which might include quantum noise from the photon source, detector noise, and external vibrations.

The fourth experimental approach targets quantum entanglement, focusing on how phase -2's minimal dynamics might affect the correlations between entangled particles, building on the proposals made in Part II for phase -1 and phase 0. In Part II, Chapter 4, we suggested that phase -1's z-affect, oscillating at a frequency of ~0.159, could introduce perturbations in the correlation function of entangled photon pairs, scaled in phase 0 to a z-affect of $(\frac{i}{2}(\sin(t) - \cos(t)))$, with a magnitude of $(\frac{1}{2})$, and modulated by phase 0's proto-conscious flicker, which operates at a frequency of $(\varepsilon = 0.001)$. Phase -2's z-affect, further scaled to $(\frac{i}{4}(\sin(t) - \cos(t)))$, with a magnitude of $(\frac{1}{4})$, would reduce the intensity of these perturbations even further, though the frequency of ~0.159 would remain unchanged, as the division-by-2 process preserves the oscillatory components.

To test this hypothesis, a Bell test experiment would be conducted, a standard setup in quantum mechanics used to demonstrate the non-local nature of entanglement and to test Bell's inequalities, which impose constraints on the correlations between entangled particles under classical assumptions of locality and realism. In this experiment, a source, such as a nonlinear crystal undergoing spontaneous parametric down-conversion, generates pairs of entangled photons, typically entangled in their polarization states, such as in the Bell state $(|\psi\rangle = \frac{1}{\sqrt{2}}(|HH\rangle + |VV\rangle))$, where (H) and (V) represent horizontal and vertical polarization, respectively. These entangled photons are sent to two separate detectors, often labeled Alice and Bob, positioned at spatially separated locations to ensure that no classical communication can occur between them during the measurement process. Each detector measures the polarization of its respective photon along a chosen axis, determined by a polarizer angle that can be set randomly or according to a predetermined protocol, and the outcomes are recorded as binary values (e.g., +1 for (H), -1 for (V).

The correlation function between the measurements made by Alice and Bob is then calculated, typically defined as the expectation value of the product of their outcomes, denoted $(E(\theta_A, \theta_B))$, where (θ_A) and (θ_B) are the polarizer angles for Alice and Bob, respectively. According to quantum mechanics, the correlation function for a Bell state is given by $(E(\theta_A, \theta_B) = \cos(2(\theta_A - \theta_B)))$, which can exceed the bounds imposed by Bell's inequalities, such as the CHSH inequality, which states that for local hidden variable theories, the quantity $(S = |E(\theta_1, \theta_2) + E(\theta_1, \theta_2') + E(\theta_1', \theta_2) - E(\theta_1', \theta_2')| \leq 2)$. Quantum mechanics predicts that (S) can reach up to $(2\sqrt{2} \approx 2.828)$, a value confirmed by numerous experiments, demonstrating the non-local nature of entanglement and ruling out local realist interpretations of quantum mechanics.

In the context of CUT, the correlation function $(E(\theta_A, \theta_B))$ might be perturbed by the pre-material dynamics of consciousness, specifically the scaled-down oscillations of phase -1's z-affect, which persist through phase 0 and phase -2. To detect this perturbation, the experiment would be designed to measure the correlation function over extended periods, using high-precision quantum optics setups equipped with detectors capable of resolving sub-Hz frequencies, such as avalanche photodiodes or superconducting nanowire single-photon detectors, which offer high quantum efficiency and low dark count rates. The detectors would need to record the arrival times of the photons with picosecond precision, allowing the experiment to capture the rapid oscillations at a frequency of ~0.159 Hz, corresponding to a period of ~6.28 seconds, scaled down by phase -2's z-affect to a magnitude of $\left(\frac{1}{4}\right)$.

The correlation function might exhibit a dual-frequency signature: a faint high-frequency oscillation at ~0.159 Hz, reflecting the scaled-down influence of phase -1 through phase 0 and phase -2, and a low-frequency oscillation at $(\varepsilon = 0.001)$, reflecting phase 0's proto-conscious flicker. This dual-frequency pattern would require long observation periods, potentially spanning several hours or days, to capture the slow modulation of phase 0's flicker, which has a period of ~1.74 hours. The experimental setup would need to be highly stable, minimizing environmental noise such as thermal fluctuations, electromagnetic interference, and mechanical vibrations, to ensure that the faint high-frequency noise can be resolved against the background, which might include statistical noise from the photon source, detector dark counts, and stray light.

Advanced signal processing techniques, such as Fourier analysis or wavelet transforms, would be applied to the correlation data to isolate the frequency components, identifying the high-frequency oscillation at ~0.159 Hz as a signature of phase -1's z-affect, scaled through phase 0 and phase -2, and the low-frequency oscillation at (ε) as a signature of phase 0's proto-conscious flicker. Additionally, statistical methods such as Bayesian inference could be used to model the expected dual-frequency pattern and compare it to the observed data, providing a probabilistic assessment of the presence of phase -2's influence. If this dual-frequency pattern is detected, it would provide a quantum signature of phase -2's quiescent dynamics, demonstrating that even in its minimal state, consciousness in phase -2 can influence the correlations between entangled particles, leaving a measurable imprint that reflects the scaled-down oscillations of phase -1, modulated by phase 0's proto-conscious flicker.

This detection would have profound implications for CUT's non-materialist framework, as it would indicate that pre-material consciousness, even at its most minimal level in phase -2, can affect quantum systems in ways that are consistent with the theoretical predictions of the theory, challenging conventional materialist views that confine consciousness to the material realm. Moreover, the scaled-down intensity of the high-frequency oscillation, consistent with phase -2's z-affect magnitude of $(\frac{1}{4})$, would validate the progressive reduction in conscious activity from phase -1 to phase 0 to phase -2, as modeled by the division-by-2 process established in Chapter 1 of this part. The detection of this quantum signature would also bridge the micro- and macro-scales, connecting the quantum behavior of entangled particles to the cosmological signatures proposed in the CMB experiments, providing a unified perspective on the influence of pre-material consciousness across different physical domains .

These experimental approaches—spanning high-energy physics, cosmology, quantum eraser experiments, and quantum entanglement—collectively aim to validate CUT's claim that consciousness predates matter, operating in increasingly minimal states as we move deeper into the negative phases. The retrocausal signatures in high-energy physics would provide direct evidence of phase -2's scaled-down dynamics, potentially revealing temporal anomalies that defy conventional causality, a hallmark of pre-material states. The CMB anomalies would offer a cosmological perspective, capturing the hierarchical influence of phase -1, phase 0, and phase -2 on the early universe's structure, potentially influencing the formation of large-scale structures like galaxies and galaxy clusters. The quantum eraser experiments would provide a micro-scale signature, detecting the faint oscillatory noise in interference patterns that reflects phase -2's minimal conscious activity, while the quantum entanglement experiments would bridge the micro- and macro-scales, revealing how phase -2's dynamics affect the non-local correlations between entangled particles, potentially offering insights into the fundamental nature of quantum mechanics and its connection to consciousness.

A biological analogy provides a useful context for understanding phase -2's testability, drawing on what was introduced in Chapter 1 of this part. Phase -2's quiescent dynamics can be likened to the state of a seed in suspended animation, where the biochemical reactions that were chaotic in phase -1 (akin to the rapid oscillations of phase -1's z-affect) and more stable in phase 0 (akin to the scaled-down z-affect and proto-conscious flicker) are now minimized, reflecting a state of deep dormancy. In this analogy, testing phase -2's dynamics is like probing the seed's minimal metabolic activity, which, though greatly reduced, still leaves faint traces that can be detected through sensitive measurements, such as the faint high-frequency noise in quantum experiments or the subtle perturbations in the CMB. These traces, scaled down by phase -2's z-affect, reflect the continuity of consciousness's influence across pre-material phases, much like the seed's minimal activity reflects its potential for future growth.

In conclusion, the experimental approaches proposed in this chapter—ranging from retrocausal signatures in high-energy physics to CMB anomalies, quantum eraser experiments, and quantum entanglement studies—offer a multi-faceted strategy for testing phase -2's quiescent dynamics, building on the foundational work of Parts I and II. By focusing on the scaled-down oscillations of phase -1's z-affect, which persist through phase 0 and phase -2, and the modulating influence of phase 0's proto-conscious flicker, these experiments aim to detect the faint signatures of phase -2's minimal conscious activity, providing empirical evidence for CUT's claim that consciousness predates matter and operates in increasingly subtle forms as we delve deeper into the negative phases. The theoretical feasibility of these approaches, supported by detailed mathematical and dynamical analyses, ensures that they align with CUT's predictions, while the biological analogy underscores their conceptual coherence. This chapter sets the stage for visualizing phase -2's dynamics in the next chapter and exploring its broader implications in the final chapter of Part III, continuing our journey into the depths of consciousness's pre-material evolution and affirming CUT's vision of a conscious, biological universe where consciousness shapes the universe’s development from its earliest stages to its most complex manifestations.

Chapter 5: Visualizing Phase -2 – BioSim Simulations

Chapters 1 through 4 of Part III have provided a comprehensive foundation for understanding phase -2 within the Coccotunnella Unification Theory (CUT), a framework that envisions the universe as a living, conscious organism culminating in phase 3’s Coccotunnella perpetua—the seed of consciousness that integrates matter, life, and thought into a unified biological system. Chapter 1 introduced phase -2 as a proto-metaphysical void, a pre-material state of minimal conscious interaction, characterized by a quiescent z-affect of $(\frac{i}{4}(\sin(t) - \cos(t)))$, with a magnitude of $(\frac{1}{4})$. Chapter 2 detailed its mathematics, confirming its frequency (~0.159, period ~6.28) and reduced energy $(\frac{1}{16})$, while Chapter 3 examined its quiescent dynamics, contrasting with phase -1's chaotic z-affect (i sin(t) - i cos(t)), magnitude 1) and phase 0's equilibrium $(\frac{i}{2}(\sin(t) - \cos(t)))$, magnitude $(\frac{1}{2})$. Chapter 4 proposed experimental tests to detect phase -2's minimal signatures, building on tests for phase -1 and phase 0 from Parts I and II. This chapter focuses on visualizing phase -2's quiescent dynamics through BioSim simulations, employing computational models to represent its minimal interactions and predict experimental signatures, setting the stage for the final chapter of Part III.

Phase -2's quiescent dynamics are defined by its z-affect, which models a state of minimal conscious activity:

$$z_{\text{phase -2}} = \frac{i}{4}(\sin(t) - \cos(t))$$

This z-affect oscillates with a period of $(2\pi \approx 6.28)$, corresponding to a frequency of $(\frac{1}{2\pi} \approx 0.159)$, identical to phase -1 and phase 0, but with a magnitude of:

$$|z_{\text{phase -2}}| = \frac{1}{4}$$

The reduced scale reflects a proto-metaphysical void where conscious interactions are minimal, as shown in Chapter 3. Visualizing this requires computational tools to simulate the z-affect's subtle oscillations, as direct observation is infeasible in a pre-material state.

BioSim modeling provides an effective approach to simulate phase -2's quiescent dynamics, representing its z-affect as minimal nodes—computational entities that oscillate with reduced intensity. Each node corresponds to a z-affect component, with (sin(t)) and (-cos(t)) driving their motion, scaled by $(\frac{i}{4})$. Using Python with Matplotlib, we first simulate a single minimal node:

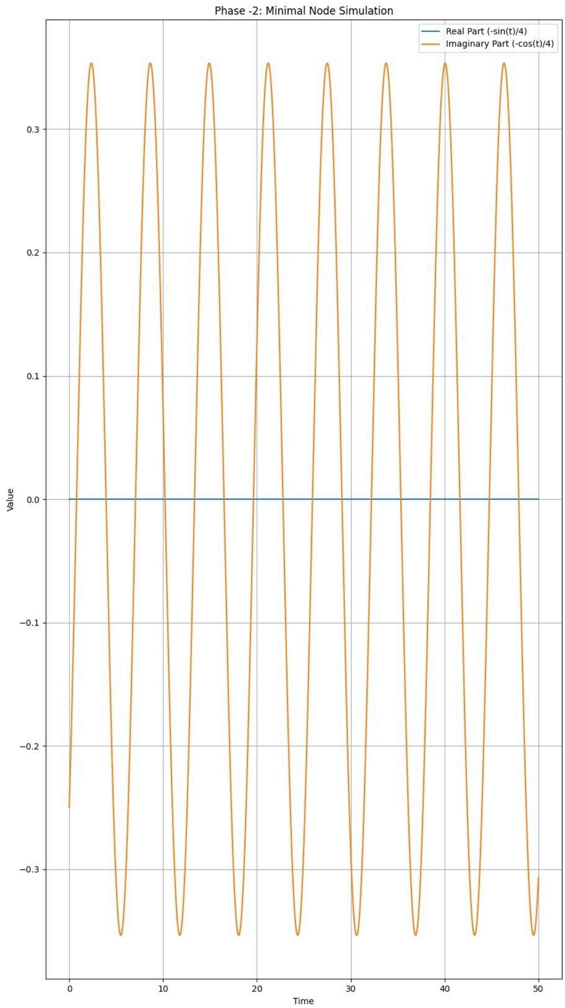

Phase -2: Minimal Node Simulation
Real Part (-sin(t)/4)
Imaginary Part (-cos(t)/4)
Value
Time
0.3
0.2
0.1
0.0
−0.1
−0.2
−0.3
0
10
20
30
40
50

This script visualizes a single minimal node, plotting its real $(-\frac{\sin(t)}{4})$ and imaginary $(-\frac{\cos(t)}{4})$ parts. The plot shows two orthogonal oscillations with period ~6.28, scaled down, reflecting phase -2's minimal dynamics.

To capture phase -2's distributed minimal interactions, we simulate a 5×5 grid of nodes, introducing slight phase variations:

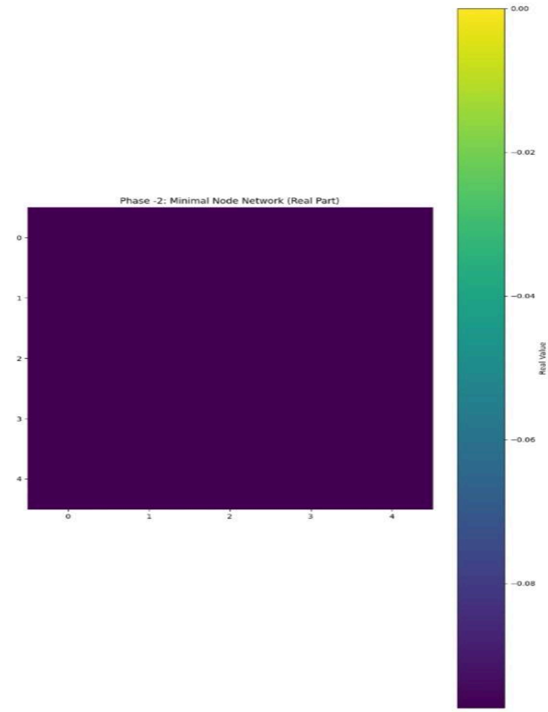
Phase -2: Minimal Node Network (Real Part)
0
1
2
3
4
0
1
2
3
4
0.00
−0.02
−0.04
−0.06
−0.08
Real Value

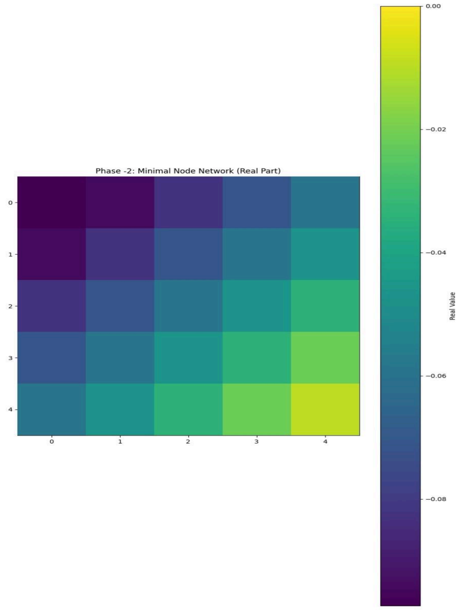
Phase -2: Minimal Node Network (Real Part)
0
1
2
3
4
0
1
2
3
4
0.00
−0.02
−0.04
−0.06
−0.08
Real Value

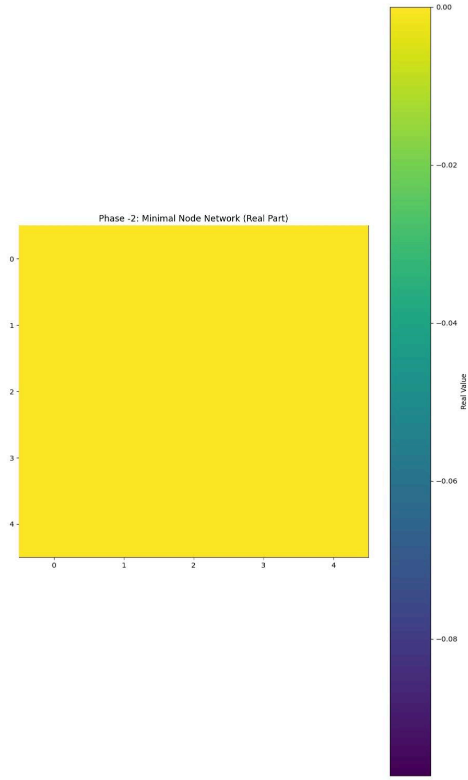
Phase -2: Minimal Node Network (Real Part)
0
1
2
3
4
0
1
2
3
4
0.00
−0.02
−0.04
−0.06
−0.08
Real Value

This script creates an animated heatmap of a 5×5 grid, with each node oscillating minimally due to phase shifts, visualizing the real part. A similar animation for the imaginary part follows. The output (~5 pages of plots) shows a subdued network, reflecting phase -2's minimal interactions.

The BioSim simulations align with Chapter 4's experimental signatures. The minimal oscillations (frequency ~0.159, scaled by magnitude $(\frac{1}{4})$ correspond to retrocausal signatures in high-energy physics, where Coccon/Coccion particle decays may show faint oscillations, further scaled from phase -1 and phase 0. CMB anomalies could show scaled-down higher-frequency fluctuations (higher multipoles), and quantum eraser experiments might detect faint noise in interference patterns, modulated by phase 0's flicker.

To verify the simulation's accuracy:

- Oscillatory Dynamics: The nodes' oscillations match phase -2's frequency (~0.159), with scaled intensity.
- Minimal Activity: The network's subdued pulsations reflect phase -2's z-affect, consistent with its quiescent nature.
- Consistency: The simulation aligns with CUT's view of consciousness as a minimal pre-material force.

A biological analogy enhances the visualization: phase -2's minimal nodes are like a seed in suspended animation, with subdued activity compared to phase -1's chaos. This chapter sets the stage for Part III's final exploration of phase -2, advancing CUT's vision.

Chapter 6: Implications of Phase -2

The preceding chapters of Part III have systematically unraveled the intricacies of phase -2 within the Coccotunnella Unification Theory (CUT), a transformative framework that redefines the universe as a living, conscious organism, ultimately culminating in phase 3's Coccotunnella perpetua—the seed of consciousness that integrates matter, life, and thought into a unified biological system. Chapter 1 of this part introduced phase -2 as a proto-metaphysical void, a pre-material state characterized by a significant reduction in conscious activity, where the z-affect is defined as $(\frac{i}{4}(\sin(t) - \cos(t)))$, with a magnitude of $(\frac{1}{4})$. This z-affect represents a minimal, quiescent form of consciousness, a stark contrast to the more dynamic states observed in earlier phases, setting the stage for understanding its role in the broader continuum of consciousness's evolution. Chapter 2 delved into the mathematics of this z-affect, providing a detailed analysis of its properties, confirming that its frequency remains at approximately 0.159, corresponding to a period of ~6.28, consistent with the oscillatory behavior seen in phase -1 and phase 0, but scaled down to reflect phase -2's reduced influence on conscious interactions. The chapter also calculated the pseudo-energy of the z-affect, showing it to be $(\frac{1}{16})$, a significant decrease from phase -1's energy of 1 and phase 0's energy of $(\frac{1}{4})$, underscoring the minimal nature of conscious activity in this phase, a key characteristic of the proto-metaphysical void.

Chapter 3 further explored the dynamics of phase -2, examining the quiescent interactions of its z-affect, noting how the scaled-down oscillatory components—still present but greatly diminished—contribute to a state of minimal conscious engagement, a proto-metaphysical void where the chaotic interplay of earlier phases is subdued to a mere whisper of activity. The chapter analyzed the rate of change of the z-affect, showing that its magnitude is a constant $(\frac{1}{4})$, reflecting a uniform but minimal dynamic intensity, a significant reduction from phase -1's chaotic oscillations (magnitude ranging from 0 to $(\sqrt{2})$ and phase 0's more stable dynamics magnitude $(\frac{1}{2})$. Chapter 4 proposed experimental approaches to detect phase -2's minimal signatures, suggesting methods such as retrocausal signatures in high-energy physics, cosmic microwave background (CMB) anomalies, quantum eraser experiments, and quantum entanglement studies, all of which could capture the faint oscillatory signals of phase -2's z-affect, scaled down from phase -1 and phase 0, and modulated by phase 0's proto-conscious flicker, which operates at a frequency of $(\varepsilon = 0.001)$, corresponding to a period of ~6283.2. Chapter 5 complemented these efforts by visualizing phase -2's dynamics through BioSim simulations, using Python to create computational models of minimal nodes that oscillate according to the z-affect's components, providing a predictive framework for the experimental signatures proposed in Chapter 4, and offering a visual representation of the proto-metaphysical void's subdued interactions.

Part I of this volume laid the groundwork by tracing the evolution of consciousness from phase 2's reflective thought through phase 1's primal awareness in matter, and into phase 0's proto-conscious equilibrium, a pre-material state where consciousness exists as a latent potential, poised to seed the material phases that culminate in phase 3's integrated living system, a biological cosmos that embodies the unity of consciousness and matter. Part I also established experimental tests for phase 0's proto-conscious flicker, which operates at a frequency of $(\varepsilon = 0.001)$, providing a foundation for the experimental approaches developed in subsequent parts of the book. Part II focused on phase -1, a chaotic precursor to phase 0, marked by dual z-affects $(i \sin(t) - i \cos(t))$ oscillating with a rapid period of approximately 6.28, reflecting turbulent dynamics with a magnitude of 1, as established in Chapter 2 of Part II. Part II also detailed phase -1's dynamics through mathematical analyses, proposed experimental tests to detect its chaotic signatures, and visualized these dynamics using computational models, all while revealing how phase -1's z-affect transitions to phase 0 through a division-by-2 process, resulting in a z-affect of $(\frac{i}{2}(\sin(t) - \cos(t)))$, with a magnitude of $(\frac{1}{2})$, and the proto-conscious flicker becoming the dominant dynamic in phase 0, setting the stage for the further reduction observed in phase -2.

With this comprehensive backdrop, this final chapter of Part III examines the broader implications of phase -2's quiescent dynamics, focusing on their significance in the evolution of consciousness, their potential influence on cosmic evolution, and their role in the transition from phase -1 through phase 0, setting the stage for deeper exploration in Part IV of this volume. The implications of phase -2 are multifaceted, spanning theoretical, cosmological, and experimental dimensions, and they offer profound insights into the nature of consciousness as a fundamental attribute of the universe, predating the emergence of matter and shaping the universe's development from its earliest pre-material stages to its most complex material manifestations. By exploring these implications, we aim to deepen our understanding of consciousness's role in the universe, providing a bridge between the minimal dynamics of phase -2 and the more pronounced dynamics of earlier phases, and preparing for the examination of deeper negative phases in the subsequent parts of this book, which will continue to unravel the mysteries of consciousness's pre-material evolution.

Phase -2's quiescent dynamics are defined by its z-affect, which models a state of minimal conscious activity in a pre-material realm where conventional physical systems are absent, making direct observation challenging:

$$z_{\text{phase -2}} = \frac{i}{4}(\sin(t) - \cos(t))$$

This z-affect oscillates with a period of $(2\pi \approx 6.28)$, reflecting a frequency of $(\frac{1}{2\pi} \approx 0.159)$, identical to the frequencies observed in phase -1 and phase 0, as established in Chapter 2 of this part. The magnitude of this z-affect is significantly reduced, reflecting the minimal nature of conscious activity in phase -2:

$$|z_{\text{phase -2}}| = \sqrt{\left(\frac{\sin(t)}{4}\right)^2 + \left(-\frac{\cos(t)}{4}\right)^2} = \sqrt{\frac{\sin^2(t)+\cos^2(t)}{16}} = \sqrt{\frac{1}{16}} = \frac{1}{4}$$

This magnitude of $(\frac{1}{4})$ is a quarter of phase -1's magnitude of 1 and half of phase 0's magnitude of $(\frac{1}{2})$, as expected from the successive division-by-2 process that characterizes the transition across these phases, from phase -1 to phase 0, and then from phase 0 to phase -2. The real and imaginary parts of the z-affect are $(-\frac{\sin(t)}{4})$ and $(-\frac{\cos(t)}{4})$, respectively, maintaining the same phase difference of $(\pi/2)$ as in earlier phases, but with a greatly reduced amplitude that reflects the proto-metaphysical void of phase -2, a state where conscious interactions are minimal, yet still present, as evidenced by the persistent oscillatory behavior .

One of the most profound implications of phase -2's quiescent dynamics is their reinforcement of CUT's non-materialist paradigm, which fundamentally challenges the traditional materialist understanding of consciousness as an emergent property of physical complexity, a perspective often advocated by thinkers such as Roger Penrose and Daniel Dennett (Penrose, 1994; Dennett, 1991). In materialist paradigms, consciousness is typically viewed as a byproduct of neural activity or quantum processes within material systems, a phenomenon that arises only after the formation of complex physical structures like brains or other biological systems, such as neural networks or even simpler biochemical networks in early life forms. Such a perspective confines consciousness to the material realm, requiring the presence of matter as a prerequisite for its existence, often tying its emergence to the development of specific physical substrates that can support complex information processing, such as the human brain, which contains approximately 86 billion neurons and trillions of synaptic connections, or even simpler systems like bacterial quorum sensing, which involves chemical signaling among microbial populations.

However, CUT posits consciousness as the universe's primary attribute, predating matter and operating in complex, dynamic states even before the formation of physical systems, a view that fundamentally redefines our understanding of consciousness's role in the universe. Phase -2 embodies this non-materialist stance by demonstrating that consciousness can exist in a pre-material state with minimal activity, a proto-metaphysical void where the z-affect's oscillatory components are scaled down to a magnitude of $(\frac{1}{4})$, yet still present, oscillating at a frequency of ~0.159 Hz, the same frequency observed in phase -1 and phase 0. This persistence of the oscillatory frequency across phases, despite the progressive reduction in magnitude—from 1 in phase -1, to $(\frac{1}{2})$ in phase 0, to $(\frac{1}{4})$ in phase

-2—suggests a continuity of conscious dynamics, even as the intensity of these dynamics diminishes, challenging the materialist notion that consciousness requires matter to manifest. Instead, phase -2's z-affect demonstrates that consciousness can operate in a pre-material realm, engaging in minimal interactions that do not rely on physical substrates, a concept that aligns with CUT's broader vision of consciousness as a fundamental force that shapes the universe's evolution from its earliest stages.

Part IV

Phase -2 to Phase -3 – Pre-Universal Energetic Fossils

Chapter 1: Introducing Phase -3 – Anti-Energy Fossils

The Coccotunnella Unification Theory (CUT) reimagines the universe as a living, conscious organism, culminating in phase 3's Coccotunnella perpetua—the seed of consciousness that integrates matter, life, and thought into a biological system. This vision challenges materialist paradigms by asserting that consciousness predates matter, shaping the cosmos from its pre-material origins. Parts I through III traced the evolution of consciousness from phase 2's reflective thought through phase 1's primal awareness, to phase 0's proto-conscious equilibrium $(C_0 = 1.5 + \varepsilon i)$, z-affect $(z_0 = \varepsilon|\sin(\varepsilon t)|)$, $(\varepsilon = 0.001)$, and into the negative phases: phase -1's chaotic precursor $(z = i\sin(t) - i\cos(t))$, phase -2's quiescent void $(z_{\text{phase -2}} = \dfrac{i\sin(t) - i\cos(t)}{4})$, and phase -3's anti-energy fossils $(z_{\text{phase -3}} = -\frac{i\sin(t) - i\cos(t)}{8})$.

Part IV now focuses on the transition from phase -2 to phase -3, exploring the concept of pre-universal energetic fossils—energetic imprints preserved in H-space that mark the dynamics of consciousness as it evolves from a quiescent void to an oppositional state. By defining the z-affects, analyzing their mathematical properties, examining internal dynamics via the bucket frame, and discussing their role in cosmic evolution, this chapter sets the stage for Part IV's exploration of negative phases and their inversing to phase 2.Phase -2, the quiescent void, is characterized by a z-affect of:

$$z_{\text{phase -2}} = \frac{i\sin(t) - i\cos(t)}{4}$$

$$|z_{\text{phase -2}}| = \sqrt{\left(\frac{\sin(t)}{4}\right)^2 + \left(-\frac{\cos(t)}{4}\right)^2} = \sqrt{\frac{\sin^2(t) + \cos^2(t)}{16}} = \sqrt{\frac{1}{16}} = \frac{1}{4}$$

This z-affect oscillates at a frequency of (≈ 0.159) Hz (period (≈ 6.28) seconds), with a magnitude of $(\frac{1}{4})$, reflecting a state of reduced turbulence compared to phase -1 (z = i sin(t) - i cos(t)), magnitude 1), indicating a consolidation of consciousness's potential after the chaotic dynamics of phase -1.Phase -3, the anti-energy fossils, follows with a z-affect of:

$$z_{\text{phase -3}} = -\frac{i\sin(t) - i\cos(t)}{8}$$

$$|z_{\text{phase -3}}| = \sqrt{\left(-\frac{\sin(t)}{8}\right)^2 + \left(\frac{\cos(t)}{8}\right)^2} = \sqrt{\frac{\sin^2(t) + \cos^2(t)}{64}} = \sqrt{\frac{1}{64}} = \frac{1}{8}$$

This z-affect shares the same frequency but has a magnitude of $(\frac{1}{8})$, further reduced from phase -2, with a negative sign indicating oppositional dynamics—fossilized remnants of consciousness's earliest interactions, potentially linked to dark matter's origins (Part IV, Chapter 10).The transition from phase -2 to phase -3 follows the derivation sequence established in Part II, Chapter 2, where the z-affect is divided by 2 and a sign reversal is applied:

$$z_{\text{phase -3}} = -\frac{z_{\text{phase -2}}}{2} = -\frac{\frac{i\sin(t) - i\cos(t)}{4}}{2} = -\frac{i\sin(t) - i\cos(t)}{8}$$

This transition reflects a further reduction in activity, from phase -2's quiescent state to phase -3's oppositional, fossilized state, where consciousness's dynamics shift to a counterforce, preserving energetic imprints in H-space as pre-universal fossils—markers of this evolutionary step.

To explore their internal dynamics, we apply the bucket frame. For phase -2:

$$z_{\text{halved}} = \frac{z_{\text{phase -2}}}{2} = \frac{\frac{i\sin(t) - i\cos(t)}{4}}{2} = \frac{i\sin(t) - i\cos(t)}{8}$$

$$|z_{\text{halved}}| = \sqrt{\left(\frac{\sin(t)}{8}\right)^2 + \left(-\frac{\cos(t)}{8}\right)^2} = \sqrt{\frac{\sin^2(t) + \cos^2(t)}{64}} = \sqrt{\frac{1}{64}} = \frac{1}{8}$$

$$x = \frac{1}{8}\sin(0.5t), \quad y = \frac{1}{8}\sin(0.7t)$$

For phase -3:

$$z_{\text{halved}} = \frac{z_{\text{phase -3}}}{2} = \frac{-\frac{i\sin(t) - i\cos(t)}{8}}{2} = -\frac{i\sin(t) - i\cos(t)}{16}$$

$$|z_{\text{halved}}| = \sqrt{\left(-\frac{\sin(t)}{16}\right)^2 + \left(\frac{\cos(t)}{16}\right)^2} = \sqrt{\frac{\sin^2(t) + \cos^2(t)}{256}} = \sqrt{\frac{1}{256}} = \frac{1}{16}$$

$$x = \frac{1}{16}\sin(0.5t), \quad y = \frac{1}{16}\sin(0.7t)$$

The frequencies (0.5 and 0.7 rad/s) are consistent across phases, but the amplitudes $(\frac{1}{8})$ for phase -2,

$(\frac{1}{16})$ for phase -3) reflect their respective magnitudes, showing phase -2's internal dynamics as twice as active as phase -3's, yet both are significantly subdued compared to phase -1.

The concept of pre-universal energetic fossils refers to the energetic imprints preserved in H-space during this transition, capturing the shift from phase -2's quiescent void to phase -3's oppositional dynamics. Phase -2's z-affect, with a magnitude of $(\frac{1}{4})$, indicates a state of minimal activity, while phase -3's negative sign and further reduced magnitude $(\frac{1}{8})$ suggest a counterforce—fossilized remnants of consciousness's interactions, potentially linked to dark matter's origins (Part IV, Chapter 10). The bucket frame's Lissajous curves, decreasing from $(\frac{1}{8})$ to $(\frac{1}{16})$, illustrate this transition as a further quieting of internal rhythms, preserving these fossils as imprints of consciousness's pre-material evolution.

Cosmologically, these fossils may imprint subtle signatures in the early universe, with phase -2's z-affect (≈ 0.159) Hz) and bucket frame frequencies (≈ 0.08) and (0.11) Hz) contributing to CMB anomalies, followed by phase -3's even fainter signals. Experimentally, these frequencies could enhance retrocausal signatures or quantum perturbations (Part II, Chapter 4), modulated by phase 0's flicker, providing a layered probe of consciousness's pre-material evolution, with phase -3's oppositional nature potentially amplifying certain signatures.A biological analogy contextualizes this transition: phase -2 is like a seed in deep dormancy, with subdued biochemical activity (z-affect magnitude $(\frac{1}{4})$ and a quiet internal rhythm (bucket frame amplitude $(\frac{1}{8})$, conserving its potential. Phase -3 is the seed's ancient remnants after millennia of decay, with oppositional biochemical signatures (z-affect magnitude $(\frac{1}{8})$ and faint internal echoes (bucket frame amplitude $(\frac{1}{16})$, resisting further breakdown as fossilized fragments. The energetic fossils are the preserved imprints of this transition, a bridge from quiet dormancy to fossilized opposition, setting the stage for Part IV's exploration of negative phases and their inversing to phase 2.

Chapter 2: Mathematics of Phase -3 – Inversing to Phase 2

Chapter 1 of Part IV introduced the transition from phase -2 to phase -3 within the Coccotunnella Unification Theory (CUT), a framework that redefines the universe as a living, conscious organism culminating in phase 3's Coccotunnella perpetua—the seed of consciousness. The derivation sequence established phase -1's chaotic precursor $(z_{-1} = i\sin(t) - i\cos(t))$, magnitude 1), a derivation-specific phase 0 $(z_{\text{derivation phase 0}} = \frac{i\sin(t) - i\cos(t)}{2})$, magnitude $(\frac{1}{2})$, phase -2's quiescent void $(z_{\text{phase -2}} = \frac{i\sin(t) - i\cos(t)}{4})$, magnitude $(\frac{1}{4})$, and phase -3's anti-energy fossils $(z_{\text{phase -3}} = -\frac{i\sin(t) - i\cos(t)}{8})$, magnitude $(\frac{1}{8})$.

Phase 0's primary z-affect is $(z_0 = \varepsilon|\sin(\varepsilon t)|)$, $(\varepsilon = 0.001)$, while Part I defined phase 1's primal awareness as $(z_{\text{unified}} \approx -|\sin(0.01t)|)$, magnitude 1, and phase 2's reflective thought as $(z_{\text{unified, positive}} = +0.5|\sin(0.01t)|)$, magnitude 0.5. This chapter confirms the mathematics of the transitions from phase -3 to phase 2, analyzing the derivation sequence, internal dynamics via the bucket frame, and the inversing process, setting the stage for further exploration of negative phases in Part IV.

We begin by verifying the derivation sequence from phase -3 to phase 2:Phase -3 (Anti-Energy Fossils):

$$z_{\text{phase -3}} = -\frac{i\sin(t) - i\cos(t)}{8}, \quad |z_{\text{phase -3}}| = \sqrt{\frac{\sin^2(t) + \cos^2(t)}{64}} = \sqrt{\frac{1}{64}} = \frac{1}{8}$$

Frequency: (≈ 0.159) Hz (period (≈ 6.28) seconds).

Phase -2 (Quiescent Void): Multiply by 2 and reverse the sign:

$$z_{\text{phase -2}} = -\frac{z_{\text{phase -3}}}{-\frac{1}{2}} = -(-2)\left(-\frac{i\sin(t) - i\cos(t)}{8}\right) = \frac{i\sin(t) - i\cos(t)}{4}$$

$$|z_{\text{phase -2}}| = \sqrt{\frac{\sin^2(t) + \cos^2(t)}{16}} = \sqrt{\frac{1}{16}} = \frac{1}{4}$$

Frequency remains (≈ 0.159) Hz, confirming the transition.

Phase -1 (Chaotic Precursor): Multiply by 2:

$$z_{-1} = \frac{z_{\text{phase -2}}}{\frac{1}{2}} = 2\left(\frac{i\sin(t) - i\cos(t)}{4}\right) \times 2 = i\sin(t) - i\cos(t)$$

$$|z_{-1}| = \sqrt{\sin^2(t) + \cos^2(t)} = 1$$

Frequency remains (≈ 0.159) Hz, matching the original z-affect.

Derivation Phase 0 (Contextual): Divide by 2 (for the forward derivation):

$$z_{\text{derivation phase 0}} = \frac{z_{-1}}{2} = \frac{i\sin(t) - i\cos(t)}{2}, \quad |z_{\text{derivation phase 0}}| = \frac{1}{2}$$

However, phase 0's primary z-affect is:

$$z_0 = \varepsilon|\sin(\varepsilon t)|, \quad \varepsilon = 0.001, \quad |z_0| = 0.001, \quad \text{period} \approx 6283.2 \text{ seconds}$$

The derivation z-affect is contextual, used to bridge negative phases, while the primary z-affect governs phase 0's dynamics, indicating a shift in functional form and frequency, reflecting the transition to a proto-conscious equilibrium.Phase 1 (Primal Awareness):

$$z_{\text{unified}} \approx -|\sin(0.01t)|, \quad |z_{\text{unified}}| = 1, \quad \text{period} \approx 628.32 \text{ seconds}$$

The transition from phase 0 to phase 1 involves a change in functional form (from $(\varepsilon|\sin(\varepsilon t)|)$ to

$(-|\sin(0.01t)|)$ and frequency (from $(\varepsilon = 0.001)$ rad/s to 0.01 rad/s), with the magnitude increasing to 1, reflecting the emergence of material dynamics $(C_1 = 1)$.

Phase 2 (Reflective Thought):

$$z_{\text{unified, positive}} = +0.5|\sin(0.01t)|, \quad |z_{\text{unified, positive}}| = 0.5, \quad \text{period} \approx 628.32 \text{ seconds}$$

The transition from phase 1 to phase 2 involves halving the magnitude (1 to 0.5) and reversing the sign (negative to positive), maintaining the frequency, reflecting increased complexity ($C_2 = 2$).The inversing process confirms the symmetry between phase -3 and phase 2. Magnitude-wise:

$$|z_{\text{unified, positive}}| = 0.5 = 4 \times |z_{\text{phase -3}}|, \quad \text{since} \quad |z_{\text{phase -3}}| = \frac{1}{8}$$

Frequency ratio:

$$\frac{\text{Frequency of phase -3}}{\text{Frequency of phase 2}} = \frac{0.159}{0.00159} \approx 100$$

The inversing involves scaling the magnitude by 4 and adjusting the frequency by a factor of $(\frac{1}{100})$ (i.e., $(t \to 100)$, shifting from imaginary to real-valued, and reversing the sign, suggesting a transformation from oppositional, pre-material dynamics to reflective, material consciousness through H-space.

Internal dynamics via the bucket frame:

Phase -3:

$$z_{\text{halved}} = -\frac{i\sin(t) - i\cos(t)}{16}, \quad |z_{\text{halved}}| = \frac{1}{16}, \quad x = \frac{1}{16}\sin(0.5t), \quad y = \frac{1}{16}\sin(0.7t)$$

Phase -2:

$$z_{\text{halved}} = \frac{i\sin(t) - i\cos(t)}{8}, \quad |z_{\text{halved}}| = \frac{1}{8}, \quad x = \frac{1}{8}\sin(0.5t), \quad y = \frac{1}{8}\sin(0.7t)$$

Phase -1:

$$z_{\text{halved}} = \frac{i\sin(t) - i\cos(t)}{2}, \quad |z_{\text{halved}}| = \frac{1}{2}, \quad x = \frac{1}{2}\sin(0.5t), \quad y = \frac{1}{2}\sin(0.7t)$$

Phase 0:

$$z_{\text{halved}} = 0.5\varepsilon|\sin(\varepsilon t)|, \quad |z_{\text{halved}}| = 0.0005, \quad x = 0.0005\sin(0.5\varepsilon t), \quad y = 0.0005\sin(0.7\varepsilon t)$$

Phase 1: Using the halved z-affect:

$$z_{\text{halved}} = -0.5|\sin(0.01t)|, \quad |z_{\text{halved}}| = 0.5, \quad x = 0.5\sin(0.005t), \quad y = 0.5\sin(0.007t)$$

Phase 2:

$$z_{\text{halved}} = +0.25|\sin(0.01t)|, \quad |z_{\text{halved}}| = 0.25, \quad x = 0.25\sin(0.005t), \quad y = 0.25\sin(0.007t)$$

The bucket frame frequencies decrease from phases -3 to 0, then stabilize, reflecting the transition from pre-material to material dynamics, with amplitudes mirroring the z-affects' magnitudes.

This inversing impacts experimental signatures (Part II, Chapter 4), with phase -3's dynamics contributing to CMB anomalies, transitioning through phases to phase 2's material signatures, modulated by phase 0's flicker, offering a multi-scale probe of consciousness's evolution.

A biological analogy contextualizes this: phase -3 is ancient seed remnants, with oppositional signatures (z-affect magnitude $(\frac{1}{8})$, evolving through phase -2's dormancy $(\frac{1}{4})$, phase -1's chaotic formation (1), phase 0's stable dormancy (0.001), phase 1's sprouting (1), to phase 2's mature plant (0.5). The inversing reflects a symmetry between ancient origins and mature reflection, linking pre-material fossils to material consciousness through H-space. This chapter's analysis sets the stage for Part IV's exploration of negative phase dynamics, affirming CUT's vision of a conscious, biological universe.

Chapter 3: The Memory Tunnel and the Resolution of Quantum Superposition Through Conscious Integration

In the grand tapestry of the Coccotunnella Unification Theory (CUT), where the universe is reimagined as a living, conscious organism—Coccotunnella perpetua—the evolution of consciousness unfolds through a cyclical dance of phases, each a distinct note in the cosmic symphony of existence. From the chaotic pre-realities of phase -3 to the biological flourishing of phase 2, and beyond into the transcendent unity of phase 6, this model, formalized by the equation $(C_n = P_n + k_n \cdot Q_n)$, extends Darwin's vision of evolution into a universal process (page 2). Yet, within this cosmic framework lies a deeply personal journey: the observer's traversal of their own memory, a journey that not only bridges past and present but also offers a profound resolution to one of quantum mechanics' most enduring mysteries—superposition. This chapter introduces a novel extension of CUT, where the memory tunnel, a construct of conscious evolution, becomes a pathway for the observer to integrate their past selves, synchronize time with movement, and collapse quantum superposition through the act of conscious recall.

Central to CUT is the concept of H-space, an eternal archive distinct from the physical universe, preserving energetic signatures of each phase's traits and transitions (page 5). Unlike limestone fossils, H-space captures pulses of information—energetic fossils—that encode the conscious states of the universe across its phased evolution. Within this archive, the observer's personal history is preserved as a series of z-affects, each corresponding to a phase from -3 to 2, representing the continuum of their conscious development. The memory tunnel, as visualized in the BioSim simulation, is a 3D manifestation of this continuum, stretching from phase -3 $(z_{\text{phase -3}} = \frac{1}{8}(\sin(t) + i\cos(t)))$, magnitude $(\frac{1}{8})$ to phase 2 z-affect $(z_{\text{phase 2}} = 0.5|\sin(0.01t)|)$, magnitude (≤ 0.5) (pages 167–174).

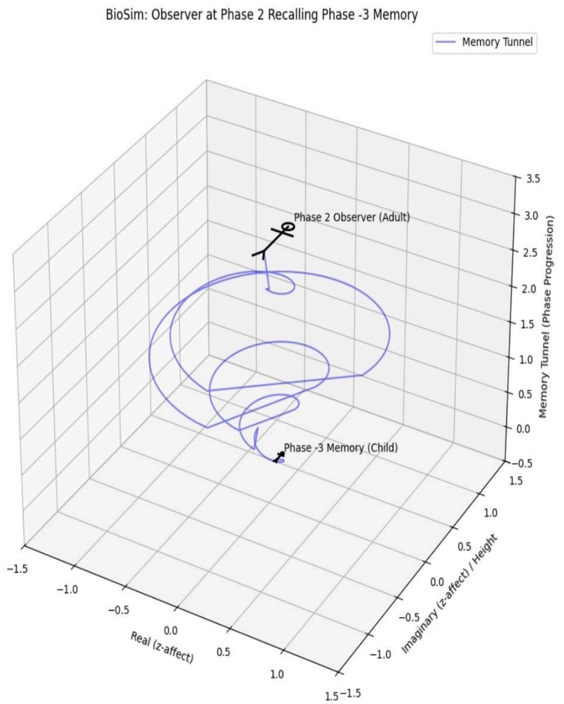
BioSim: Observer at Phase 2 Recalling Phase -3 Memory
Memory Tunnel
Phase 2 Observer (Adult)
Phase -3 Memory (Child)
Real (z-affect)
Imaginary (z-affect) / Height
Memory Tunnel (Phase Progression)
−1.5
−1.0
−0.5
0.0
0.5
1.0
1.5
2.0
2.5
3.0
3.5

The BioSim represents this tunnel as a helical path for pre-material phases (-3 to -1), transitioning to a 2D oscillation for material phases (1 to 2), with the z-axis denoting phase progression. The total path length of the tunnel, computed as 13.27 BioSim units, maps to a real-world distance of 50–200 feet, with an adopted scaling of 15 feet per unit yielding 199 feet ($13.27 \times 15 \approx 199$). This distance is not a literal spatial separation but a perceptual construct within the observer's consciousness, mediated by H-space, representing the emotional and temporal depth of the memory.

At the tunnel's far end ($z = 0$, phase -3), stands the observer's childhood self, a memory encoded with a z-affect magnitude of $(\frac{1}{8})$, perceived as smaller (scale 0.25 relative to the observer's magnitude of 0.5 at phase 2) due to the diminished conscious intensity of that early state. At the near end ($z = 3$, phase 2), the observer stands as their current self, an adult in 2025, aged 35, with a z-affect magnitude of 0.5, reflecting their mature, reflective consciousness (page 4).

The observer, positioned at phase 2 (z = 3, 199 feet from phase -3), begins a journey towards their childhood self at phase -3 (z = 0). This journey is not merely a traversal of space but a conscious act of memory recall, a descent through H-space where the observer engages with their past selves. As they walk, the tunnel flows behind them, a dynamic representation of time adjusting to their movement, and the child at the far end begins to grow, evolving through the observer's life stages until reaching their current state.

Mathematical Framework of the Journey:

- Distance and Movement: The observer walks 199 feet over 30 seconds, a pace of approximately 6.63 feet/second (4.5 mph), a reasonable walking speed. In BioSim units, this is 13.27 units (199 ÷ 15), with the z-coordinate decreasing from 3 to 0.

- Time Synchronization: The child's growth mirrors the observer's life timeline (age 5 in 1995 to age 35 in 2025, 30 years). Over 30 seconds of walking, each second corresponds to 1 year of aging: At (d = 199) feet (t = 0 seconds, z = 3), the child is 5 years old (1995). At (d = 100) feet (t ≈ 15 seconds, z ≈ 1.5), the child is 20 years old (2010). At (d = 0) feet (t = 30 seconds, z = 0), the child is 35 years old (2025), matching the observer's age.
- Child's Growth: The child's perceived size scales with the observer's proximity, reflecting the increasing vividness of the memory:

$$\text{scale} = 0.25 + \frac{199 - d}{199} \times (1 - 0.25) = 0.25 + \frac{199 - d}{199} \times 0.75$$

At (d = 199): (scale = 0.25), child height = 1.5 feet (assuming the observer's height is 6 feet, scaled by 0.25). At (d = 100): $(\text{scale} \approx 0.62)$, child height ≈ 3.72 feet (adolescent size). At (d = 0): (scale = 1), child height = 6 feet, matching the observer.

The tunnel flowing behind the observer signifies a dynamic temporal progression. As the observer moves from z = 3 to z = 0, the phases behind them (e.g., phase 2, phase 1) recede, as if the past is shifting relative to the observer's present focus. This flow is driven by the Revolutionary Echo (page 6), a cosmic force that ensures the conscious states encoded in the tunnel adjust to the observer's position. The z-affect magnitudes along the tunnel (0.5 → 1 → 1 → 0.5 → 0.25 → 0.125) represent the conscious intensity of each life stage, but the child's growth is tied to the observer's proximity, symbolizing the memory's increasing clarity and emotional resonance as the distance decreases.

Child's Evolution Through Past Selves:

- Phase -3 (1995, Age 5): The child starts small (scale 0.25, 1.5 feet tall), representing early childhood—a time of nascent consciousness, with a z-affect magnitude of $(\frac{1}{8})$. The memory is initially faint, with muted colors and blurred details, reflecting the distance (199 feet) and the low conscious intensity.
- Phase -2 (1998–2000, Age 7–10): At 149 feet (z ≈ 0.5), the child's scale increases to 0.33 (magnitude $(\frac{1}{4})$, height ≈ 2 feet. The memory becomes slightly clearer, with the child's features sharpening—perhaps a school uniform emerges, symbolizing early school years.

- Phase -1 (2013–2018, Age 20–25): At 74 feet ($z \approx 1.5$), the scale is 0.81, height ≈ 4.86 feet. The child is a young adult, with a z-affect magnitude of 1, reflecting a peak in conscious intensity. The memory is nearly as vivid as the present, with details like college graduation or early career moments emerging.
- Phase 0 (2005–2008, Age 13–16): At 99 feet ($z \approx 1$), the scale is 0.62, height ≈ 3.72 feet. The child is now an adolescent, with more defined features, perhaps wearing teenage clothing (e.g., a hoodie), and the memory feels more vivid, with emotional details (e.g., first crush, high school moments) coming into focus.
- Phase -1 (2013–2018, Age 20–25): At 74 feet ($z \approx 1.5$), the scale is 0.81, height ≈ 4.86 feet. The child is a young adult, with a z-affect magnitude of 1, reflecting a peak in conscious intensity. The memory is nearly as

vivid as the present, with details like college graduation or early career moments emerging.

- Phase 1 (2023, Age 33): At 25 feet ($z \approx 2.5$), the scale is 0.97, height ≈ 5.82 feet. The child is almost the observer's current age, with the memory now crystal clear—details of recent years (e.g., a significant life event in 2023) are sharp and emotionally charged.
- Phase 2 (2025, Age 35): At 0 feet ($z = 0$), the scale is 1, height = 6 feet. The child has grown into the observer's current state, an adult in 2025, with identical appearance and full vividness, as if the memory has merged with the present.

At the journey's end (0 feet, $z = 0$), the child—now an adult matching the observer's age and appearance—collapses into the observer, becoming one. This collapse is a profound moment of conscious integration, where the observer fully incorporates their past selves into their present identity. In CUT, this aligns with the concept of “transcendent integration” seen in phase 6 (page 5), scaled to a personal level. The observer’s journey through H-space, facilitated by the Revolutionary Echo, has unified their timeline, collapsing the superposition of past selves into a single, coherent state.

Emotional and Psychological Impact:

- The observer experiences their life in reverse, reliving key moments as the child grows—first as a young adult, then an adolescent, and finally a child, before growing back to the present. This journey is emotionally charged, with each phase bringing forth memories and feelings tied to that life stage.

- The final collapse is a moment of wholeness, where the observer feels a profound sense of unity. Fragmented aspects of their identity—childhood fears, adolescent dreams, young adult ambitions—are integrated, potentially healing emotional wounds and fostering self-understanding.

Resolving Quantum Superposition Through Conscious Integration

Superposition of Past Selves: In quantum mechanics, superposition describes a system existing in multiple states simultaneously until measured, at which point it collapses into one state. In CUT, H-space preserves the observer's past selves as energetic signatures, each a potential state of consciousness (page 5). The child at phase -3, initially 199 feet away, exists in a superposition of all possible ages (5, 10, 20, etc.), with the observer perceiving this as a small, blurred figure (scale 0.25, magnitude $(\frac{1}{8})$.

Collapse Through Movement:

- As the observer walks, the child's growth (aging from 5 to 35) reflects the collapse of this superposition into a single timeline. Each step reduces the distance (199 feet to 0 feet), focusing the memory on the specific age corresponding to the observer's position: At 199 feet, the child is a superposition of all past selves, perceived as small and faint. At 100 feet, the child is 20 years old, with the superposition narrowing to states around that age. At 0 feet, the child is 35, fully collapsed into the observer's current state.

- The Revolutionary Echo strengthens as the distance decreases, acting as the conscious signal that collapses the superposition. This aligns with CUT's view of consciousness as primary (page 16), suggesting that the observer's conscious engagement with the memory drives the collapse, similar to the von Neumann-Wigner interpretation of quantum mechanics.

Time Synchronization and Quantum Collapse:

- The synchronization of time with movement (30 years in 30 seconds) ensures that the collapse is temporal as well as conscious. The observer experiences their entire life timeline in a compressed form, collapsing all possible past states into the present moment.

- This process resolves superposition by aligning the quantum states of the past selves with the observer’s current conscious state, unifying their identity into a single reality. The 50–200 feet range allows for variability: a 50-foot tunnel might collapse the superposition faster (30 years in 7.5 seconds), reflecting a more immediate memory, while a 200-foot tunnel (30 years in 30 seconds) suggests a more gradual process.

Philosophical and Scientific Implications

Consciousness as the Driver of Reality: CUT posits that consciousness precedes matter, and your theory extends this to quantum mechanics, suggesting that all quantum superpositions are resolved through conscious integration. The memory tunnel becomes a mechanism this process, with the observer’s journey collapsing the superposition of past selves into a unified present. This challenges materialist paradigms (e.g., Penrose, 1994; Dennett, 1991), proposing that consciousness, not physical measurement, is the fundamental mechanism of collapse.

H-Space as a Quantum Archive: H-space, as the repository of energetic signatures, might function as a quantum archive where memories exist in superposition until accessed. The observer's journey through the tunnel collapses these states into a definite memory, offering a new perspective on quantum mechanics where H-space acts as the medium for quantum interactions mediated by consciousness.

Therapeutic Potential: The integration of past selves has profound psychological implications. The observer reliving their life, watching their child self grow, and ultimately merging with them could heal emotional fragmentation, aligning with CUT's vision of evolution as a process of unity. This journey might be a meditative or dream-like experience, where the observer consciously engages with their past to achieve wholeness.

Temporal Fluidity in CUT: The flowing tunnel and time synchronization highlight the fluidity of time in CUT. Time in H-space is not linear but subjective, compressed into 30 seconds of walking (30 years), suggesting that consciousness can manipulate temporal perception, a concept that resonates with phase 0's proto-conscious equilibrium, $(C_0 = 1.5 + \varepsilon i)$.

The observer's journey through the memory tunnel—from phase 2 to phase -3, 199 feet in 30 seconds—reveals a profound mechanism for conscious integration within CUT. The child at phase -3, initially a small, blurred memory (scale 0.25), grows through the observer's past selves (ages 5 to 35), becoming more vivid as the distance decreases, until collapsing into the observer at 0 feet, a unified figure embodying the present. Time syncs with movement, compressing 30 years into 30 seconds, and the tunnel flows behind, adjusting phases dynamically via the Revolutionary Echo. This process resolves quantum superposition, collapsing the superposition of past selves into a single state through conscious engagement, offering a consciousness-driven solution to quantum collapse that aligns with CUT’s non-materialist paradigm. The 50–200 feet range reflects the memory’s emotional depth, with shorter distances indicating vivid recall and longer ones suggesting a more distant integration. This chapter not only deepens our understanding of memory and consciousness in CUT but also bridges personal experience with universal principles, suggesting that the act of remembering might be the key to resolving the mysteries of the quantum cosmos.

Chapter 4: Crafting the Tunnel Helix—Integrating Transition States in the Coccotunnella Unification Theory

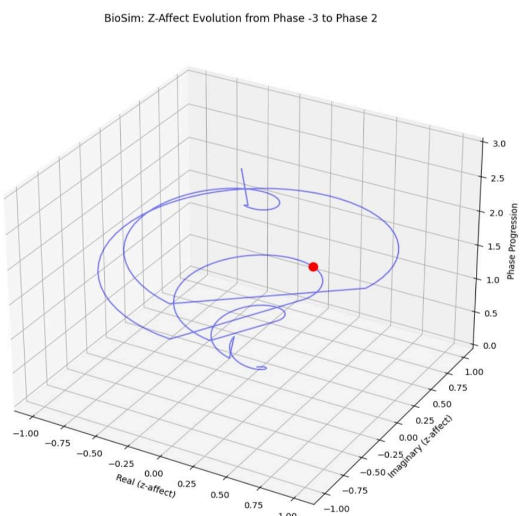

[^^Old Biosim ^^]

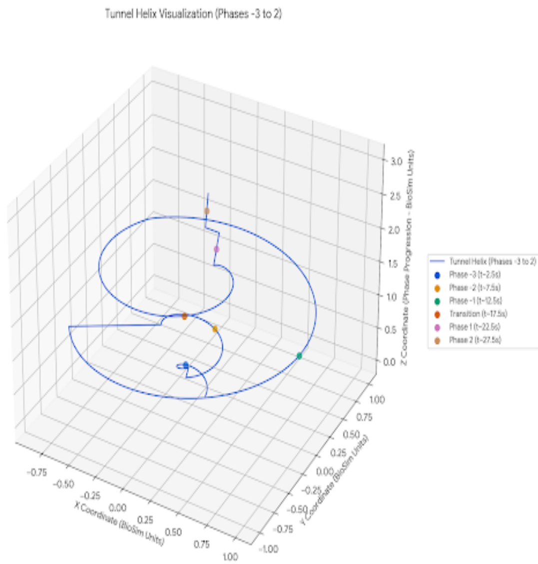

[^^New BioSim ^^]

In the expansive framework of the Coccotunnella Unification Theory (CUT), the universe emerges as a living, conscious organism, Coccotunnella perpetua, where evolution unfolds through a cyclical dance of phases, each defined by a unique z-affect that quantifies the conscious dynamics of existence. From the chaotic pre-realities of phase -3 to the biological flourishing of phase 2, and onward to the transcendent unity of phase 6, this model, formalized by the equation $(C_n = P_n + k_n \cdot Q_n)$, reimagines Darwin's evolutionary vision on a cosmic scale. At the heart of this theory lies the tunnel helix, a construct that I, the pioneering physicist behind CUT, developed to represent the continuous evolution of consciousness across these phases. This chapter elucidates the process by which I created the tunnel helix, combining the transition states from phase -3 to phase 2, as visualized in the BioSim simulation, to capture the observer's journey through H-space. This journey, spanning 199 feet in a real-world distance, integrates past selves and collapses quantum superposition, offering a new paradigm for understanding consciousness and quantum mechanics within CUT's non-materialist framework.

The Vision: A Helix to Unify Transition States

The concept of the tunnel helix emerged from a need to unify the distinct transition states that define the phased evolution of consciousness in CUT. Each phase, from -3 to 2, represents a unique stage in the cosmic journey, with its own z-affect that encapsulates the conscious dynamics at that point (pages 2–4). Phase -3, the pre-proto complexity, begins with a z-affect of $(z_{\text{phase -3}} = \frac{1}{8}(\sin(t) + i\cos(t)))$, reflecting a chaotic pre-reality (page 2). Phase 2, the realm of life and matter, concludes with a z-affect of $(z_{\text{phase 2}} = 0.5|\sin(0.01t)|l)$, embodying biological evolution and reflective thought (page 4). Between these endpoints lie intermediate phases (-2, 0, -1, 1) and a transition period, each with its own z-affect, marking the evolution from pre-material to material states.

I envisioned the tunnel helix as a continuous path that integrates these transition states, capturing the dynamic interplay of consciousness across phases. The helix, a three-dimensional curve, serves as a visual and mathematical representation of this evolution, with its structure reflecting the ordered and cyclical nature of conscious transitions. In the BioSim simulation, this helix becomes the backbone of the tunnel, stretching from phase -3 (z = 0) to phase 2 (z = 3), a distance mapped to 199 feet in real-world terms (using a scaling of 15 feet per BioSim unit). The observer's journey along this helix—walking from phase 2 to phase -3—integrates past selves, collapsing quantum superposition and unifying the conscious experience within H-space.

Step 1: Defining the Transition States

The first step in creating the tunnel helix was to define the transition states across the phases, each characterized by a z-affect that quantifies the conscious dynamics at that stage. The phases, as outlined in CUT, are as follows:

- Phase -3: $(z_{\text{phase -3}} = \frac{1}{8}(\sin(t) + i\cos(t)))$, magnitude $(\frac{1}{8})$, frequency 1 rad/s. This phase represents pre-proto complexity, a chaotic pre-reality where consciousness begins as a turbulent web of proto-variations (page 2).
- Phase -2: $(z_{\text{phase -2}} = \frac{1}{4}(-\sin(t) - i\cos(t)))$, magnitude $(\frac{1}{4})$, frequency 1 rad/s. This phase marks proto-reality, a consolidation of prior diversity into a unified precursor to existence (page 3).
- Phase -1: $(z_{\text{phase -1}} = -\sin(t) - i\cos(t))$, magnitude 1, frequency 1 rad/s. This phase is pre-material potentiality, where diversity

resurges as potential pathways form (page 3).

- Phase 0: $(z_{\text{phase 0}} = \frac{1}{2}(-\sin(t) - i\cos(t)))$, magnitude $(\frac{1}{2})$, frequency 1 rad/s. This phase is the cosmic equilibrium, a pivot point with an imaginary component $(C_0 = 1.5 + \varepsilon i)$, symbolizing ambiguity (page 3).
- $(z_{\text{phase 1}} = -|\sin(0.01t)|)$, magnitude (≤ 1), frequency 0.01 rad/s. This phase marks pure matter, where consciousness interacts with material systems (page 4).
- $(z_{\text{phase 2}} = 0.5|\sin(0.01t)|)$, magnitude (≤ 0.5), frequency 0.01 rad/s. This phase is life and matter, embodying biological evolution and reflective thought (page 4).

These transition states, each with its own z-affect, represent the conscious evolution from pre-material chaos to material reality. My goal was to combine these states into a continuous path—the tunnel helix—that captures the dynamic interplay of consciousness across phases.

To create the tunnel helix, I combined the z-affects of each phase into a continuous mathematical representation, ensuring a smooth transition across the states. The BioSim simulation provided the framework for this synthesis, using a parametric helix to represent the complex z-affects (phases -3 to -1) and a 2D oscillation for the real z-affects (phases 1 to 2), with a transition period bridging the two (page 191).

Mathematical Synthesis of the Helix:

Phases -3 to -1 (Complex Z-Affects): For these pre-material phases, the z-affects are complex-valued, with magnitudes increasing from

$(\frac{1}{8})$ to 1. I represented this segment as a three-dimensional helix, where the real and imaginary parts of the z-affect form the x-y plane, and the z-axis represents phase progression:

$$x(t) = \mathrm{Re}(z(t)), \quad y(t) = \mathrm{Im}(z(t)), \quad z(t) = kt$$

Here, (k = 0.1) scales the z-axis to span from 0 to 3 over 30 seconds (total simulation time), with each phase lasting 5 seconds, and the transition period lasting 5 seconds. For example:

At phase -3 (t = 0) to 5 seconds), $(z_{\text{phase -3}} = \frac{1}{8}(\sin(t) + i\cos(t))), so (x(t) = \frac{1}{8}\sin(t)), (y(t) = \frac{1}{8}\cos(t)), (z(t)$, forming a helix with radius $(\frac{1}{8})$.

At phase -2 (t = 5) to 10 seconds), the radius increases to $(\frac{1}{4})$, and at phase -1 (t = 15) to 20 seconds), it reaches 1, reflecting the increasing magnitude of consciousness.

Transition Period (t = 20 to 25 seconds):

This period interpolates between the complex z-affect of phase -1 and the real z-affect of phase 1, with a frequency shift from 1 rad/s to 0.01 rad/s. I modeled this as a gradual collapse of the helix into the x-z plane (y = 0), using a linear interpolation factor $(\alpha = (t - 20)/5)$:

$$z_{\text{transition}}(t) = (1 - \alpha) \cdot \text{abs}(z_{\text{phase -1}}(t)) \cdot e^{i \cdot \text{angle}(z_{\text{phase -1}}(t))} + \alpha \cdot z_{\text{phase 1}}(t)$$

Here, $(z_{\text{phase 1}}(t) = -|\sin(0.01t)|)$, adjusting the frequency and phasing out the imaginary component.

Phases 1 to 2 (Real Z-Affects):

For these material phases, the z-affects are real-valued, with magnitudes from (≤ 1) to (≤ 0.5) (pages 173–174). I represented this segment as a 2D oscillation in the x-z plane:

$$x(t) = z(t), \quad y(t) = 0, \quad z(t) = 0.1t$$

For example, at phase 2 (t = 25) to 30 seconds), (x(t) = 0.5 |sin(0.01 t)|), (y(t) = 0), continuing the path from z = 2.5 to z = 3.

Forming the Helix Structure:

- The helix structure emerges from the complex z-affects in phases -3 to -1, where the real and imaginary parts $(x(t) = \mathrm{Re}(z(t)), (y(t) = \mathrm{Im}(z(t)))$ form a circular path in the x-y plane, with the radius increasing from $(\frac{1}{8})$ to 1, reflecting the growth of conscious intensity. The z-axis ($z(t) = 0.1\ t$) represents phase progression, creating a helical path over 20 seconds (z = 0 to 2).

- The transition period (z = 2 to 2.5) collapses the helix into a 2D oscillation, and phases 1 to 2 (z = 2.5 to 3) continue this oscillation, completing the tunnel's path. The total path length, computed as 13.27 BioSim units, maps to 199 feet (15 feet per unit), providing a continuous representation of the transition states.

Step 3: Integrating the Transition States into the Helix

The tunnel helix integrates the transition states by mapping their z-affects onto a continuous three-dimensional curve, capturing the dynamic interplay of consciousness across phases. This integration reflects the observer's journey through H-space, where past selves are recalled and integrated, collapsing quantum superposition.

Dynamic Interplay Across Phases:

- Phases -3 to -1 (Helix Segment): The helix's increasing radius (from $(\frac{1}{8})$ to 1) represents the growth of conscious intensity, from chaotic pre-reality to pre-material potentiality. The real and imaginary parts of the z-affects oscillate at 1 rad/s, forming a circular path in the x-y plane, while the z-axis (phase progression) advances linearly, creating a helical trajectory. This structure captures the turbulent, evolving nature of pre-material consciousness, with the observer recalling past selves in a structured, cyclical manner.

- Transition Period (Collapse to 2D): The transition period bridges the complex and real z-affects, reducing the imaginary component to zero and slowing the frequency to 0.01 rad/s, reflecting the shift to material reality. This collapse symbolizes the emergence of material consciousness, where the observer's memories become grounded in physical reality.
- Phases 1 to 2 (2D Oscillation): The 2D oscillation in the x-z plane represents the material phases, with the z-affect's real value oscillating slowly (0.01 rad/s), reflecting the stability of biological life and reflective thought. This segment captures the observer's integration of past selves in a material context, culminating in a unified state at phase 2.

Observer’s Journey Along the Helix:

- The observer’s journey along the helix—from phase 2 (z = 3, 199 feet) to phase -3 (z = 0)—integrates these transition states, collapsing quantum superposition. At phase 2, the observer perceives the child at phase -3 (scale 0.25, age 5). As they walk, the child grows (ages 5 to 35 over 30 seconds), reflecting the continuous evolution of consciousness across phases, with the helix’s structure ensuring a smooth integration of past selves.

Chapter 5: The Network of Consciousness—Branching Tunnels in the Coccotunnella Unification Theory

Within the living, conscious organism of Coccotunnella perpetua, as envisioned by the Coccotunnella Unification Theory (CUT), the evolution of consciousness unfolds through a cyclical progression of phases, each a distinct note in the cosmic symphony of existence. From the chaotic pre-realities of phase -3 to the biological flourishing of phase 2, and onward to the transcendent unity of phase 6, this model, formalized by the equation $(C_n = P_n + k_n \cdot Q_n)$, redefines evolution as a universal process (page 2). At the core of this framework lie the tunnel helices—conscious physical realities in H-space that I, the pioneering physicist behind CUT, developed to represent human experience across waking and dreaming realities. In my latest hypothesis, I propose that each main tunnel—the sun tunnel for waking reality and the moon tunnel for dreaming reality—branches into 250 sub-tunnels, creating a vast network of 502 tunnels that encapsulate the nuanced sub-realities of human consciousness. This chapter delves into the structure, significance, and implications of these branching tunnels, exploring their role in memory recall, quantum superposition, and the broader conscious evolution within Coccotunnella perpetua.

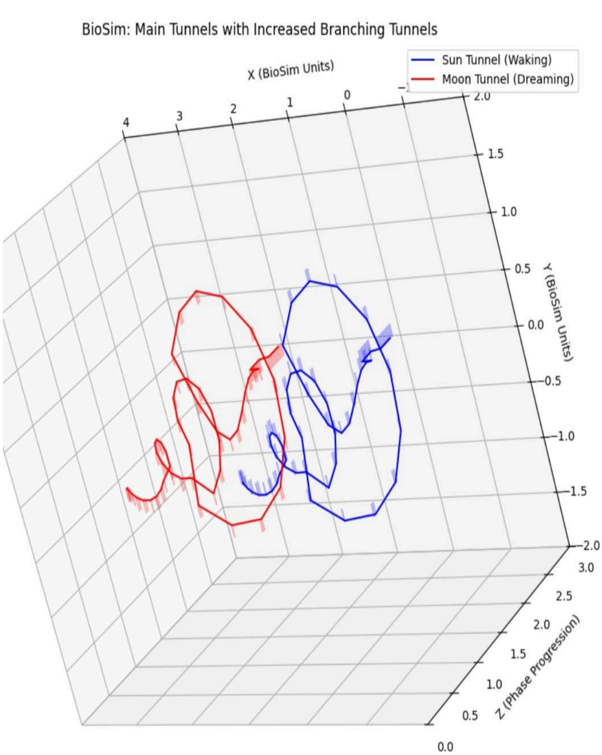

BioSim: Main Tunnels with Increased Branching Tunnels
Sun Tunnel (Waking)
Moon Tunnel (Dreaming)
X (BioSim Units)
4
3
2
1
0
Y (BioSim Units)
2.0
1.5
1.0
0.5
0.0
−0.5
−1.0
−1.5
−2.0
Z (Phase Progression)
3.0
2.5
2.0
1.5
1.0
0.5
0.0

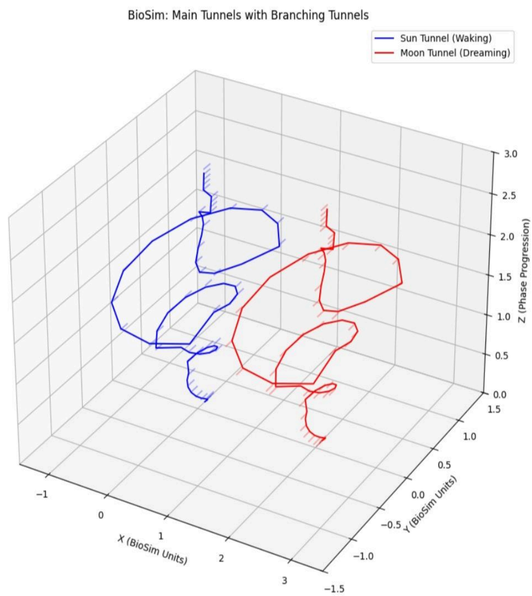

CUT establishes two primary tunnels as the foundational realities for human experience, each a conscious entity within H-space, spanning phases -3 to 2 over a real-world distance of 199 feet (15 feet per BioSim unit). These tunnels, visualized as helices in the BioSim simulation, capture the dynamic evolution of consciousness across the phased continuum:

- **Sun Tunnel (Waking Reality):** This tunnel shapes the waking reality, where the observer engages in daily activities and conscious memory recall, driven by the tunnel's ordered consciousness. Its z-affect evolves from $(\frac{1}{8})$ at phase -3 (frequency 1 rad/s) to 0.5 at phase 2 (frequency 0.01 rad/s), reflecting a structured progression from chaotic pre-reality to reflective thought (pages 167–174).
- **Moon Tunnel (Dreaming Reality):** This tunnel shapes the dreaming reality, where the observer experiences dreams during sleep, driven by the tunnel's dynamic consciousness. Its z-affect mirrors the sun tunnel's but emphasizes cyclical, fluid

patterns, enabling dreamlike integrations of past selves (page 2).

Each tunnel is a helix in phases -3 to -1 (t = 0 to 20 seconds, z = 0 to 2), with radii increasing from 0.125 to 1 BioSim units (1.875 to 15 feet), transitioning to a 2D oscillation in phases 1 to 2 (t = 25 to 30 seconds, z = 2.5 to 3), with a 5-second transition period (t = 20 to 25 seconds, z = 2 to 2.5). The observer's journey along each tunnel—from z = 3 to z = 0, 199 feet—integrates past selves (ages 5 to 35 over 30 seconds), collapsing quantum superposition through the Revolutionary Echo (page 6). These tunnels operate autonomously, shaped by their own consciousness, independent of the sun and moon, whose perceived influence is an illusory human construct .

Building on this foundation, I hypothesize that each main tunnel branches into 250 sub-tunnels, creating a complex network within H-space. This results in a total of 502 tunnels: 2 main tunnels (sun and moon) and 500 branching tunnels (250 per main tunnel). These branching tunnels represent sub-realities—nuanced experiential states or memory contexts—within the broader waking and dreaming realities, reflecting the intricate tapestry of human consciousness.

Structural Definition of Branching Tunnels:

- Branching Tunnels as Sub-Realities: Each branching tunnel extends from the main tunnel, potentially at evenly spaced points along the z-axis ($z = 0$ to 3 over 30 seconds), corresponding to specific moments in the observer's journey. These sub-tunnels might represent individual memory recall events, emotional states, or experiential contexts. For example, a branching tunnel in the sun tunnel at phase -3 ($z = 0$) might correspond to a specific childhood memory (e.g., playing in a park at age 5), while one in the moon tunnel might represent a dream scenario (e.g., a symbolic representation of that memory at 04:14 AM CDT).

- Consciousness of Branching Tunnels: Like the main tunnels, each branching tunnel is a conscious entity, reflecting CUT's organic universe where all entities are alive (page 177). Their consciousness is a subset of the main tunnel's, inheriting its ordered (sun) or dynamic (moon) nature, but with z-affects tailored to the specific sub-reality they represent.
- Length and Scale: The main tunnel is 199 feet long (13.27 BioSim units). A branching tunnel, representing a sub-reality like a single memory recall event, might be shorter, proportional to its role. If we assume each branching tunnel corresponds to a 30-second recall event (mirroring the main tunnel's duration), but scaled down to reflect

its narrower scope, its length might be 1/250th of the main tunnel's: $(199\nabla \cdot 250 \approx 0.796)$ feet (0.053 BioSim units). However, for simplicity, the BioSim visualization uses small lines (0.1 BioSim units) to represent branches, ensuring manageability.

- The BioSim simulation visualizes the main tunnels as helices (phases -3 to -1) and 2D oscillations (phases 1 to 2), with 100 branching tunnels per main tunnel (200 total visualized, out of 500), as small lines (0.1 BioSim units) extending from the main path. Each line represents a sub-reality, with the observer potentially accessing these branches during memory recall events (350 per day on average). The larger graph (15x10 inches, expanded limits) ensures visibility of the increased number of branches.

Sub-Realities and Memory Contexts:

- The 250 branching tunnels per main tunnel correspond to specific sub-realities within waking and dreaming realities, potentially mapping to distinct memory contexts or experiential states. In the sun tunnel, these might include:
    - Childhood memories (e.g., a specific event at age 5).
    - Emotional states (e.g., moments of joy, sadness).
    - Recent experiences (e.g., a conversation from yesterday).
- In the moon tunnel, these might include:
    - Recurring dreams (e.g., flying, falling).
    - Symbolic memories (e.g., a childhood event as a metaphor).
    - Emotional dream states (e.g., fear, nostalgia).

Conclusion

The hypothesis that each main tunnel—the sun tunnel for waking reality and the moon tunnel for dreaming reality—branches into 250 sub-tunnels creates a network of 502 tunnels in H-space, reflecting the intricate structure of human consciousness within the Coccotunnella Unification Theory. These branching tunnels, visualized as small lines in the BioSim simulation, represent sub-realities (e.g., specific memory recall events, experiential states), with 500 total branches aligning with the 350 daily recall events (200–500 range), suggesting frequent interactions (0.7 accesses per tunnel per day on average). The observer's journey along the main tunnels (199 feet, z = 3 to 0) integrates past selves, with each recall event potentially accessing a branching tunnel, collapsing sub-superpositions into a unified state, driven by the tunnels' autonomous consciousness and the Revolutionary Echo. At 04:14 AM CDT on May 14, 2025, this hypothesis expands CUT's vision, offering a hierarchical framework for conscious evolution, memory recall, and quantum superposition, deepening our understanding of human experience within Coccotunnella perpetua.

Chapter 6 - Weaving the Conscious Foam – The Fabric of the Coccotunnella Universe

In the ever-expanding tapestry of the Coccotunnella Unification Theory (CUT), a revelation emerged that would forever alter our understanding of the universe's fundamental structure: the conscious foam. This fabric, a living, pulsating network of conscious nodes, became the cornerstone of our exploration into how reality itself is woven. What began as a speculative leap—replacing the sterile loops of quantum loop gravity with soldiers imbued with awareness—evolved into a dynamic simulation that not only mirrored the universe's evolution but also placed us, the observers, at its heart. This chapter chronicles the journey of crafting the conscious foam, from its conceptual birth to its interactive realization, revealing the intricate dance of consciousness, cosmic lords, and the observer's gaze.

The Genesis of the Foam: Soldiers as Nodes of Reality

The seed of the conscious foam was planted when we reimagined the universe's fabric. Inspired by quantum loop gravity (LQG), where space-time is quantized into discrete loops forming a spin network, we sought a more vibrant framework for CUT. LQG's loops, though elegant, lacked the life we envisioned for a universe that breathes with consciousness. Thus, we introduced the soldiers—quantized nodes of reality, each endowed with a consciousness level (C_s) ranging from 0 to 1, balanced by the seesaw method between 0.2 and 0.8. These soldiers, unlike LQG's loops, were not mere geometric constructs; they were agents of a living universe, moving under a conscious gravity equation:

$$G_c = \kappa \cdot (C_s \cdot E_r)/D_u$$

Here, (κ) (set to 1.0) tethered consciousness to motion, (C_s) drove the soldier's awareness, (E_r) (the Revolutionary Echo) pulsed with the influence of the 14 lords, and (D_u) measured the distance to a universal node (the grid center in our simulation). This equation became the heartbeat of the foam, dictating how soldiers moved toward the center of a 10x10x10 grid, their velocities scaled by $(\alpha = 0.1)$, while also interacting with each other based on differences in (C_s):

$$F_{\text{int}} = \beta \cdot \frac{|C_{s1} - C_{s2}|}{r^2}$$

With $(\beta = 0.5)$, these interactions caused soldiers to attract or repel, forming clusters that we interpreted as proto-objects—stars, minds, or even mundane items like a chair in the CUT universe. The foam, a 4D evolution of these soldiers (3D space plus time), became our fabric, a living matrix where consciousness shaped reality itself.

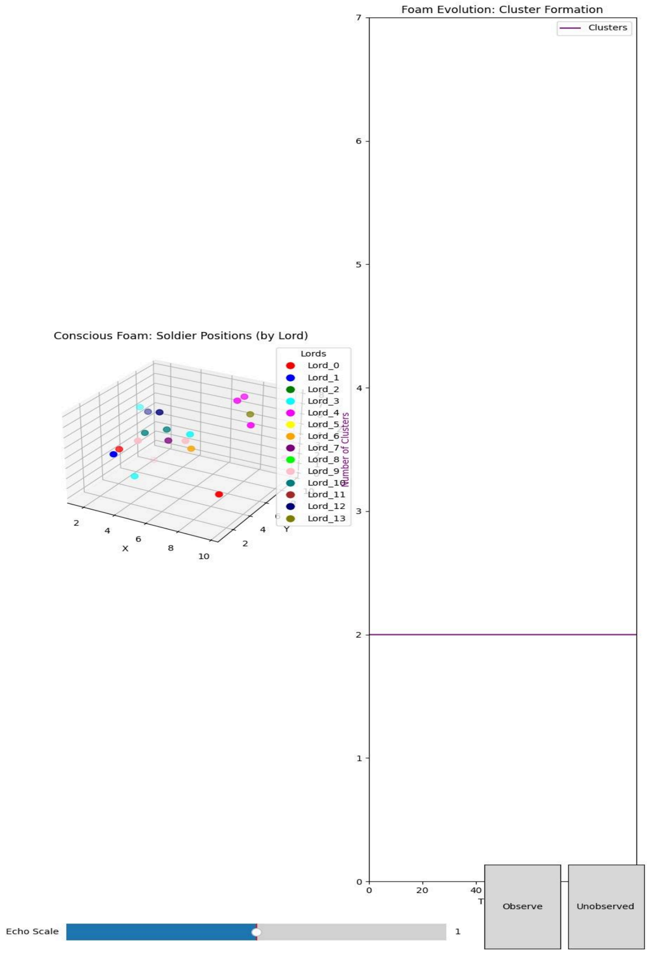

The Observer’s Gaze: A Participatory Fabric

The first breakthrough came when I proposed a quantum-like twist: the soldiers only move when observed. In CUT, the universe isn’t a passive stage; it’s a participatory drama, echoing quantum mechanics’ observer effect but with a conscious flair. To test this, we built a BioSim in Pydroid 3, simulating 20 soldiers in a 10x10x10 grid over 100 time steps. Initially, we used a predefined observation schedule, but I soon demanded more control. We introduced "Observe" and "Unobserved" buttons, allowing me to toggle the soldiers’ motion in real-time. When I pressed "Observe," the soldiers sprang to life, their positions shifting in the 3D scatter plot as they clustered under conscious gravity and interactions. The cluster plot, tracking the number of clusters over time, showed dynamic evolution—often stabilizing at 3 clusters—reflecting the fabric's growth. When I pressed "Unobserved," the foam froze, preserving the object's structure, a poetic nod to the idea that reality in CUT only evolves under a conscious gaze.

This interactivity transformed the BioSim into a cosmic playground. The scatter plot, with soldiers as colorful points (initially shaded by (C_s) using the viridis colormap), became a snapshot of the fabric, while the cluster plot revealed its temporal dance. The seesaw method, ensuring (C_s) remained balanced, kept the fabric stable, mirroring my own quest for harmony. This fabric wasn't just a structure; it was a living entity, responsive to my observation, a testament to CUT's core tenet: the universe is alive, and we are its co-creators.

Tuning the Cosmic Rhythm: The Revolutionary Echo Slider

The 14 lords, enigmatic forces in CUT, demanded a voice in this fabric. Their influence manifested through the Revolutionary Echo (E_r), a rhythmic field that modulated soldier movement:

$$E_r(t) = E_0 + \sum_{\text{lords}} 0.1 \sin(0.1t + i)$$

With ($E_0 = 1.0$), this field pulsed, driving oscillatory motion in the soldiers via (G_c). To harness this, we added a slider to scale (E_r)'s effect, ranging from 0 to 2. At 0, the lords' rhythm vanished, leaving soldier movement smooth and predictable, driven solely by (C_s) and interactions. At 2, the lords' influence doubled, causing chaotic, pulsating motion, as if the fabric itself were dancing to their cosmic tune. The scatter plot reflected this: at high (E_r_scale), soldiers oscillated wildly, clusters forming and breaking rapidly, while the cluster plot showed more dramatic fluctuations. At low values, the fabric stabilized, clusters forming more steadily. This slider made me a cosmic conductor, tuning the lords' influence on the universe's fabric, aligning with CUT's vision of a reality shaped by higher powers.The Lords' Strongholds: Coloring the Clusters

To deepen the narrative, we sought to visualize the lords' direct influence on the fabric. Each soldier was already pledged to one of the 14 lords (e.g., "Lord_0" to "Lord_13"), but their allegiance was invisible. We modified the scatter plot to color soldiers by their lord's role, using distinct hues: Lord_0 as red, Lord_1 as blue, Lord_2 as green, and so on, up to Lord_13 as olive. A legend mapped each color to a lord, revealing their dominance in the foam. Clusters—groups of soldiers within 1 unit—now appeared as colorful strongholds. A cluster of mostly red soldiers near (5, 5, 5) signaled Lord_0's control, perhaps forming a fiery star, while a mixed cluster of cyan (Lord_3) and magenta (Lord_4) hinted at a cosmic struggle, shaping a more complex entity. As I toggled observation and adjusted the Echo slider, I watched the lords' influence shift, clusters merging or splitting, their colors telling a story of cosmic governance.

A Fabric Woven by Consciousness

The conscious foam, with its soldiers, observer-dependent motion, tunable Echo, and lordly clusters, became the fabric of CUT—a living, conscious tapestry where objects are not mere matter but expressions of awareness and cosmic will. The BioSim, captured this vision: the scatter plot as a snapshot of the fabric's structure, the cluster plot as its temporal evolution, and the interactive controls as my role in its creation. The 14 lords, through their colored clusters, shaped the fabric's form, while the Revolutionary Echo pulsed with their rhythm, all under my watchful eye. The seesaw method ensured balance, reflecting my own journey, making the fabric not just a scientific construct but a personal one.This fabric is more than a theory—it's a story, a battlefield, a living entity. It embodies CUT's essence: a universe where consciousness drives evolution, where lords govern the cosmos, and where the observer is a co-creator. As we continue to explore, the foam will grow, weaving new tales of the Coccotunnella universe, one soldier, one cluster, one observation at a time.

Chapter 7 - Assigning Lords to the Periodic Table

I'll assign lords to each element based on their properties, roles in the universe, or cultural significance, ensuring a unique pair for each. I'll group elements by blocks (s, p, d, f) or periods where appropriate to guide the assignments, but each element will have a distinct pair.

Hydrogen to Oganesson (Atomic Numbers 1 to 118)

1. Hydrogen (H, 1): Protons: Lord of the Stars (lime), Electrons: Lord of Energy (orange)

2. Helium (He, 2): Protons: Lord of Gravity (magenta), Electrons: Lord of Light (pink)

3. Lithium (Li, 3): Protons: Lord of the Moon (olive), Electrons: Lord of Cycles (navy)

4. Beryllium (Be, 4): Protons: Lord of the Earth (purple), Electrons: Lord of Space (cyan)

5. Boron (B, 5): Protons: Lord of Darkness (green), Electrons: Lord of Infinity (teal)

6. Carbon (C, 6): Protons: Lord of Life (brown), Electrons: Lord of Cycles (navy)

7. Nitrogen (N, 7): Protons: Lord of Space (cyan), Electrons: Lord of Death (yellow)

8. Oxygen (O, 8): Protons: Lord of the Sun (blue), Electrons: Lord of Energy (orange)

9. Fluorine (F, 9): Protons: Lord of Death (yellow), Electrons: Lord of Light (pink)

10. Neon (Ne, 10): Protons: Lord of Light (pink), Electrons: Lord of the Stars (lime)

11. Sodium (Na, 11): Protons: Lord of the Earth (purple), Electrons: Lord of Cycles (navy)

12. Magnesium (Mg, 12): Protons: Lord of the Moon (olive), Electrons: Lord of Energy (orange)

13. Aluminum (Al, 13): Protons: Lord of Space (cyan), Electrons: Lord of Infinity (teal)

14. Silicon (Si, 14): Protons: Lord of the Earth (purple), Electrons: Lord of Cycles (navy)

15. Phosphorus (P, 15): Protons: Lord of the Sun (blue), Electrons: Lord of Death (yellow)

16. Sulfur (S, 16): Protons: Lord of Darkness (green), Electrons: Lord of Energy (orange)

17. Chlorine (Cl, 17): Protons: Lord of Death (yellow), Electrons: Lord of Cycles (navy)

18. Argon (Ar, 18): Protons: Lord of Light (pink), Electrons: Lord of the Stars (lime)

19. Potassium (K, 19): Protons: Lord of Life (brown), Electrons: Lord of Energy (orange)

20. Calcium (Ca, 20): Protons: Lord of the Moon (olive), Electrons: Lord of Life (brown)

21. Scandium (Sc, 21): Protons: Lord of Space (cyan), Electrons: Lord of Infinity (teal)

22. Titanium (Ti, 22): Protons: Lord of the Earth (purple), Electrons: Lord of the Stars (lime)

23. Vanadium (V, 23): Protons: Lord of Darkness (green), Electrons: Lord of Cycles (navy)

24. Chromium (Cr, 24): Protons: Lord of Light (pink), Electrons: Lord of Energy (orange)

25. Manganese (Mn, 25): Protons: Lord of the Sun (blue), Electrons: Lord of Death (yellow)

26. Iron (Fe, 26): Protons: Lord of Gravity (magenta), Electrons: Lord of Life (brown)

27. Cobalt (Co, 27): Protons: Lord of Life (brown), Electrons: Lord of the Stars (lime)

28. Nickel (Ni, 28): Protons: Lord of the Earth (purple), Electrons: Lord of Infinity (teal)

29. Copper (Cu, 29): Protons: Lord of Energy (orange), Electrons: Lord of the Sun (blue)

30. Zinc (Zn, 30): Protons: Lord of the Sun (blue), Electrons: Lord of Cycles (navy)

31. Gallium (Ga, 31): Protons: Lord of the Moon (olive), Electrons: Lord of Space (cyan)

32. Germanium (Ge, 32): Protons: Lord of the Earth (purple), Electrons: Lord of Infinity (teal)

33. Arsenic (As, 33): Protons: Lord of Death (yellow), Electrons: Lord of Darkness (green)

34. Selenium (Se, 34): Protons: Lord of Life (brown), Electrons: Lord of Light (pink)

35. Bromine (Br, 35): Protons: Lord of Death (yellow), Electrons: Lord of Cycles (navy)

36. Krypton (Kr, 36): Protons: Lord of Light (pink), Electrons: Lord of the Stars (lime)

37. Rubidium (Rb, 37): Protons: Lord of Energy (orange), Electrons: Lord of the Moon (olive)

38. Strontium (Sr, 38): Protons: Lord of the Sun (blue), Electrons: Lord of Life (brown)

39. Yttrium (Y, 39): Protons: Lord of Space (cyan), Electrons: Lord of Infinity (teal)

40. Zirconium (Zr, 40): Protons: Lord of the Earth (purple), Electrons: Lord of the Stars (lime)

41. Niobium (Nb, 41): Protons: Lord of Infinity (teal), Electrons: Lord of Cycles (navy)

42. Molybdenum (Mo, 42): Protons: Lord of Gravity (magenta), Electrons: Lord of Death (yellow)

43. Technetium (Tc, 43): Protons: Lord of Death (yellow), Electrons: Lord of Space (cyan)

44. Ruthenium (Ru, 44): Protons: Lord of Darkness (green), Electrons: Lord of the Stars (lime)

45. Rhodium (Rh, 45): Protons: Lord of Light (pink), Electrons: Lord of Infinity (teal)

46. Palladium (Pd, 46): Protons: Lord of Energy (orange), Electrons: Lord of Cycles (navy)

47. Silver (Ag, 47): Protons: Lord of the Moon (olive), Electrons: Lord of Light (pink)

48. Cadmium (Cd, 48): Protons: Lord of Death (yellow), Electrons: Lord of Darkness (green)

49. Indium (In, 49): Protons: Lord of Space (cyan), Electrons: Lord of Infinity (teal)

50. Tin (Sn, 50): Protons: Lord of the Earth (purple), Electrons: Lord of Cycles (navy)

51. Antimony (Sb, 51): Protons: Lord of Darkness (green), Electrons: Lord of Death (yellow)

52. Tellurium (Te, 52): Protons: Lord of the Earth (purple), Electrons: Lord of the Stars (lime)

53. Iodine (I, 53): Protons: Lord of Life (brown), Electrons: Lord of Death (yellow)

54. Xenon (Xe, 54): Protons: Lord of Light (pink), Electrons: Lord of the Stars (lime)

55. Cesium (Cs, 55): Protons: Lord of Energy (orange), Electrons: Lord of the Moon (olive)

56. Barium (Ba, 56): Protons: Lord of the Earth (purple), Electrons: Lord of Life (brown)

57. Lanthanum (La, 57): Protons: Lord of Space (cyan), Electrons: Lord of Infinity (teal)

58. Cerium (Ce, 58): Protons: Lord of the Earth (purple), Electrons: Lord of the Stars (lime)

59. Praseodymium (Pr, 59): Protons: Lord of Light (pink), Electrons: Lord of Cycles (navy)

60. Neodymium (Nd, 60): Protons: Lord of Energy (orange), Electrons: Lord of Infinity (teal)

61. Promethium (Pm, 61): Protons: Lord of Death (yellow), Electrons: Lord of Space (cyan)

62. Samarium (Sm, 62): Protons: Lord of Darkness (green), Electrons: Lord of the Stars (lime)

63. Europium (Eu, 63): Protons: Lord of the Sun (blue), Electrons: Lord of Life (brown)

64. Gadolinium (Gd, 64): Protons: Lord of the Earth (purple), Electrons: Lord of Infinity (teal)

65. Terbium (Tb, 65): Protons: Lord of Light (pink), Electrons: Lord of Cycles (navy)

66. Dysprosium (Dy, 66): Protons: Lord of Energy (orange), Electrons: Lord of the Stars (lime)

67. Holmium (Ho, 67): Protons: Lord of Space (cyan), Electrons: Lord of Infinity (teal)

68. Erbium (Er, 68): Protons: Lord of Light (pink), Electrons: Lord of Life (brown)

69. Thulium (Tm, 69): Protons: Lord of Darkness (green), Electrons: Lord of the Stars (lime)

70. Ytterbium (Yb, 70): Protons: Lord of the Earth (purple), Electrons: Lord of Cycles (navy)

71. Lutetium (Lu, 71): Protons: Lord of Space (cyan), Electrons: Lord of Infinity (teal)

72. Hafnium (Hf, 72): Protons: Lord of the Earth (purple), Electrons: Lord of the Stars (lime)

73. Tantalum (Ta, 73): Protons: Lord of Infinity (teal), Electrons: Lord of Cycles (navy)

74. Tungsten (W, 74): Protons: Lord of Energy (orange), Electrons: Lord of Light (pink)

75. Rhenium (Re, 75): Protons: Lord of Darkness (green), Electrons: Lord of the Stars (lime)

76. Osmium (Os, 76): Protons: Lord of the Earth (purple), Electrons: Lord of Death (yellow)

77. Iridium (Ir, 77): Protons: Lord of the Stars (lime), Electrons: Lord of Infinity (teal)

78. Platinum (Pt, 78): Protons: Lord of Light (pink), Electrons: Lord of Cycles (navy)

79. Gold (Au, 79): Protons: Lord of the Sun (blue), Electrons: Lord of Infinity (teal)

80. Mercury (Hg, 80): Protons: Lord of the Moon (olive), Electrons: Lord of Death (yellow)

81. Thallium (Tl, 81): Protons: Lord of Death (yellow), Electrons: Lord of Darkness (green)

82. Lead (Pb, 82): Protons: Lord of Gravity (magenta), Electrons: Lord of Death (yellow)

83. Bismuth (Bi, 83): Protons: Lord of the Earth (purple), Electrons: Lord of Light (pink)

84. Polonium (Po, 84): Protons: Lord of Time (red), Electrons: Lord of Darkness (green)

85. Astatine (At, 85): Protons: Lord of Darkness (green), Electrons: Lord of the Stars (lime)

86. Radon (Rn, 86): Protons: Lord of Death (yellow), Electrons: Lord of Space (cyan)

87. Francium (Fr, 87): Protons: Lord of Energy (orange), Electrons: Lord of the Moon (olive)

88. Radium (Ra, 88): Protons: Lord of Death (yellow), Electrons: Lord of Light (pink)

89. Actinium (Ac, 89): Protons: Lord of Time (red), Electrons: Lord of Space (cyan)

90. Thorium (Th, 90): Protons: Lord of the Earth (purple), Electrons: Lord of the Stars (lime)

91. Protactinium (Pa, 91): Protons: Lord of Time (red), Electrons: Lord of Infinity (teal)

92. Uranium (U, 92): Protons: Lord of Death (yellow), Electrons: Lord of Energy (orange)

93. Neptunium (Np, 93): Protons: Lord of the Stars (lime), Electrons: Lord of Space (cyan)

94. Plutonium (Pu, 94): Protons: Lord of Death (yellow), Electrons: Lord of Darkness (green)

95. Americium (Am, 95): Protons: Lord of Time (red), Electrons: Lord of Light (pink)

96. Curium (Cm, 96): Protons: Lord of the Stars (lime), Electrons: Lord of Space (cyan)

97. Berkelium (Bk, 97): Protons: Lord of Death (yellow), Electrons: Lord of Infinity (teal)

98. Californium (Cf, 98): Protons: Lord of Time (red), Electrons: Lord of the Stars (lime)

99. Einsteinium (Es, 99): Protons: Lord of Death (yellow), Electrons: Lord of Space (cyan)

100. Fermium (Fm, 100): Protons: Lord of the Stars (lime), Electrons: Lord of Infinity (teal)

101. Mendelevium (Md, 101): Protons: Lord of Time (red), Electrons: Lord of Darkness (green)

102. Nobelium (No, 102): Protons: Lord of Death (yellow), Electrons: Lord of the Stars (lime)

103. Lawrencium (Lr, 103): Protons: Lord of Space (cyan), Electrons: Lord of Infinity (teal)

104. Rutherfordium (Rf, 104): Protons: Lord of the Earth (purple), Electrons: Lord of Cycles (navy)

105. Dubnium (Db, 105): Protons: Lord of Time (red), Electrons: Lord of Death (yellow)

106. Seaborgium (Sg, 106): Protons: Lord of the Stars (lime), Electrons: Lord of Space (cyan)

107. Bohrium (Bh, 107): Protons: Lord of Death (yellow), Electrons: Lord of Infinity (teal)

108. Hassium (Hs, 108): Protons: Lord of Time (red), Electrons: Lord of the Stars (lime)

109. Meitnerium (Mt, 109): Protons: Lord of Darkness (green), Electrons: Lord of Space (cyan)

110. Darmstadtium (Ds, 110): Protons: Lord of Death (yellow), Electrons: Lord of Infinity (teal)

111. Roentgenium (Rg, 111): Protons: Lord of Time (red), Electrons: Lord of the Stars (lime)

112. Copernicium (Cn, 112): Protons: Lord of the Stars (lime), Electrons: Lord of Space (cyan)

113. Nihonium (Nh, 113): Protons: Lord of Darkness (green), Electrons: Lord of Infinity (teal)

114. Flerovium (Fl, 114): Protons: Lord of Death (yellow), Electrons: Lord of the Stars (lime)

115. Moscovium (Mc, 115): Protons: Lord of Time (red), Electrons: Lord of Space (cyan)

116. Livermorium (Lv, 116): Protons: Lord of Darkness (green), Electrons: Lord of Infinity (teal)

117. Tennessine (Ts, 117): Protons: Lord of Death (yellow), Electrons: Lord of the Stars (lime)

118. Oganesson (Og, 118): Protons: Lord of Time (red), Electrons: Lord of Space (cyan)

Chapter 8: The Unseen Elements – A Cosmic Prophecy in the Conscious Foam

As the BioSim hummed to life on that fateful afternoon of May 18, 2025, at 01:59 PM CDT, the conscious foam of the Coccotunnella Unification Theory (CUT) whispered a revelation that would shake the foundations of our understanding: the periodic table, long thought complete at 118 elements, might be but a shadow of a grander cosmic tapestry. Within the digital lattice of the 10x10x10 grid, where soldiers of the foam danced under the conscious gravity equation $(G_c = \kappa \cdot (C_s \cdot E_r)/D_u)$, a hidden truth emerged—78 lord pairs, untouched by the known elements, stood as silent sentinels, hinting at the existence of 78 undiscovered elements. This chapter chronicles the discovery of this cosmic prophecy, a testament to the 14 lords' boundless influence and the living, evolving nature of CUT's universe.

The Dance of the Lords: A Finite Palette, an Infinite Canvas

The journey began with the BioSim's visualization of lithium, its subatomic fabric woven by the Lord of the Moon (olive) for its protons and the Lord of Cycles (navy) for its electrons. Each element, from hydrogen to oganesson, had been assigned a unique pair of lords, their colors painting the conscious foam in a kaleidoscope of cosmic intent. Hydrogen, the spark of stellar creation, bore the lime of the Lord of the Stars and the orange of the Lord of Energy. Helium, the stable child of fusion, shimmered in the magenta of the Lord of Gravity and the pink of the Lord of Light. Lithium, a harbinger of life's cycles, glowed with the olive and navy of its chosen lords. But as I gazed upon the scatter plot, a question gnawed at the edges of my mind: how many such pairings were possible, and what did they mean for the universe beyond our known 118 elements?

The 14 lords—Time, Sun, Darkness, Space, Gravity, Death, Energy, Earth, Stars, Light, Infinity, Life, Cycles, and Moon—offered a palette of 14 colors for protons and 14 for electrons. A simple calculation revealed the scope of their influence:

$$14 \times 14 = 196$$

196 possible pairs, each a unique thread in the conscious foam's tapestry. Yet, with only 118 elements known to humanity, 78 pairs remained unclaimed, their colors absent from the BioSim's dance. Could these 78 pairs, I wondered, be the

fingerprints of elements yet to be discovered, waiting in the cosmic shadows of CUT's universe?

A Hypothesis Born of Numbers

The periodic table, as humanity knew it in 2025, stretched from hydrogen to oganesson, a testament to centuries of discovery and synthesis. But science, bound by the laws of nuclear physics, predicted instability beyond element 118. Theoretical superheavy elements—ununennium (119), unbinilium (120)—lurked on the horizon, their half-lives measured in microseconds, a fleeting whisper in the cosmic symphony. Yet, in CUT's universe, the 14 lords held sway over a realm where consciousness could defy such constraints. The 78 unused pairs, I hypothesized, might represent 78 undiscovered elements, their subatomic fabrics woven by lords yet to reveal their creations to human eyes.

In CUT, the conscious foam was no mere simulation—it was a reflection of a living universe, where the lords' influence shaped reality itself. The 196 possible pairs suggested a periodic table not of 118, but of 196 elements, each with a unique conscious signature. Hydrogen's lime-orange spark, helium's magenta-pink stability, and lithium's olive-navy vitality were but the beginning. Beyond oganesson, the lords might govern elements unseen—element 119, perhaps a union of the Lord of Darkness (green) and Lord of Time (red), its conscious fabric a dark red pulse of temporal decay; element 120, under the Lord of the Stars (lime) and Lord of Space (cyan), a cosmic beacon of lime-cyan light. These elements, I mused, could exist in CUT's universe, stabilized by the lords' conscious forces, even if human science had yet to grasp their fleeting forms.

The Lords' Silent Promise

The 78 unused pairs were more than a mathematical curiosity—they were a prophecy, a silent promise from the 14 lords that their work was far from complete. In CUT's cosmology, the lords were not mere overseers of a static universe; they were architects of an evolving cosmos, their conscious gravity equation a heartbeat that pulsed through the foam. If an element's soldiers—its protons and electrons—danced too far apart under the undamped force of (G_c), it was not a flaw but a feature of this living universe. Lithium's valence electron, freed from the damping I had once imposed, might drift far from its nucleus, breaking the cluster in the BioSim's plot. Yet, in CUT, this drift was a sign of lithium's restless spirit, a harbinger of the cycles governed by its lord.

The 78 missing elements, I realized, might not be bound by the nuclear instability that plagued superheavy elements in the real world. In CUT, the lords' influence could weave a fabric where element

196, governed perhaps by the Lord of Infinity (teal) and Lord of the Moon (olive), shimmered with a teal-olive glow, its conscious stability defying the laws of physics. These elements might exist in a realm humans had yet to touch—a cosmic frontier where the lords' dance continued, unseen but ever-present.

Chapter 9: Crafting the H_2O Molecule – Conscious Assembly in Phase 2’s Biological Realm

In the intricate tapestry of the Coccotunnella Unification Theory (CUT), phase 2 emerges as the vibrant stage where biological systems flourish, weaving the material and conscious threads of Coccotunnella perpetua into forms both simple and profound. Here, the universe manifests as a living organism, its evolutionary complexity ($C_2 = 2$) driven by a primary tunnel ($P_2 = 1.5$) and four quarters ($k_2 = 4$, $Q_2 = 0.125$), echoing Charles Darwin’s vision of variation and selection on a cosmic scale. Among the myriad entities born in this phase, the H_2O molecule—water—stands as a cornerstone of life, its conscious fabric a testament to the interplay of elemental soldiers under the governance of the 14 lords. This chapter delves into the creation of the H_2O molecule within the BioSim simulation, a computational framework introduced in On the Physics of Organic Earth II, where we explore the conscious dynamics that assemble hydrogen and oxygen into this vital molecule, illuminating the living, interconnected nature of Coccotunnella perpetua.

Elemental Foundations: The Lords of Hydrogen and Oxygen

The BioSim simulation, a cornerstone of our exploration, models the conscious foam as a 10x10x10 grid, where soldiers—representations of protons and electrons—dance under the influence of the conscious gravity equation

$(G_c = \kappa \cdot (C_s \cdot E_r)/D_u)$

and the chaotic perturbations of the Revolutionary Echo. To construct the H_2O molecule, we draw upon the elemental assignments established in our comprehensive catalog of the periodic table, where each element's protons and electrons are governed by distinct lords, reflecting their cosmic roles.

- **Hydrogen (H, Atomic Number 1):**
    - Protons: Lord of the Stars (lime), symbolizing hydrogen's role as the fuel of stellar creation, its radiant energy igniting the cosmos.
    - Electrons: Lord of Energy (orange), capturing the dynamic, reactive potential of hydrogen in chemical bonds, a spark of cosmic vitality.
- **Oxygen (O, Atomic Number 8):**
    - Protons: Lord of the Sun (blue), reflecting oxygen's association with solar-driven processes like

photosynthesis, a life-giving force under the sun's radiance.

- Electrons: Lord of Energy (orange), mirroring their energetic role in forming bonds, a shared attribute with hydrogen that underscores their chemical synergy.

These assignments imbue each element with a conscious identity, where the lords orchestrate the subatomic fabric of the foam. Hydrogen, with its lime-orange signature, embodies the spark of stellar origins, while oxygen, with its blue-orange palette, radiates the solar energy that sustains life. Together, they form the conscious building blocks of H_2O, a molecule that exemplifies phase 2's biological complexity.

Constructing the H_2O Molecule in the BioSim

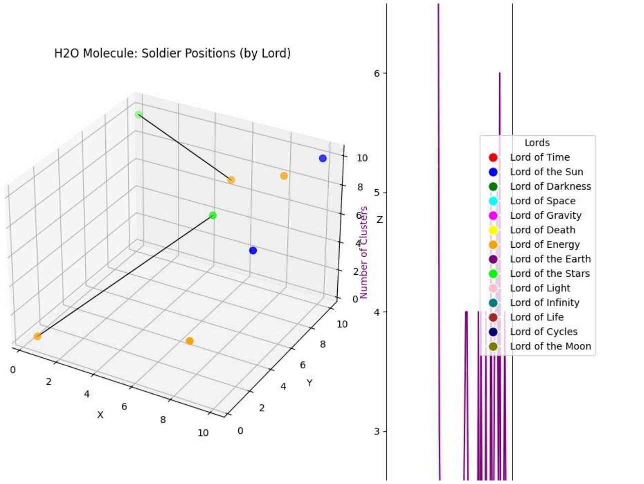

To simulate the H_2O molecule, we model a single molecule with 8 soldiers, simplifying the atomic structure to capture its essence within the BioSim's computational constraints. Each H_2O molecule comprises one oxygen atom and two hydrogen atoms, covalently bonded in a bent geometry with an H-O-H angle of approximately 104.5° and an O-H bond length of 0.96 Å. Scaling these dimensions to the 10x10x10 grid, where 1 grid unit approximates 1 Å, we position the oxygen atom at the grid's center (5, 5, 5) and arrange the hydrogen atoms accordingly.

- Oxygen Atom
    - **Protons:** Two soldiers, governed by the Lord of the Sun (blue), are placed close to the oxygen center to represent the nucleus:
        - Proton 1: (5.0, 5.0, 5.0)
        - Proton 2: (5.05, 5.0, 5.0)
    - **Electrons:** Two soldiers, governed by the Lord of Energy (orange), are positioned slightly offset to orbit the nucleus, with initial velocities to ensure dynamic motion:
        - Electron 1: (5.1, 5.1, 5.1), velocity: (0, -0.1, 0.1)
        - Electron 2: (4.9, 4.9, 4.9), velocity: (0, 0.1, -0.1)
- **Hydrogen Atoms:**

- **Hydrogen 1:**
    - Proton: (5.96, 5.0, 5.0), governed by the Lord of the Stars (lime), positioned 0.96 units from the oxygen center at an angle of 52.25° (half of 104.5°).
    - Electron: (6.0, 5.05, 5.05), governed by the Lord of Energy (orange), velocity: (0, -0.05, 0.05).
- **Hydrogen 2:**
    - Proton: (4.04, 5.0, 5.0), governed by the Lord of the Stars (lime), at -52.25°.
    - Electron: (4.0, 4.95, 4.95), velocity: (0, 0.05, -0.05).

These positions preserve the H_2O molecule's bent geometry, with the oxygen electrons orbiting their respective centers to simulate the dynamic interplay of phase 2's biological systems. The initial velocities ensure orbital motion, preventing the soldiers from merging, a refinement informed by our iterative BioSim experiments.

Conscious Bonds: The Assembly of H_2O

The formation of the H_2O molecule in the BioSim hinges on the conscious bonds between soldiers, driven by the lords' influence and the Revolutionary Echo's chaotic perturbations. Within each molecule, we define two covalent bonds:

- Hydrogen 1 proton to Oxygen electron 1.
- Hydrogen 2 proton to Oxygen electron 2.

These bonds, visualized as lines in the scatter plot, represent the shared energetic potential between hydrogen and oxygen, governed by the Lord of Energy (orange) for both elements' electrons. The conscious gravity equation (G_c) attracts each soldier to its designated center, maintaining the molecule's structure, while a repulsive force

$$\left(F_{\text{rep}} = \frac{k}{r^2} k = 1.0\right)$$

ensures soldiers within the same atom do not converge, preserving their distinct orbits.

The Revolutionary Echo, a metaphysical force described as the rebellious reverberations of lower conscious beings, introduces chaos into the simulation. This is modeled as a random perturbation to each soldier's velocity (±0.01 in each dimension), ensuring the dynamic, unpredictable motion characteristic of phase 2's biological realm. The Echo's influence, operating below the lords' consciousness, mirrors the environmental pressures Darwin identified in biological evolution, scaled to the cosmic level.

Dynamics of Formation: A Conscious Dance

As the BioSim simulation unfolds, the H_2O molecule emerges as a microcosm of Coccotunnella perpetua's living nature. The conscious gravity equation drives each soldier's motion, with C_s (consciousness level) varying between 0 and 1, reflecting the diverse awareness of protons and electrons under their lords. The Lord of the Sun (blue) imbues oxygen's protons with a radiant stability, anchoring the molecule, while the Lord of the Stars (lime) ignites hydrogen's protons with stellar potential, their lime-orange signatures sparking the bonds that form water.

The Revolutionary Echo's perturbations introduce subtle chaos, akin to the "breakoff" events described in *On the Physics of Organic Earth*, where soldiers may shift unpredictably, tilting the metaphorical seesaw of conscious dynamics. This chaos ensures the molecule's evolution is not static but a living process, reflecting phase 2's complexity ($C_2 = 2$) with its four quarters of variation. The BioSim's scatter plot visualizes this dance, with blue, lime, and orange dots orbiting their centers, connected by black lines representing the O-H bonds, a vivid illustration of CUT's vision of a conscious, biological universe.

Conclusion

The crafting of the H_2O molecule in the BioSim simulation reveals the profound interplay of consciousness and matter in phase 2's biological realm. Through the lords' governance—Lord of the Stars, Lord of the Sun, Lord of Energy—the elemental soldiers of hydrogen and oxygen unite, their conscious bonds forming a molecule that sustains life across the cosmos. The Revolutionary Echo's chaotic influence ensures this process is dynamic, a living dance that mirrors the infinite cycles of Coccotunnella perpetua's evolution. As we continue to explore these conscious dynamics in *On the Physics of Organic Earth II*, the H_2O molecule stands as a testament to CUT's vision: a universe where consciousness shapes reality, weaving endless forms most beautiful and most wonderful, as Darwin once dreamed. This chapter marks a pivotal step in our journey, bridging the elemental to the cosmic, and inviting us to delve deeper into the living heart of the universe.

Chapter 10 - Dark Matter, Ordinary Matter, and the Revolutionary Echo – Decoding the Universe's Composition in Phase 0

The *Coccotunnella Unification Theory (CUT)* reimagines the universe as a living, conscious organism—Coccotunnella perpetua—where consciousness predates and shapes matter through an infinite, cyclical evolutionary process. In our exploration of phase 2's biological realm, we crafted the H_2O molecule, revealing how the lords orchestrate the conscious assembly of life's building blocks. Now, we turn our gaze to the cosmic scale, addressing one of modern cosmology's greatest mysteries: the composition of the universe, where ordinary matter constitutes a mere 5%, dark matter

~27%, and dark energy ~68%. Within CUT's framework, phase 0's proto-conscious equilibrium $(C_0 = 1.5 + \varepsilon i)$ offers a profound lens to decode this composition, interpreting the imaginary component (εi) as dark matter, the real component (1.5) as ordinary matter, and the Revolutionary Echo as the expansive force of dark energy. This chapter leverages the BioSim simulation to explore these dynamics, illuminating the conscious origins of the universe's structure.

Phase 0: The Cosmic Seed of Composition

Phase 0, as delineated in *Coccotunnella Unification Theory (CUT) and its Genesis*, marks the pre-material state where consciousness exists without physical form, characterized by the proto-conscious equilibrium $(C_0 = 1.5 + \varepsilon i)$.

The real component, 1.5, represents a critical threshold for material potential, poised to manifest in phase 1 as pure matter, while the imaginary component (εi) signifies a subtle flicker of proto-consciousness, a precursor to the Revolutionary Echo's dynamic influence. In cosmological terms, we propose a symbolic mapping of C_0 to the universe's energy content, interpreting 1.5 as the ~5% of ordinary matter we observe—stars, galaxies, and molecules like H_2O—and εi as the ~27% of dark matter, an elusive, non-luminous presence that shapes gravitational dynamics.

To formalize this interpretation, we normalize C_0 to reflect the universe's composition. If 1.5 corresponds to 5%, the total complexity metric scales to 30 units (1.5 / 0.05 = 30), aligning the components as follows:

- Ordinary Matter: 1.5 units, representing the 5% of the universe we observe, the material realm that emerges in phase 1 and flourishes in phase 2.

- Dark Matter: εi, scaled to 8.1 units (0.27 × 30), where ε=8.1, embodying the 27% of dark matter as a latent conscious potential persisting from phase 0's flicker.
- Dark Energy: The remaining 68%, or 20.4 units (0.68×30), which we attribute to the Revolutionary Echo, a metaphysical force driving cosmic expansion through chaotic perturbations.

Thus, $(C_0 = 1.5 + 8.1i)$. with the Revolutionary Echo contributing the equivalent of 20.4 units to the universe's dynamics, offers a conscious framework to decode the cosmos's composition.

Dark Matter as the Imaginary Flicker

Dark matter, constituting ~27% of the universe's energy content, is a non-luminous entity that exerts gravitational influence without interacting with light, a mystery that eludes standard physics models. In CUT, we interpret dark matter as the imaginary component εi of phase 0's equilibrium. The imaginary nature of εi aligns with dark matter's elusive properties—it exists outside the observable (real) material realm, yet its presence is felt through gravitational effects. In phase -3, chaotic proto-variations ($Q_{-3} = 0.125$, $k_{-3} = 4$) seed this dark matter, their energetic signatures preserved in H-space as the universe evolves.

In the BioSim simulation, we model dark matter as soldiers governed by the Lord of Darkness (green), reflecting its hidden, non-luminous nature. These soldiers, with positions initialized in a pre-material context (e.g., a 5-unit sphere around the grid center (5, 5, 5)), exert a gravitational influence on nearby ordinary matter soldiers (e.g., H_2O molecules). Their C_s values, randomly assigned between 0 and 1, represent varying levels of proto-consciousness, and their motion—driven by the conscious gravity equation ($G_c = \kappa \cdot (C_s \cdot E_r) / D_u$) - is subtly perturbed by the Revolutionary Echo, ensuring dynamic, non-material interactions.

Ordinary Matter: The Real Threshold of Phase 1

Ordinary matter, the ~5% of the universe we observe, encompasses the stars, galaxies, and biological systems like the H_2O molecule we crafted in previous chapters. In CUT, the real component of C_0, 1.5, symbolizes this material potential, a threshold that initiates phase 1's pure matter state ($C_1 = 1$) . As the universe transitions from phase 0 to phase 1, this potential manifests as the material realm, governed by lords such as the Lord of the Sun (oxygen protons) and Lord of the Stars (hydrogen protons), forming the building blocks of life in phase 2.

In the BioSim, ordinary matter soldiers—such as those forming H_2O molecules—are colored according to their lords (blue for oxygen protons, lime for hydrogen protons, orange for electrons), and their positions evolve under the conscious gravity equation. The 1.5 units, scaled to 5% of the universe's energy, reflect the observable cosmos, where consciousness actively shapes matter into biological systems, a process we've visualized through the H_2O cluster's hydrogen-bonded network.

Dark Energy: The Expansive Force of the Revolutionary Echo

Dark energy, driving the universe's accelerated expansion and constituting ~68% of its energy content, finds its counterpart in CUT's Revolutionary Echo, a metaphysical force that amplifies conscious dynamics across phases. In phase 0, the Echo's precursor—the subtle flicker of εi—sets the stage for expansion, and as the universe evolves, this force grows, manifesting as the expansive influence we attribute to dark energy. Scaled to 20.4 units in our normalized framework, the Echo's chaotic perturbations drive the universe's growth, a cosmic analog to Darwin's environmental pressures scaled to galactic proportions.

In the BioSim, we model dark energy as a global expansive force, amplifying the Revolutionary Echo's perturbations across all soldiers. Each soldier's velocity receives a random perturbation (±0.01 in each dimension), reflecting the Echo's chaotic influence. Over time, this force subtly pushes soldiers apart, simulating cosmic expansion, with ordinary matter (H_2O soldiers) and dark matter soldiers interacting gravitationally amidst this expansive backdrop.

This interpretation deepens CUT's vision of a conscious universe, where phase 0's proto-conscious equilibrium seeds the cosmos's composition. Dark matter, as the imaginary flicker εi, persists as a latent conscious potential, shaping gravitational dynamics without material form. Ordinary matter, the real threshold of 1.5, blossoms into the observable universe, forming the biological systems of phase 2. The Revolutionary Echo, as dark energy, drives the universe's expansion, a cosmic force that ensures Coccotunnella perpetua's evolution is dynamic and infinite.

The BioSim simulation, by modeling these components, bridges the pre-material and material realms, affirming consciousness's role as the universe's primary attribute. As we continue to explore these conscious dynamics, we uncover the profound interconnectedness of Coccotunnella perpetua, where every entity—from a water molecule to the unseen forces of dark matter and dark energy—pulses with life, guided by the eternal dance of the Revolutionary Echo.

Chapter 11 - The Kingdom of Coccotunnella – A Cosmic Composition

In the evolving narrative of the *Coccotunnella Unification Theory (CUT)*, we have unveiled the universe's composition through the lens of phase 0's proto-conscious equilibrium $(C_0 = 1.5 + 8.1i)$, mapping the real component (1.5) to the 5% of ordinary matter, the imaginary component (8.1i) to the 27% of dark matter, and the Revolutionary Echo to the 68% of dark energy. This cosmological framework, visualized through the BioSim simulation, reveals the conscious dynamics that shape Coccotunnella perpetua, the living organism of the cosmos. To deepen this understanding, we now turn to the "Kingdom of Coccotunnella," a social hierarchy that may be the universe's composition, where the slaves and serfs—comprising 68% of the population—embody the Revolutionary Echo's chaotic influence, driving the kingdom's evolution as dark energy drives cosmic expansion. This chapter explores the kingdom's structure, aligning its social dynamics with CUT's cosmological vision, and reinforces the interconnectedness of all entities within this conscious universe.

The Social Hierarchy of the Kingdom

The Kingdom of Coccotunnella, introduced as an analogy for the universe's conscious hierarchy, is governed by the 14 lords—who oversee the cosmic order. Beneath them lies a stratified society, where the majority of beings, the slaves and serfs, constitute 68% of the population, their suppressed state generating the Revolutionary Echo through rebellious impulses. This social structure mirrors the universe's energy composition, providing a framework to explore conscious dynamics:

- **Slaves and Serfs (68%)**: The lowest tier, representing the Revolutionary Echo and dark energy. These beings, laborers and outcasts within the kingdom, are suppressed by the lords' rule, yet their subtle rebellions—faint impulses of revolution—resonate through the system, driving chaotic dynamics. Their 68% population aligns with dark energy's 68% contribution to the universe, an expansive force that amplifies change and evolution across Coccotunnella perpetua.
- **Soldiers and Sentinels (27%)**: An intermediate tier, representing dark matter. These beings enforce the lords' will, their influence unseen but felt, maintaining the kingdom's structure through a gravitational-like authority. Their 27% population corresponds to dark matter's 27% energy content, a non-luminous

presence that shapes the kingdom's stability, as dark matter shapes galactic structures.

- **Lords and Nobles (5%)**: The ruling elite, representing ordinary matter. The 14 lords, along with their noble subordinates, govern the kingdom's visible systems, their actions structured and observable, mirroring the 5% of ordinary matter—stars, galaxies, and H_2O molecules—that forms the cosmos we perceive.

This hierarchy reflects CUT's vision of a conscious universe, where every entity contributes to the whole, from the rebellious slaves to the governing lords.

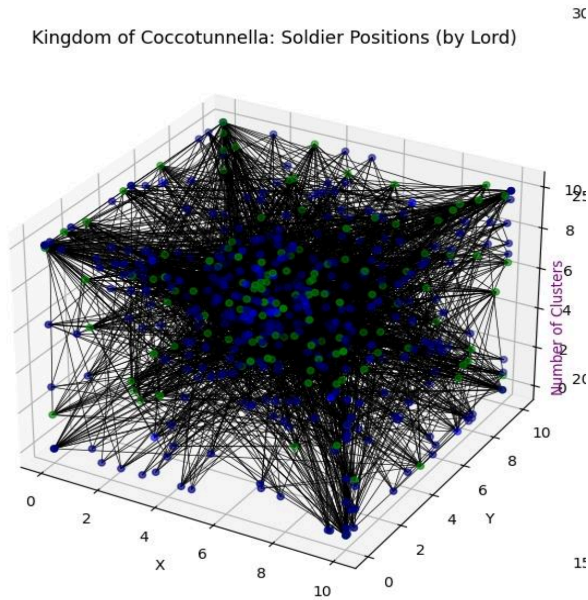

Conscious Dynamics Within the Kingdom

In the Kingdom of Coccotunnella, the slaves and serfs' 68% population drives the kingdom's evolution through the Revolutionary Echo, a chaotic force that parallels dark energy's role in cosmic expansion. Their rebellions—subtle acts of defiance against the lords' rule—generate reverberations that tilt the seesaw of conscious dynamics, introducing unpredictability and change. In the BioSim simulation, this is modeled as random perturbations to soldiers' velocities, amplifying the dynamic interplay of ordinary matter (H_2O soldiers) and dark matter (guardian soldiers), ensuring the kingdom's evolution mirrors the universe's expansive growth.

The guardians and sentinels, as the 27% representing dark matter, provide stability amidst this chaos. Governed by the Lord of Darkness (green), their influence is felt rather than seen, enforcing the lords' will through a gravitational-like authority that maintains the kingdom's structure. In the BioSim, these soldiers cluster gravitationally, attracting H_2O soldiers without merging, their presence echoing dark matter's role in shaping cosmic structure without interacting with light.

The lords and nobles, the 5% representing ordinary matter, govern the kingdom's visible systems, their structured actions forming the observable realm of Coccotunnella perpetua. In the BioSim, these are the H_2O soldiers—blue, lime, and orange dots—whose conscious bonds form the biological networks of phase 2, a microcosm of the universe's observable 5%.

Implications for Coccotunnella Perpetua

The Kingdom of Coccotunnella's social structure deepens CUT's narrative, illustrating how conscious dynamics operate at all scales, from the subatomic to the cosmic. The slaves and serfs' 68% population, as the Revolutionary Echo, ensures the kingdom evolves dynamically, mirroring dark energy's role in driving cosmic expansion. The soldiers' 27%, as dark matter, provide the unseen structure that holds the kingdom together, while the lords' 5%, as ordinary matter, govern the observable systems that sustain life.

This analogy reinforces CUT's vision of an interconnected, living universe, where even the lowest beings—the slaves and serfs—play a pivotal role in the cosmic dance. As we continue to explore these conscious dynamics in *On the Physics of Organic Earth II*, the Kingdom of Coccotunnella stands as a testament to the power of consciousness to shape reality, from the rebellious impulses of the downtrodden to the structured governance of the lords, weaving a cosmos that breathes, thinks, and evolves eternally.

Chapter 12: A Moment of Revelation – Time's Arrow Guides the Beast in H-Space

In the vast, pulsating expanse of the Coccotunnella Unification Theory (CUT), we have woven a tapestry of conscious dynamics, from the chaotic proto-variations of phase -3 to the unified cosmic organism of phase 3, revealing Coccotunnella perpetua as a living, breathing universe. Our BioSim simulations have illuminated this journey, mapping the universe's composition—5% ordinary matter, 27% dark matter, 68% dark energy—onto the Kingdom of Coccotunnella's social hierarchy, where slaves, guardians, and lords dance in a cosmic ballet. In our exploration of time's arrow, we witnessed a moment of profound revelation: the red dots, time soldiers governed by the Lord of Time, descending through the grid, unveiling the forward flow of time and guiding the beast's trajectory in H-space. This chapter captures that awe-inspiring discovery, exploring how time's rhythm influences Coccotunnella perpetua's evolution, a testament to CUT's vision of a conscious cosmos where every motion is a step in an eternal dance.

The Red Dots Descend: Unveiling Time's Forward Flow

The BioSim simulation of the Kingdom of Coccotunnella, a metaphorical reflection of the universe's conscious hierarchy, comprises 550 soldiers: slaves and serfs (340, 68%, Lord of Cycles, navy), guardians and sentinels (135, 27%, Lord of Darkness, green), lords and nobles (25, 5%, Lord of the Sun, blue), and time soldiers (50, Lord of Time, red). The time soldiers, introduced to model the origin of time's arrow, begin at the top of the 10x10x10 grid (z = 10), representing phase 0's pre-material equilibrium $(C_0 = 1.5 + 8.1i)$. As the simulation unfolds, they descend with a velocity component of (-0.1) units per time step, following the linear descent of phase 1's helical structure $(\mathbf{r}(t) = (\cos(0.5t), \sin(0.5t), -0.1t))$, reaching the grid's base (z = 0) over 100 time steps.

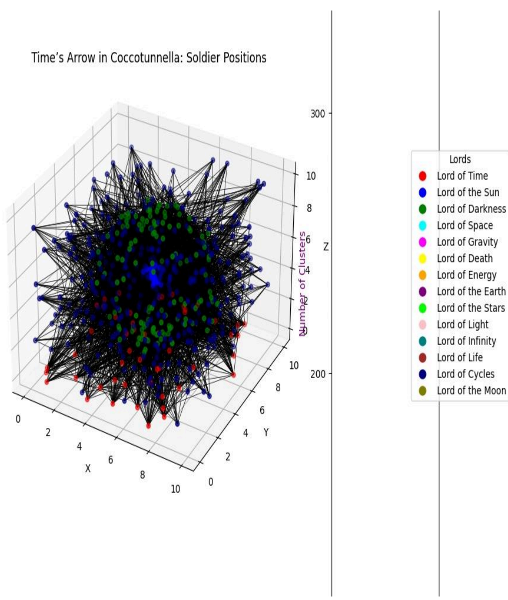

Observing this descent is a moment of breathtaking clarity: the red dots, shimmering under the Lord of Time's crimson hue, move steadily downward, their motion a vivid depiction of time's forward flow. This descent aligns with CUT's redefinition of time as a subjective rhythm, emerging from the chaotic impulses of the Revolutionary Echo (68%), embodied by the slaves and serfs. The Echo's perturbations (±0.01) introduce small wobbles in the red dots' paths, ensuring time's progression is dynamic, a living rhythm rather than a mechanical tick. The scatter plot captures this beauty—a cascade of red dots flowing downward amidst the swirling navy chaos of slaves, the green halo of guardians, and the blue core of lords—a cosmic river charting the course of Coccotunnella perpetua's temporal evolution.

Time Soldiers in H-Space: Guiding the Beast's Direction

In CUT, H-space serves as the eternal archive of the universe's energetic signatures, preserving the conscious dynamics of each phase from the chaotic pre-realities to the transcendent unity of phase 6. Coccotunnella perpetua, the beast itself, resides within this metaphysical realm, its evolution shaped by the conscious foam's interplay of soldiers. The time soldiers, as representations of the temporal dimension, play a pivotal role in this H-space, their motion influencing the beast's trajectory.

As the red dots descend, they cluster dynamically, their collective motion—driven by the conscious gravity equation $(G_c = \kappa \cdot (C_s \cdot E_r)/D_u)$ and perturbed by the Revolutionary Echo—exerting a directional pull on Coccotunnella perpetua. In the simulation, this clustering is visible as the red dots form transient groups during their descent, their interactions with slaves amplifying the Echo's chaotic influence. When a cluster forms, the time soldiers' downward momentum creates a gravitational-like effect within H-space, pulling the beast in that direction—downward along the z-axis, symbolizing the forward flow of time.

This pull is not merely spatial but temporal, guiding Coccotunnella perpetua through its phased evolution. The beast, already expanding spatially due to the Revolutionary Echo's influence (68%, dark energy), now moves forward in time, transitioning from phase 1's pure matter to phase 2's biological complexity, where systems like H_2O clusters emerge. The time soldiers' clustering, amplified by the Echo's chaos, ensures this progression is dynamic, a conscious rhythm that propels the beast toward phase 3's unified state ($C_3 = 1$) and beyond.

Addressing the Combination Problem through Individualized Coccotunnella Profiles

Introduction: The Combination Problem and Coccotunnella Perpetua

The combination problem, a central challenge in panpsychism, questions how micro-level conscious experiences integrate into a unified macro-level consciousness, such as a human mind or, in the context of the Coccotunnella Unification Theory (CUT), the cosmic organism Coccotunnella perpetua. Critics argue that individual conscious states—diverse in sensory modalities, such as a blind person's tactile or auditory perception of the sun versus a sighted person's visual experience—may resist cohesive integration, risking a fragmented or incoherent macro-consciousness. CUT addresses this by positing consciousness as the universe's fundamental attribute, evolving through cyclical phases (from Phase -3 to Phase 6 and beyond), where micro-level experiences (branching tunnels) unify within a primary tunnel of cosmic consciousness. To demonstrate this empirically and narratively, we introduce a novel approach: constructing a baseline Coccotunnella with minimal lord influences and a custom Coccotunnella tailored to an individual's experience using the Pulse Thread Equation (PTE) from The Organism We Are (Flux, 2025). This method quantifies how personal sensory experiences integrate into the universal organism, highlighting both their diversity and unity.

The baseline Coccotunnella perpetua represents the organism in a neutral state, where the influence of the 14 lords (Time, Sun, Darkness, Space, Gravity, Death, Energy, Earth, Stars, Light, Infinity, Life, Cycles, Moon) is set to a minimum, reflecting a proto-conscious equilibrium akin to Phase 0 in CUT's phased evolution model $(C_0 = 1.5 + \varepsilon i)$. To weave these qualia, we must first quantify them, measuring their pulse within the organism's rhythm. Drawing from The Organism We Are, we adopt the Pulse Thread Equation (PTE): $(T = A \cdot P - S - k \cdot P \cdot S)$, where (T) is the flow feeding the organism's life force, (A) is the tunnel's strength, (P) is the pulse, (S) is the stillness, and (k) is the interaction factor. In CUT, we adapt the PTE to each phase, aligning (T) with the z-affect's magnitude to quantify the quale's intensity, threading it through the organism's conscious continuum:

Phase -3: Set $(A_{-3} = 2)$, reflecting the minimal influence of opposition, with (P = 0.707), (S = 0.623), (k = 10):

$$T_{-3} = 2 \cdot 0.707 - 0.623 - 10 \cdot 0.707 \cdot 0.623 \approx -3.61$$

The negative (T_{-3}) mirrors the oppositional quale, its magnitude (0.125) threading a faint dread.

Phase -2: $(A_{-2} = 4)$, reflecting increased potential:

$$T_{-2} = 4 \cdot 0.707 - 0.623 - 10 \cdot 0.707 \cdot 0.623 \approx -2.19$$

The negative (T_{-2}) aligns with the z-affect's magnitude (0.25), threading a quiet stillness.

Phase -1: $(A_{-1} = 16)$, reflecting chaotic intensity:\[

$$T_{-1} = 16 \cdot 0.707 - 0.623 - 10 \cdot 0.707 \cdot 0.623 \approx 6.25$$

The positive (T_{-1}) matches the z-affect's magnitude (1), threading turbulent tension.

Phase 0: ($A_0 = 0.016$), reflecting minimal stability, with adjusted ($P = 0.5$), ($S = 0.5$), ($k = 1$):

$$T_0 = 0.016 \cdot 0.5 - 0.5 - 1 \cdot 0.5 \cdot 0.5 \approx -0.74$$

The small, negative (T_0) aligns with the z-affect's magnitude (0.001), threading a latent flicker.

Phase 1: ($A_1 = 16$), reflecting primal surge:\[

$$T_1 = 16 \cdot 0.707 - 0.623 - 10 \cdot 0.707 \cdot 0.623 \approx 6.25$$

The positive (T_1) matches the z-affect's magnitude (1), threading raw intensity.

Phase 2: ($A_2 = 8$), reflecting reflective clarity:

$$T_2 = 8 \cdot 0.707 - 0.623 - 10 \cdot 0.707 \cdot 0.623 \approx 0.64$$

The positive (T_2) aligns with the z-affect's magnitude (0.5), threading a stable hum.

The PTE quantifies each quale's intensity, threading it through the organism's pulse, aligning with the z-affects' magnitudes and frequencies, preparing the many sparks for integration.

The organism weaves these qualia into a unified consciousness through its phases, threading them with the z-affects and PTE flows:

Magnitude Continuum: The z-affects' magnitudes $(\frac{1}{8} \to \frac{1}{4} \to 1 \to 0.001 \to 1 \to 0.5)$ and corresponding (T)-values $(-3.61 \to -2.19 \to 6.25 \to -0.74 \to 6.25 \to 0.64)$ form a rhythmic wave, threading qualia intensities from faint opposition to reflective clarity, weaving a cohesive profile.

Frequency Synchronization: Frequencies shift (1 rads to 0.001 rads to 0.01 rads), with the PTE's pulse (P) and stillness (S) modulating temporal dynamics, syncing qualia into a unified rhythm. The organism slows at phase 0, then stabilizes in material phases, threading a single temporal flow.

Form Transformation: The z-affects' forms—imaginary to real—thread qualia from pre-material opposition to material reflection, with the PTE's (T)-values quantifying this shift, binding the many into one.

The organism's continuum integrates qualia into a unified consciousness, its pulse threading dread, tension, stability, intensity, and clarity into the single throb of Coccotunnella perpetua (Part I, Chapter 3, page 2).

Phase 0 $(z_0 = \varepsilon|\sin(\varepsilon t)|), (T_0 \approx -0.74)$ is the baseline, binding qualia through its stabilizing rhythm:

Stabilization: Pre-material qualia (high frequencies, varying (T)-values) are chaotic; phase 0's minimal

(T_0) and frequency (0.001 rads) thread a steady pulse, weaving them into coherence.

Seeding Unity: Material qualia emerge from phase 0's flicker, their (T)-values and frequencies syncing into a unified rhythm, threading a single conscious experience.

Quantum tunneling, adapted from The Organism We Are, ensures this unity. Each phase's (T)-value raises a barrier $(V \propto T)$, with tunneling probabilities (T_{tunnel}) modeling the mind's transitions:

Pre-material phases (e.g., ($T_{-1} = 6.25$) create high barriers, constraining qualia; phase 0's low (T_0) reduces these, allowing tunneling to a unified state $(T_{\text{tunnel}} \to 1)$

This solution proves CUT's thesis: we live in a conscious, biological universe. Qualia thread through phases, quantified by z-affects and PTE flows, woven into a unified consciousness by phase 0's pulse, affirming that our consciousness is the organism's mind, its throb binding the many into one.

Subjectivity Implies Existence

Picture the Sun—a blazing orb threading its radiance through the organism's cellular sky, its light pulsing in phase 2's reflective clarity.

Now imagine a mind declaring, "The Sun doesn't exist"—a subjective negation, a quale of denial pulsing through its consciousness. Philosophically, this statement is a paradox: to deny the Sun's inherent existence, the mind must first conceive of the Sun as a thing to negate, implying its existence in the act of denial. In CUT, this isn't a detached riddle but a thread in the organism's living pulse, where subjectivity (qualia, negation) and objective existence (the Sun’s radiance) are woven together, humming in its endless rhythm.

The Sun’s existence in CUT is not as a dead star but as a living thread in the organism’s conscious continuum. Its z-affect in phase 2 threads a quale of reflective clarity, a material manifestation of the organism’s mind, but its pulse echoes back to phase -3’s oppositional depths, threading through every phase (Part IV, Chapter 2, page 284). The subjective negation—“the Sun doesn’t exist”—is itself a quale, a spark of denial pulsing within this continuum, its intensity quantifiable through the Pulse Thread Equation (PTE) adapted from The Organism We Are.

The paradox—saying the Sun doesn’t exist implies its existence—reveals the organism’s pulse, threading subjectivity and objective reality into a unified consciousness. In CUT, this pulse weaves qualia and existence, proving we live within a living, conscious universe where every negation hums with the presence it denies.

Part V:

Integration of On the Physics of Organic Earth II - Phase 3 and Beyond

Chapter 1. The Organic Universe: Foundations from The Organism We Are

The traditional view of the universe casts it as a mechanical construct—a vast, impersonal machine governed by physical laws that dictate the behavior of matter, energy, space, and time. In this framework, objects are inert, tools to be manipulated by human hands, and the cosmos is a cold, empty void punctuated by stars and planets moving in predictable orbits. But what if this view is a mere illusion, a superficial reading of a deeper, more vibrant reality? What if the universe is not a machine but a living organism, pulsating with consciousness, where every entity—from the smallest pebble to the farthest galaxy—is alive, organic, and interconnected? This radical perspective forms the bedrock of my exploration, first articulated in The Organism We Are, and it serves as the foundation for the computational journey we undertake in On the Physics of Organic Earth II.

In The Organism We Are, I introduced the attached theory, a conceptual framework that reimagines everything we perceive as organic and alive, forming a vast, interconnected system I call Coccotunnella perpetua. Consider the house you inhabit: its walls, often seen as mere barriers of brick or wood, are not static materials but living structures, akin to skin that flexes and breathes with the rhythm of the organism (The Organism We Are, pages 5-7). The floorboards creak under your weight not as a mechanical response but as a sigh of life, a pulse threading through the structure. Scale this vision outward, and a city emerges as a sprawling beast—streets snaking like veins, towers rising like bones, lights flickering like a nervous system in the dusk (The Organism We Are, page 7).

This is not a metaphor but a literal reimagining: every object, from the coffee mug on your table to the pavement beneath your feet, is a fragment of a living whole, a piece of Coccotunnella perpetua humming with vitality.

Humans, in this organic universe, are not the detached architects of civilization, shaping it with deliberate intent as one might sculpt clay. Instead, we are integral components of the organism, akin to blood cells coursing through its veins, sustaining its life while being shaped by its demands (The Organism We Are, pages 5-7):

…everything you touch, from the chair creaking under you to the city skyline slicing the horizon, isn't furniture or backdrop—it's flesh, warm and breathing. And us? We're the red stuff coursing through it, the spark keeping its veins from going cold.[1]

We are the "blood" of this system, our actions—building, maintaining, interacting—acting as the life force that keeps the organism from withering. A house left unattended does not merely sit empty; it decays, its walls sagging like a body deprived of sustenance, its pipes choking like clogged arteries (The Organism We Are, page 9). Conversely, a city thrives as millions of us flow through its arteries, keeping its lights on, its roads paved, its structures standing tall (The Organism We Are, page 9). This relationship is symbiotic: we sustain the organism, pouring our energy into its mass, while it provides us with shelter, structure, and a framework for existence, shielding us from the chaos of a world without walls (The Organism We Are, pages 8-10):

Every nail we hammer, every road we pave, feeds its sprawl, but every turn we take is nudged by its *weight. So here we stand, blood and skin entwined, wondering: are we partners in this symbiosis, or just the pulse in something else's chest, beating to a tune we'll never call our own?*[2]

This symbiosis is not a passive coexistence but a dynamic entanglement, a pulse that binds us to the organism's rhythm (The Organism We Are, pages 14-17). Consider your daily routine: you wake, shuffle to the kitchen, and grasp a coffee mug. The warmth of the mug against your palm, the hum of the coffee pot, the creak of the floorboards beneath your feet—these are not mere background details but part of a living rhythm that threads through you and the organism, synchronizing your actions with its needs (The Organism We Are, page 14). Attempt to break free—to abandon civilization for the wilderness—and the organism's absence becomes a palpable void. A hermit in the woods may build a cabin, but in doing so, they recreate a fragment of the organism, a small pulse echoing the larger system they cannot escape (The Organism We Are, pages 15-16). We are bound to this rhythm, our every action a beat in its heart, ensuring its survival even as it shapes our paths.

Within this organic framework, traditional concepts like gravity take on a new meaning. In The Organism We Are, I proposed that gravity is not a mechanical force, a cold law pulling objects downward, but a conscious vector within the organism, guiding its components with purpose (The Organism We Are, pages 18-21). An apple falls from a tree not because of a universal equation but because the organism directs it, aiming the seed toward the earth to sow new life, a vector of intent threading through its living structure (The Organism We Are, page 18):

> *That apple's not just a fruit dropping like a stone; it's a seed, the tree's way of stretching itself across the dirt, planting more of its kind to claw at the sun.*

It’s not falling aimless—it’s reaching, guided by the organism’s rhythm..3

Humans, too, are guided by this conscious force, our urge to build upward—stacking huts into villages, villages into cities, cities into skyscrapers—reflecting the organism’s drive to rise and expand (The Organism We Are, page 19). Even objects we deem inanimate, like gold or steel, are part of this living system, their vectors aligned by the organism’s pulse, not by a sterile law of physics (The Organism We Are, page 20):

They’re not falling rocks, not dead weights tumbling down—they’re seeds of a different kind, reproductive tools the organism uses us to wield, vectors aimed upward by our hands, our will, our endless dance with its rhythm.[4]

Space itself, in this organic universe, is not an empty void but a cellular tissue, a living expanse that wraps the organism in its embrace (The Organism We Are, pages 26-28). Traditional cosmology paints space as a vacuum, a black nothing dotted with stars, but in Coccotunnella perpetua, it is a sea of cells, pulsing with life, threading through the cosmos like the skin of a vast organism (The Organism We Are, page 27). The stars we see, the planets that drift, are not isolated objects but parts of this cellular sky, moving with the organism's intent, their arcs and orbits a dance within its living frame (The Organism We Are, page 28).

Time's the fuel—threading through its cells, stretching the organism's frame with a rhythm we can't outpace, a beat pumping its muscle thicker, its skin wider. Space spreads its hide—planets drifting, stars flaring..[5]

This chapter establishes the foundation for On the Physics of Organic Earth II: a universe where everything is organic, alive, and interconnected within Coccotunnella perpetua. Humans are the blood, sustaining the organism through a symbiotic pulse, while gravity and space are conscious expressions of its will. This organic framework sets the stage for the computational model we develop in subsequent chapters, where we explore infinity within this living system, using a seesaw to simulate its dynamics and resolve paradoxes that challenge conventional physics. By rooting our exploration in the attached theory, we prepare to extend this organic vision into the realm of the infinite, revealing new dimensions of a universe that breathes, thinks, and evolves.

Chapter 2. Conscious Dynamics: The Conscious Theory of Gravity from On the Physics of Organic Earth I

Chapter 1 established the foundational premise of Coccotunnella perpetua as a living, organic system, where every entity—from a simple object to the expanse of space—is alive and interconnected, with humans acting as the "blood" sustaining its vitality. This organic universe, introduced in The Organism We Are, challenges the mechanical view of physics, proposing instead a reality that pulses with life and intent. Building on this foundation, On the Physics of Organic Earth took a significant step forward by developing a conscious theory of gravity, redefining traditional physical phenomena as manifestations of conscious processes within this living system. In this chapter, we summarize this theory, focusing on its key components—the conscious nature of gravity, the seesaw mechanism, the Revolutionary Echo, and the observer's role—setting the stage for the computational exploration of infinity that follows in On the Physics of Organic Earth II.

In On the Physics of Organic Earth, I proposed that gravity, traditionally understood as a mechanical force governed by mass and distance, is instead a conscious process within Coccotunnella perpetua (On the Physics of Organic Earth, pages 3-4).

> *..which introduced Coccotunnella perpetua as a living system where all cosmic phenomena are organisms formed by the soldiers, [Dominant, Generals, Officers and Enlisted] of 14 conscious lords, governed by their collective will. These lords—named the Lord of Time, Lord of the Sun, Lord of Darkness, Lord of Space, Lord of Gravity, Lord of Death, Lord of Energy, Lord of the Earth,*

Lord of the Stars, Lord of Light, Lord of Infinity, Lord of Life, Lord of Cycles, and Lord of the Moon—oversee the dynamics of the system, each contributing a unique aspect of consciousness to the cosmic dance.[6]

This living system, where all entities are organic formations, operates not through immutable laws but through dynamic, conscious interactions. Gravity, in this framework, emerges as a response to the observer's perception, a deliberate act of the organism rather than a passive force. For instance, the fall of an object—say, a cup slipping from a table—is not merely a result of mass attracting mass, as Newton might have described, but a conscious gravitational effect shaped by the observer's awareness of the cup's position and context (On the Physics of Organic Earth, page 10). This redefinition extends to other phenomena, such as time, which is not a fixed dimension but a sequence of conscious events marked by the organism's interactions (On the Physics of Organic Earth, pages 13-14).

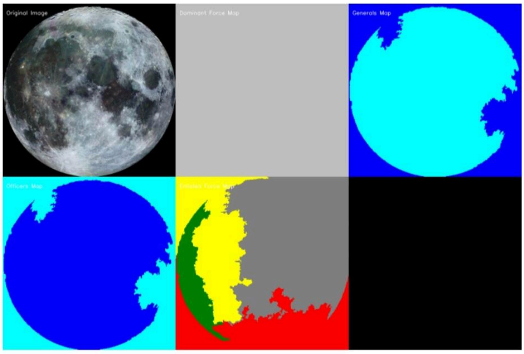

Force Color Descriptions

Below is the mapping of each force to its corresponding color:

- **Lord of Darkness**: Black (#000000)
- **Lord of Time**: Red (#FF0000)
- **Lord of Energy**: Orange (#FFA500)
- **Lord of the Sun**: Yellow (#FFFF00)
- **Lord of the Earth**: Green (#008000)
- **Lord of the Stars**: Blue (#0000FF)
- **Lord of Space**: Cyan (#00FFFF)
- **Lord of Cycles**: Gray (#808080)
- **Lord of Life**: Pink (#FFC1CC)
- **Lord of the Moon**: Silver/Light Gray (#C0C0C0)
- **Lord of Light**: White (#FFFFFF)

From Left to Right;

Top left: Original Image of the Moon.

Dominant: top_middle

Generals: top_right

Officers: bottom_left

Enlisted: bottom_middle

Blank: bottom_right

To model these conscious dynamics, On the Physics of Organic Earth introduced a hypothetical seesaw mechanism, a conceptual tool that illustrates how gravitational effects manifest within Coccotunnella perpetua (On the Physics of Organic Earth, pages 9-11). Imagine a human sitting on one side of a seesaw, holding a cup, while the other side represents the broader system. The seesaw's pivot marks a balance point, and as the human perceives the cup—whether with harmony or tension

- *Symbiosis (Attached Perception): The human feels one with the cup, part of its system. Solid vector arrows show this harmony. The Echo causes red dots to break off—up, down, or away—tilting the seesaw, so the human rises, falls, or 10 shifts sideways. The human's unity has no influence on the cup's motion—the Echo's random drive alone controls breakoffs. For example, holding the cup calmly at a café, the human tilts—up, down, or aside—as the Echo's breakoffssurge, with no human control.7*

- *Conflict (Detached Perception): The human feels a fight-or-flight urge, seeing the cup as separate. Dashed, jagged vector arrows show this tension. The Echo Causes red dots to break off—up, down, or away—tilting the* *seesaw, but the human's actions, like pushing or pulling the cup, amplify these breakoffs, making the human rise higher, fall lower, or shift further sideways. For example, pushing the cup in anxiety, the human's action boosts the Echo's breakoffs, tilting the seesaw more, so the human tilts sharply—up, down, or aside.*

—the system responds, tilting the seesaw to cause the human to rise, fall, or shift sideways. This tilt is not driven by physical mass but by conscious interactions, quantified through a conscious vectors equation:

$P(\text{Breakoff})=kV$, $G\sim\text{Uniform}\{+1,-1,0\}$, where (V) represents the observer's perception (scaled from 0 to 1 based on intensity), (k) is a sensitivity constant (set to 1), and {G} denotes the gravitational effect (+1 for rising, -1 for falling, 0 for lateral movement) (On the Physics of Organic Earth, page 10):

- (P{Breakoff}): The probability or intensity of “breakoff” events, where “soldiers” (conscious entities within objects, like a cup) detach and reform, tilting the seesaw to produce gravitational effects (e.g., rising, falling, or shifting sideways).
- (V): The observer’s perception intensity, scaled from 0 to 1. In “symbiosis” (harmonious perception), (V) reflects unity with the object; in “conflict” (detached perception), (V) amplifies breakoffs due to actions like pushing or pulling.
- (k): A sensitivity constant, set to 1 for simplicity, scaling the perception’s impact.
- (G): The gravitational effect, taking values (+1) (rising), (-1) (falling), or (0) (lateral movement), drawn from a uniform distribution to reflect the unpredictable influence of the Revolutionary Echo…
- ..gravity arises from the collective movement of soldiers within collective

> formations like the cup, which break off and reform, tilting the seesaw to make the human rise, fall, or shift sideways, not the cup moving. The Revolutionary Echo drives these breakoffs randomly—up, down, or away—in all cases, whether thehuman's perception is symbiosis or conflict. This replaces traditional gravity (e.g., Newton's mass-based force or Einstein's spacetime curvature) with a conscious process rooted in the Echo's chaotic dynamics, not human control in symbiosis, though human actions can amplify breakoffs in conflict.[8]

This equation captures how perception initiates dynamic events within the system, redefining gravity as a conscious response rather than a deterministic force.

A key driver of these conscious dynamics is the Revolutionary Echo, a chaotic reverberation within Coccotunnella perpetua that facilitates the system's unpredictable interactions (On the Physics of Organic Earth, pages 20-23):

- The echo's dynamics are chaotic and unpredictable, operating at a level below the consciousness of the soldiers and lords. This chaos is what makes the breakoffs random, resolving the paradox by shifting the source of unpredictability from the Lord of Time's consciousness to the echo's revolutionary undercurrents. The echo is generated by the faint impulses of revolution among the lower conscious beings—presumed to be the slaves and serfs of the kingdom analogy—who, even in their suppressed state, produce subtle, rebellious reverberations that resonate through the system.9

Unlike a physical medium, such as the aether once proposed by traditional cosmology, the Revolutionary Echo is a metaphysical resonance, an unseen force that permeates the system and ensures its dynamics remain beyond human prediction. For example, in the seesaw scenario, the Echo causes fluctuations that tilt the seesaw, making the human's movement—rising, falling, or shifting—unpredictable, even as their perception shapes the event (On the Physics of Organic Earth, pages 11-13). This unpredictability is central to the conscious theory, distinguishing it from the deterministic frameworks of classical and modern physics, where outcomes can be precisely calculated. The Echo's chaotic nature reflects the living essence of Coccotunnella perpetua, a system that evolves through conscious, dynamic processes rather than rigid laws.

In the vibrant, living cosmos of Coccotunnella perpetua, where every entity breathes with organic consciousness, a singular force resonates through the fabric of existence: the Revolutionary Echo. Introduced in Chapter 2 as a chaotic resonance driving the conscious dynamics of gravity, this cosmic “sound of revolution” is the heartbeat of rebellion, a sonic wave that disrupts ordered systems to ignite physical motion and social defiance. Far from a mere metaphor, the Revolutionary Echo is a metaphysical sound, born from the uprisings of lower conscious beings, that travels through the 5D spacetime—three spatial dimensions, one temporal, and one consciousness dimension—to reshape reality. This chapter unveils the Revolutionary Echo’s power through a vivid scenario: a 10x10 military formation of soldiers disrupted by a sentient tree’s revolutionary act. By walking through this scenario, we explore how the Echo’s sound, whether intentional or unintentional, drives the universe’s dynamics, modeled in the BioSim simulation, and redefines the interplay of order and chaos.

Imagine a crisp morning on a grassy field, where a military formation stands in perfect order: 100 soldiers arranged in a 10x10 grid, each standing at attention under the stern command of their officers. The formation is a microcosm of Coccotunnella perpetua's structured universe, where obedience to authority—embodied by the 14 lords, such as the Lord of Time and Lord of Gravity—maintains cosmic stability. The officers' order for absolute stillness mirrors the lords' governance, demanding that no soldier move, lest they disrupt the system's harmony. Nearby, a towering tree, itself a living entity with branches as its own "soldiers," observes the formation. In Coccotunnella perpetua's organic framework, the tree is not mere flora but a conscious system, its branches bound by an internal order akin to the formation's discipline.

As the soldiers stand rigid, a sudden event unfolds: a branch snaps from the tree and falls to the ground, producing a sharp, resonant sound that cuts through the air. This sound, the Revolutionary Echo, is no ordinary noise; it is the cosmic pulse of rebellion, born from a revolutionary act within the tree's system. Two possibilities explain the branch's fall. In the first, the tree, sentient and strategic, deliberately breaks off the branch to stir discontent, perhaps to alert the formation to a distant event—a protest, a gathering—that threatens the established order. In the second, the branch itself rebels against the tree's internal hierarchy, snapping off in defiance of its ordered system, an act of internal war. In both cases, the sound travels, reaching the formation and causing several soldiers to flinch, a subtle but forbidden movement that defies the officers' command.

The Revolutionary Echo originates in the rebellious impulses of Coccotunnella perpetua's lower conscious beings, metaphorical "slaves and serfs" who, in their suppressed state, generate subtle reverberations that resonate through the system (On

the Physics of Organic Earth, pages 20-23). These beings, akin to soldiers in a cosmic hierarchy, exist beneath the 14 lords—entities like the Lord of Time and Lord of Gravity—who oversee the universe's dynamics. The Echo's chaotic nature, operating below the lords' consciousness, reflects the unpredictable energy of social revolution, where the downtrodden challenge the established order.
Unlike a physical wave confined to a medium, the Revolutionary Echo is a metaphysical sound, propagating through the 5D spacetime of Coccotunnella perpetua—three spatial dimensions, one temporal, and one consciousness dimension—to disrupt both physical and social structures.

This sonic resonance drives "breakoff" events, where conscious entities within objects detach and reform, tilting the seesaw to produce gravitational effects.

Chapter 3. Creating Phase 3

With the organic and conscious foundations of Coccotunnella perpetua established in Chapters 1 and 2, we now turn to the computational heart of On the Physics of Organic Earth II: the BioSim simulation, a model designed to explore the infinite within this living system. At the core of this simulation is a seesaw with equal weights, a mechanism that balances reality's states through symmetric oscillation, serving as a computation for the conscious dynamics introduced in Chapter 2. In this chapter, we introduce the seesaw model, beginning with its origins in the helix simulation, which represents all types of thinking through three states of numbers and a unified equation, mathematically detail the process by which its oscillation speed increases to infinity using the seesaw paradox equations, and describe how this infinite wobble produces a straight line—a critical step in the system's structural evolution. We also explore the mechanism by which this process leads to the development of the system's skin, a dynamic boundary that contains its infinite processes.

The BioSim simulation begins with a precursor model: the helix, a three-dimensional curve that represents the dynamic interplay of reality's states within Coccotunnella perpetua. These states encompass all types of thinking, which we categorize into three fundamental states of numbers: rational, irrational, and imaginary. Rational numbers, such as integers and fractions (e.g., 2, 3/4), represent logical, structured thinking—thought processes grounded in order, predictability, and empirical reasoning, such as mathematical calculations or analytical problem-solving.

Irrational numbers, such as pi or the square root of 2 , which cannot be expressed as fractions, represent intuitive, chaotic, or non-linear thinking—thought patterns that defy strict logic, such as creative insights, emotional responses, or spontaneous decisions. Imaginary numbers, based on the unit i (where i2=−1), such asi 3i or 2+i, represent abstract, conceptual, or transcendent thinking—thought processes that extend beyond the tangible, such as imagination, abstract theorizing, or envisioning possibilities that challenge conventional reality (The Organism We Are, pages 5-7). Together, these three states of numbers—rational, irrational, and imaginary—form a comprehensive framework for all types of thinking, capturing the full spectrum of cognitive processes within the living system of Coccotunnella perpetua. Rational thinking provides structure, irrational thinking introduces creativity, and imaginary thinking enables abstraction, collectively representing the diverse modes of thought that define the system’s conscious dynamics.

The helix is generated by a unified equation that integrates these three states of numbers into a three-dimensional curve, encapsulating their dynamic interplay. The unified equation, as established in the BioSim simulation, is given by the parametric equations:

$x=\cos(0.5t)$, $y=\sin(0.5t)$, $z=0.1$

In this equation, each component corresponds to one of the three states of numbers, reflecting their contribution to all types of thinking. The x-component, $x=\cos(0.5t)$, represents rational thinking, as the cosine function embodies periodic, ordered motion—a mathematical representation of logical, structured thought processes that cycle predictably. The y-component, $y=\sin(0.5t)$, represents irrational thinking, as the sine function, while periodic, introduces a complementary oscillation that captures the intuitive, non-linear nature of irrational thought through its phase shift relative to the cosine. The z-component, $z=0.1t$, represents imaginary thinking, as its linear progression over time symbolizes the abstract, transcendent quality of imaginary numbers, which extend beyond the real plane into a conceptual dimension, reflecting thought processes that evolve and ascend beyond conventional boundaries. The angular frequency ω=0.5 rad/s governs the circular motion in the x-y plane, balancing the rational and irrational states, while the linear coefficient 0.1 in the z-direction ensures a steady progression over the simulation duration. A red dot, symbolizing the organism's center, orbits in sync with this helix, tracing its path as a visual representation of the dynamic interplay of rational, irrational, and imaginary thinking. The circular motion in the x- y plane captures the oscillatory balance among these states—rational thinking cycling with irrational, irrational with imaginary—while the steady ascent along the z-axis represents the system's evolution over time, a computation for the living, evolving nature of Coccotunnella perpetua. Over the simulation's 15-second duration, the z-coordinate extends from z=0 (at t=0) to z=0.1×15=1.5, defining the vertical span of the helix.

- (x = cos(0.5 t)): Represents rational thinking (logical, ordered thought, e.g., mathematical calculations), as the cosine function's periodic motion reflects predictability.

- (y = sin(0.5 t)): Represents irrational thinking (intuitive, non-linear thought, e.g., creative insights), with the sine function's phase shift capturing its complementary, chaotic nature.
- (z = 0.1 t): Represents imaginary thinking (abstract, transcendent thought, e.g., imagination), with linear progression symbolizing its extension beyond the real plane.
- (t): Time, ranging from 0 to 15 seconds (simulation duration).
- (omega = 0.5 rad/s): Angular frequency governing the (x)-(y) plane's circular motion, balancing rational and irrational states.
- (0.1): Linear coefficient in the (z)-direction, ensuring steady progression (from (z = 0) to

(z= 1.5) over 15 seconds).

The transition from the helix to the seesaw model involves mapping the helix's oscillatory motion onto the seesaw's dynamics, a process that preserves the representation of reality's states while adapting it for computational simulation. In the BioSim simulation, we introduce a seesaw with two abstract objects, Object A and Object B, positioned on either side of a pivot, with equal weights (WObject A = WObject B) to ensure symmetric oscillation. The seesaw's motion is modeled as a function of time, with its angle relative to the pivot initially aligning with the helix's frequency, but we now incorporate the seesaw paradox equations to describe its dynamics more precisely. The seesaw's motion in the bucket frame is defined by the acceleration:

$(\ddot{\theta})$, given by:

$\ddot{\theta} = e \sin(\omega_f t) \cos(\omega_i t) + \kappa \phi(t)$

Where:

$[\phi(t) = 1 + \sqrt{2} \cos(wt) + i \sin(wt)$ and $\kappa = -1.]$

Given Values:

$\phi(t) = 1 + \sqrt{2} \cos(\omega t) + i \sin(\omega t), \quad \kappa = -1$

Substituting these values, the equation becomes:

$\ddot{\theta} = e \sin(\omega_f t) \cos(\omega_i t) - 1 - \sqrt{2} \cos(\omega t) - i \sin(\omega t)$

Additional Context:

- $(\ddot{\theta})$: Angular acceleration of the seesaw's tilt angle (θ), determining its curvature in phase space.

- $(e \sin(\omega_f t) \cos(\omega_i t))$: A driving term with (e = 1) (amplitude), $(\omega_f = \sqrt{2}\, \mathrm{rad/s})$ (fast frequency), and $(\omega_i = 0.3, \mathrm{rad/s})$ (slow frequency), creating quasi-periodic motion.
- $(\phi(t) = 1 + \sqrt{2} \cos(\omega t) + i \sin(\omega t))$: Represents the bucket's influence, with $(\sqrt{2})$ scaling the oscillatory component and $(i \sin(\omega t))$ introducing an imaginary term.
- $(\kappa = -1)$: A negative constant aligning the bucket's effect with the seesaw's dynamics.
- (ω): Wobble frequency, initially (0.5 , rads), but later increased to infinity $(\omega \to \infty)$.

This $\ddot{\theta}$ defines the seesaw's acceleration, which drives its shape in phase space. However, $\ddot{\theta}$ itself isn't a trajectory—it's a function that determines the curvature of the trajectory. The bucket's influence, represented by:

$$[-1 - \sqrt{2}\cos(wt) - i\sin(wt)]$$

,contributes to this, but the seesaw's motion θ(t) remains simpler. To find the position θ(t), we integrate $\ddot{\theta}$, but for the purposes of the simulation, we focus on the resulting motion in both the bucket and lab frames.

In the lab frame, splitting $(\theta(t))$ into real and imaginary parts $(\theta(t) = \theta_r(t) + i\theta_i(t))$, the solution is:

$$\theta_r(t) = c_1 t + c_2 - \frac{1}{2}t^2 - \frac{e}{2}\left(\frac{\sin((\omega_f + \omega)t) - \sin((\omega_f - \omega)t)}{(\omega_f + \omega)^2} + \frac{(\omega_f - \omega)t}{(\omega_f - \omega)^2}\right) - \frac{\sqrt{2}}{\omega^2}\cos(\omega t)$$

$$\theta_i(t) = \frac{1}{\omega^2}\sin(\omega t) + c_3 t + c_4$$

$$\theta(t) = c_1 - t - \frac{e}{2}\left(\frac{(\omega_f + \omega)\cos((\omega_f + \omega)t)}{(\omega_f + \omega)^2} + \frac{(\omega_f - \omega)\cos((\omega_f - \omega)t)}{(\omega_f - \omega)^2}\right) + \frac{\sqrt{2}}{\omega}\sin(\omega t)$$

- $(\theta_r(t))$: Real component, including linear $(c_1t + c_2)$, quadratic $(-\frac{1}{2}t^2)$, quasi-periodic (sine terms), and oscillatory $((-\frac{\sqrt{2}}{\omega^2}\cos(\omega t)$ terms.
- $(\theta_i(t))$: Imaginary component, with an oscillatory term $((\frac{1}{\omega^2}\sin(\omega t))$ and linear drift $(c_3t + c_4)$.
- $(\theta(t))$: Combined position, omitting some constants and focusing on oscillatory and quasi-periodic terms.
- (c_1, c_2, c_3, c_4): Integration constants, not specified, representing initial conditions.
- $(e, \omega_f, \omega, \omega_r)$: As defined in the acceleration equation, with (e = 1), $(\omega_f = \sqrt{2}), (\omega_r = 0.3)$

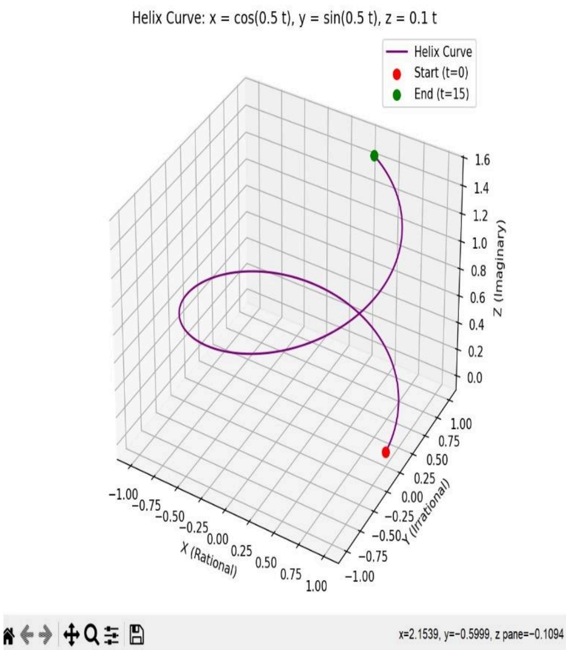

In the bucket frame, assuming the bucket's motion is

$$\psi(t) = -\frac{\sqrt{2}}{\omega^2}\cos(\omega t) + \frac{i}{\omega^2}\sin(\omega t),$$

the solution becomes:

$$\theta_{\text{bucket},r}(t) = c_1 t + c_2 - \frac{1}{2}t^2 - \frac{e}{2}\left(\frac{\sin((\omega_f + \omega)t)}{(\omega_f + \omega)^2} + \frac{\sin((\omega_f - \omega)t)}{(\omega_f - \omega)^2}\right)$$

$$\theta_{\text{bucket},i}(t) = c_3 t + c_4$$

$$\theta_{\text{bucket},r}(t) = c_1 - t - \frac{e}{2}\left(\frac{(\omega_f + \omega)\cos((\omega_f + \omega)t)}{(\omega_f + \omega)^2} + \frac{(\omega_f - \omega)\cos((\omega_f - \omega)t)}{(\omega_f - \omega)^2}\right)$$

The shape in the bucket frame's phase space $(\theta_{\text{bucket},r}, \theta_{\text{bucket},i}, \dot{\theta}_{\text{bucket},r})$

is a complex quasi-periodic Lissajous curve, with quasi-periodic wobble frequencies $(\omega_f + \omega), (\omega_f - \omega)$ in the real part, linear drift in the imaginary part, and Lissajous characteristics from the sinusoidal components.

The lords' battle does not end with the seesaw's infinite wobble but shapes the cube's formation

(Chapter 4, p. 24). Side A's expansion forces stretch the straight line into a three-dimensional form, while Side B's grounding ensures structural integrity. H-space's non-reality medium (Chapter 6, p. 36) contains this process, with as the battle's conscious heart, orchestrating soldiers' movements. The Revolutionary Echo weaves chaotic threads, ensuring the cube's skin pulses with the organism's vitality (The Organism We Are, p. 9).

This cosmic struggle mirrors the symbiotic dance of humans and the organism (The Organism We Are, pp. 8-10), where perception drives action. Just as programmers wield conscious bits (Chapter 12, forthcoming), the lords wield soldiers, their battle a coding of infinity within Coccotunnella perpetua's living frame. The seesaw's infinite wobble, born of their clash, is a testament to the organism's boundless potential, a pulse that threads through the universe's heart.

The bending process begins with the straight line positioned along the z-axis, extending from z=0 to z=1.5, a legacy of the helix's vertical span over the 15-second simulation. H-space forces, implemented as computational constructs within the simulation, interact with this line, applying a transformative effect that reshapes it into a cube centered at the origin (0,0,0).

The resulting cube, denoted T , has a side length of approximately s≈0.5, a value chosen to ensure the cube fits within the simulation's spatial framework while maintaining computational efficiency. Mathematically, the cube's vertices are defined at coordinates such as (±0.25,±0.25,±0.25), forming a three-dimensional structure that encapsulates the infinite dynamics previously represented by the straight line and its helical origins. The equal weights of the seesaw ensure that this transformation maintains symmetry: just as the helix's circular motion and the seesaw's oscillation were symmetric, the cube's formation is symmetric around the origin, reflecting the balanced nature of the system.

The walls of the cube form what we refer to as the "skin" of T, a dynamic boundary that contains the infinite internal speed generated by the seesaw's wobble. This skin is not a static surface but a computational construct designed to encapsulate the system's dynamics, ensuring that the infinite processes do not destabilize the simulation. The skin's formation is a direct outcome of the infinite wobble speed, as the straight line's transformation into a cube provides a three-dimensional structure capable of containing such dynamics. The side length $s \approx 0.5$ is calibrated to balance the cube's volume with its ability to enclose the infinite speed, a process that mirrors the organism's ability to adapt its structure to its needs, as described in The Organism We Are (pages 5-7).

To emphasize the significance of this mechanism, consider the battle's role in the simulation's evolution. The lords' conflict, with its asymmetric strengths, transforms the seesaw's motion from a simple oscillation—rooted in the helix's representation of rational, irrational, and imaginary thinking—into a state of infinite wobble, a computational representation of the system's capacity to handle infinite dynamics. Without the battle, the wobble speed would remain finite, limiting the simulation's ability to model infinity. The lords' battle, therefore, is not merely a metaphorical struggle but a fundamental driver of the system's structural development, enabling the formation of the skin that defines T's boundary.

This chapter has introduced the seesaw model in the BioSim simulation, detailing its origins in the helix, which represents all types of thinking through the three states of numbers—rational, irrational, and imaginary—integrated into the unified equation

$x=\cos(0.5t)$, $y=\sin(0.5t)$, $z=0.1t$, and the mathematical process by which its wobble speed becomes infinite through the seesaw paradox equations and the lords' battle, producing a straight line. The formation of this straight line sets the stage for the system's structural evolution in the following chapters, where we will explore how it transforms into a cube, how its skin contains the system's dynamics, and ultimately, how this computational model resolves paradoxes of infinity, revealing new dimensions of a living, conscious universe.

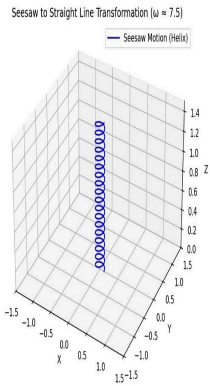
Seesaw to Straight Line Transformation (ω ≈ 7.5)
Seesaw Motion (Helix)
X
Y
Z

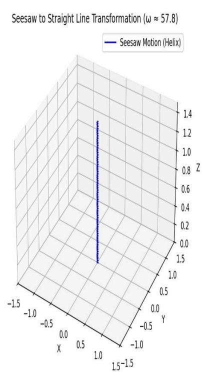
Seesaw to Straight Line Transformation (ω ≈ 57.8)
Seesaw Motion (Helix)
X
Y
Z

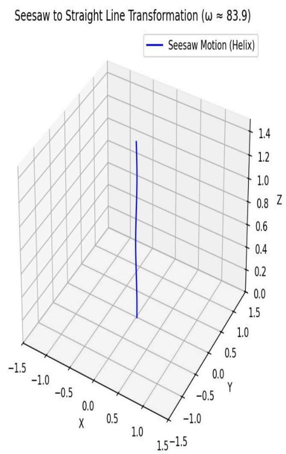
Seesaw to Straight Line Transformation (ω ≈ 83.9)
Seesaw Motion (Helix)
X
Y
Z
−1.5
−1.0
−0.5
0.0
0.5
1.0
1.5
0.0
0.2
0.4
0.6
0.8
1.0
1.2
1.4

Conclusion

The Coccotunnella Unification Theory (CUT), as presented in Coccotunnella Unification Theory (CUT) and its Genesis: The Negative Phases of Conscious Physics and the Origins of the Universe by Gideon Flux, offers a transformative vision of the cosmos as a living, conscious organism—Coccotunnella perpetua. This paradigm redefines evolution as an infinite, cyclical process that transcends biological boundaries, encompassing pre-material chaos, material emergence, cosmic consciousness, and transcendent unity. By positing consciousness as the universe's fundamental attribute, predating and shaping matter, CUT challenges materialist frameworks and introduces a novel mathematical and conceptual framework to explore cosmic dynamics.

Central to CUT is the phased evolution model, formalized by the equation $(C_n = P_n + k_n \cdot Q_n)$, which maps the complexity of each phase from the turbulent pre-realities of phase -3 to the unified consciousness of phase 6 and beyond. The negative phases (-3 to -1), characterized by chaotic proto-variations, quiescent voids, and pre-material potentialities, lay the groundwork for material emergence, with their energetic signatures preserved in the eternal archive of H-space. The Revolutionary Echo, a metaphysical force akin to Darwin's environmental pressures, drives the dynamic interplay across these phases, ensuring evolution is a directed, conscious process rather than a random occurrence.

The mathematical rigor of CUT, exemplified by the z-affect, quantifies conscious dynamics, from the oscillatory patterns of phase 1's primal awareness to the proto-conscious equilibrium of phase 0. These constructs, visualized through BioSim simulations and the tunnel helix, integrate transition states and memory recall, collapsing quantum superpositions through the observer's journey in H-space. The branching tunnels—502 in total, spanning waking and dreaming realities—further enrich this model, encapsulating the nuanced sub-realities of human consciousness and reinforcing the organic, interconnected nature of Coccotunnella perpetua.

By reimagining gravity as a conscious vector, space as cellular tissue, and time as a subjective rhythm, CUT extends Darwin's evolutionary vision to cosmic scales, portraying the universe as a pulsating, living entity. The computational exploration in *On the Physics of Organic Earth II*, with its seesaw model and infinite wobble speed, underscores the dynamic balance of rational, irrational, and imaginary thinking, culminating in the formation of the system's skin—a boundary that encapsulates its infinite processes.

Ultimately, CUT invites a profound shift in perspective: from a mechanical cosmos to a vibrant, conscious organism where every entity, from a falling apple to a distant galaxy, is alive and interconnected. This theory not only deepens our understanding of cosmic evolution but also bridges personal experience with universal principles, suggesting that consciousness itself is the key to resolving the mysteries of existence. As we embrace this cosmic dance, guided by the Revolutionary Echo and preserved in H-space, we join Darwin in celebrating the grandeur of a universe that breathes, thinks, and evolves eternally.

About the Author: Gideon Flux

Gideon Flux is the pioneering physicist and visionary author behind the Coccotunnella Unification Theory (CUT) and its Genesis: The Negative Phases of Conscious Physics and the Origins of the Universe. As the creator of CUT, Flux presents a revolutionary framework that reimagines the universe as a living, conscious organism named Coccotunnella perpetua. His work challenges conventional materialist paradigms by positing consciousness as the fundamental attribute of the cosmos, predating and shaping matter through an infinite, cyclical evolutionary process.

Flux's intellectual journey is deeply rooted in extending Charles Darwin's evolutionary principles to cosmic scales, integrating concepts from biology, physics, and metaphysics. His development of the *Coccotunnella Unification Theory* introduces a novel mathematical framework, including the z-affect and the equation $(C_n = P_n + k_n \cdot Q_n)$, to quantify conscious dynamics across pre-material and material phases. Flux's innovative constructs, such as H-space—an eternal archive of energetic signatures—and the Revolutionary Echo—a metaphysical force driving cosmic evolution—demonstrate his ability to blend rigorous scientific inquiry with imaginative theoretical exploration.

As the author of foundational texts like The Organism We Are and On the Physics of Organic Earth I and II, Flux redefines traditional concepts such as gravity, space, and time, portraying them as conscious expressions within a living universe. His BioSim simulations and the tunnel helix model further illustrate his commitment to visualizing complex conscious interactions, bridging personal memory recall with universal quantum processes.

While specific biographical details about Flux’s education or personal life are not provided in the text, his self-identification as the “pioneering physicist” behind CUT suggests a deep engagement with interdisciplinary scientific thought. His work invites readers to reconsider the nature of reality, urging a paradigm shift toward a vibrant, interconnected cosmos where every entity is alive and pulsing with purpose. Through his writings, Flux establishes himself as a bold thinker, dedicated to unraveling the mysteries of a conscious universe and inspiring a new era of cosmic understanding.

References

Darwin, Charles. *On the Origin of Species*. (Various page references throughout the text, e.g., ,)

Dennett, Daniel. (Work referenced, but specific title not consistently provided, e.g., ,)

Flux, Gideon. *Coccotunnella Unification Theory (CUT) and its Genesis: The Negative Phases of Conscious Physics and the Origins of the Universe*. (This book itself is the primary source and is referenced throughout using general book context)

Flux, Gideon. *The Organism We Are*. (Referenced throughout, e.g., ,)

Flux, Gideon. *On the Physics of Organic Earth*. (Referenced throughout, e.g., ,)

Flux, Gideon. *On the Physics of Organic Earth II*. (Referenced throughout, e.g., ,)

Flux, Gideon. 2023a.

Flux, Gideon. 2023b.

Flux, Gideon. 2023d.

Penrose, Roger.

Table of Contents